Part II

Hydrology and Micro-meteorology

Chapter 5

Grassland Hydrology and Micro-meteorology

5.1 Introduction

To quantify the effect of grassland afforestation on catchment water yield, the dry season water use of the grassland will be determined in this chapter, whereas that of the pine plantations will be treated in the following chapters. A summarising discussion will be presented in Chapter 9.

There is very little hydrological or micro-meteorological information available on natural grasslands in the humid tropics. Yet the need for such data is growing as large areas of semi-unproductive grassland are being converted to plantation forest for wood production (Evans, 1992), whereas at the same time natural forests are being converted to pasture land at a high rate, particularly in Latin America (Whitmore, 1990). .

The changes in microclimate associated with land-use conversion (*e.g.* reflected radiation, temperature, humidity) and soils (*e.g.* infiltration capacity; Shukla *et al.*, 1990) will certainly affect evapotranspiration (ET) and the water yield. In areas where rainfall is highly seasonal the distribution of streamflow over the year may change as well, leading to flooding and erosion in areas where the grassland is overgrazed and regularly burned (Andrus, 1986; Bruijnzeel, 1990). and to shortages of water during dry periods after afforestation of such areas (Kammer and Raj, 1979; van Lill *et al.* 1980; Schulze and George, 1987),

There are several factors (*e.g.* net radiation, soil moisture availability, vegetation surface characteristics) that affect ET by vegetation. During the growing season, if soil moisture is not limiting, water use will depend largely on the available energy. Due to the difference in albedo of grasslands (0.16–0.26) and of coniferous forests (0.05–0.15; Arya, 1988) amounts of the available energy will be higher above the forests than above grasslands and forest transpiration rates could therefore be higher than those of grassland under similar climatic conditions. In addition, the higher aerodynamic roughness of forests as compared to grassland results in more efficient vapour transport, especially during rainfall events when the energy for evaporation is supplied by advective cooling of the air mass just above the vegetation rather than

by radiation (Rutter, 1967; Pearce *et al.*, 1980). As such, interception of rainfall by forests should be significantly higher than that by grass (Calder, 1979, 1982; Schulze and George, 1987), also because (particularly coniferous) forest tend to have larger leaf surface areas than grassland (Jarvis *et al.*, 1976; McWilliam *et al.*, 1993) . However, no data is yet available on rainfall interception in tropical grasslands. The nearest, perhaps, is the study of rainfall interception in sugar cane in Brazil by Leopoldo *et al.* (1981) who reported an average value of 4% of incident rainfall.

When the climate is seasonal, the grassland vegetation will exhibit a pattern of growth and dieback (which may be genetically rather than just climatically controlled) coinciding with variations in the moisture content of the topsoil where the root density is largest. In the course of the dry season, when topsoil moisture levels drop to wilting point, the above-ground portion of the grassland vegetation dies and the underground parts remains dormant until the start of the next wet season. Naturally, transpiration will be low during the dormant season due to the reduction in the transpiring leaf area, whereas evaporation from the soil is prevented by the isolating capacity of the dead standing crop and litter layer. As the rooting depth of pine trees (1–10 m, Kammer and Raj, 1979) is much larger than that of the grass (<1 m) forest transpiration can be sustained for much longer periods of time during the dry season, even when topsoil moisture levels have dropped below wilting point (Edwards, 1979; Schulze and George, 1987).

The combination of all these factors suggests that higher annual ET rates may be expected for pine forests than for grasslands. In the following I will briefly review the available evidence from the literature on tropical grasslands and effects of afforestation.

The available studies comparing the water use of grassland to that of forest in the tropics deal with man-made pasture lands in Amazonia (Bastable *et al.*, 1993; Wright *et al.* 1992), annually burned grasslands in the Philippines (Baconguis and Jasmin, 1984; Dano, 1990) or grasslands at higher altitudes in Africa (Focan and Fripiat, 1953; Bailly *et al.*, 1974; Blackie, 1979). These studies all considered short grass (height <1 m) which renders their results less applicable to the taller grasslands found in Fiji. Several of these studies were carried out in small catchments and in some cases leakage must have been considerable, leading to unrealistically high ET values (*e.g.* in the Philippine case). Variations in soil type, seasonality of the climate and grass species further complicate the prediction of water use by grass.

Wright *et al.* (1992) calculated the evapotranspiration from regularly burnt pasture land in a large 12-year-old rainforest clearing in Central Amazonia, Brazil, using micro-meteorological techniques. The ground cover consisted for 85% of grass and for 4% of tree stumps and bushes whereas 13% of the soil was bare. Grass height averaged 28 cm and the leaf area index (LAI) was 1.2 m^2 m^{-2}. ET rates were obtained for a 35-day period which included a dry period of 20 days during which soil moisture stress occurred, although this did not result in dying of the grass. Average ET rates decreased from 3.8 mm day^{-1} shortly after a rainfall event to 2.1 mm day^{-1} after 20 dry days with the ratio of ET/E_0 decreasing from 0.7–0.8 in the beginning to 0.5–0.6 for conditions with increasing moisture stress. The surface resistance increased from 150–180 m s^{-1} shortly after rainfall to 240–330 m s^{-1} at the end of the 20 dry days.

Baconguis and Jasmin (1984) measured the streamflow from a 0.95 ha grassland drainage basin in Luzon, the Philippines, over a period of 8 years. The average annual precipitation input was 3129 mm with a corresponding runoff of only 567 mm. This would imply the very high annual ET value of 2561 mm and basin leakage can therefore not be excluded (Bruijnzeel, 1990).

Blackie (1979) monitored rainfall inputs (2062 mm) and streamflow outputs (1008

mm) from a 37 ha highland catchment (catchment M, 2400 m a.s.l.) in Kenya which was covered by grass (*Pennisetum clandestinum*, 33%), bamboo (47%) and a pine plantation (13%) from 1966 to 1973. He reported an average annual ET of 1054 mm over this period compared to an E_0 of 1513 mm.

In the warm-temperate and less humid environment of South Africa, Van Lill *et al.* (1980) reported on a paired catchment study where decreases in streamflow of 300–380 mm year^{-1} were observed on a total rainfall of 1100–1200 mm after the conversion of (pasture) grasslands on shallow soils to *Eucalyptus grandis*. The effect of afforestation on streamflow became apparent in the third year after planting, and the decline in streamflow reached a maximum in the fifth year after planting and remained fairly constant thereafter. The dry season winter flows were reduced by some 100–130 mm and soil moisture storage was not sufficient to meet evaporative demands in this period. These reductions in water yield were comparable to those observed after afforestation with pine species elsewhere in South Africa (Van Wijk, 1977). Bosch (1982) showed that ET from former grasslands areas afforested with pines in South Africa increased with age of the forest, with maximum increases of 300–450 mm year^{-1} at age 15–25 years. The effect of afforestation was largest on low flows and reductions of around 50% were observed in catchments planted to *Pinus radiata* (Banks and Kromhout, 1963) and *Pinus patula* six to eight years after planting (Bosch, 1979). In a paired catchment study involving small (<40 ha) *Themeda triandra* grassland catchments with shallow soils which were planted to *Pinus patula*, *Pinus radiata* and *Eucalyptus grandis* Smith and Scott (1992) observed reductions of 40 to 60% in low flows after afforestation with pines within 6–8 years after planting. Even higher reductions (90–100%) were observed for the catchments planted to eucalypts, indicating that the water use is also species dependent, at least during the first eight years after planting.

Bosch and Hewlett (1982) reviewed 94 catchment studies world-wide in terms of effects of afforestation and deforestation on water yield. They concluded that water yield reductions after afforestation increased with increasing annual rainfall totals, as well as with the growth rates (age) of the forest.

The only available study on the effect of converting grasslands to *Pinus caribaea* forest in Fiji is the work of Kammer and Raj (1979) However, the study was based on incidental measurements of minimum flows made in the Varaciva, Teidamu and Vitogo catchments between 1969 and 1979, rather than a rigorous comparison of catchment water yield. The forest cover of the Teidamu catchment (55.4 km^2, elevation 10–600 m a.s.l.) increased from less than 10% in 1969 (very young pines) to 60% in 1978, which corresponded with a decrease in minimum flows in the order of 50%. The Varaciva catchment (29.6 km^2, elevation 60–600 m a.s.l.) was completely under forest in 1979 (6–7 year old pines) and a reduction of 65% had been observed for the minimum flows after 1974. Total rainfall measured in the adjacent lowlands at Drasa between April 1978 and December 1979 was 45% below average and minimum flows in the Vitogo catchment (46.9 km^2, only 10% forest cover) decreased as well, particularly from October 1977 onwards. However, as the rate of decrease in minimum flows from the Vitogo catchment was less pronounced than those observed for the Varaciva and Teidamu catchments, the below-average rainfall in 1978 and 1979 will have accounted for only part of the reduction in the minimum flows in the forested catchments.

In the following the water use of a *Pennisetum polystachyon* grassland during the dry season of 1991 will be discussed.

5.2 Field Instrumentation and Methods

Dry season ET of the Nabou grassland was evaluated by:

1. The soil water depletion method at times with a divergent zero-flux plane (Cooper, 1979; Wellings and Bell, 1980)
2. The Penman-Monteith evapotranspiration model (Monteith, 1965)

Daily rainfall (9:00 h) was measured with a standard gauge at Nabou station situated some 100 m from the site. No attempts were made to measure rainfall interception from grassland due to time and material constraints. However, as detailed in Section 5.5, an attempt was made to model this component.

A capacitance soil moisture probe (Didcot Instruments Co. Ltd.) was used to measure profiles of **volumetric soil moisture content** (θ). Two access tubes (G1 and G2) were installed 6 m apart to a depth of 1.2 m on March 28 and April 24, 1991 respectively. Both tubes were installed carefully to avoid damage to the surrounding grass but in order to gain access to the tubes it was inevitable that some of the surrounding grass had to be removed. Details of the measurement procedures and probe calibration are given in Appendix 24. Soil moisture profiles at 2 cm depth intervals were frequently measured (*e.g.* at least once a week) until October 4, 1991. ET was calculated as the total soil moisture loss above a divergent zero flux plane during periods without drainage (Cooper, 1979; Wellings and Bell, 1980). For this the following conditions had to be met:

- No redistribution of moisture within the profile
- Development of a zero flux plane (as indicated by zero moisture loss)
- No significant rainfall between two consecutive measurements

Small amounts of rainfall (amounts <4 mm between two consecutive measurements were found not to influence the moisture profiles) were added to ET as all of this would have been intercepted by the grass cover and litter layer.

A ceramic cup tensiometer was installed close to access tube G1 on June 18 with the cup at a depth of 20 cm to provide information on **soil moisture tension** in the topsoil. The soil moisture tension was read regularly with an electronic pressure transducer connected to a hypodermic needle which was inserted into the tensiometer through a rubber septum. Soil moisture tensions could be measured in this way to the nearest cm up to a tension of 900 cm H_2O (pF= 2.9).

Wet season micro-meteorological measurements were made in a grassland site of limited areal extent on a ridge top close to the Oleolega catchment (Figure 3.4) between January 30 and April 12, 1991. A meteorological mast was erected and equipped with the following instruments.

Solar radiation ($R_s \downarrow$) was measured at 4.65 m above the soil surface with a pyranometer (Skye Instruments Ltd. SP-1110) mounted on a support arm extending 0.8 m from the mast. Care was taken that the instrument was placed horizontally and that the shadow of the mast could not interfere with the measurements. Calibration of the pyranometer by the manufacturer referred to solar radiation in the 300–3000 nm waveband, with absolute errors <5% and typically much better than 3%.

The **incoming and reflected ($R_s \uparrow$) radiation** in a waveband of 300–2500 nm were measured with an albedometer (Kipp & Zonen, Model CM-7). The albedometer was placed level at 4.25 m above the soil surface on a 1–m boom extending from the mast in such a way that the shadow of the mast would not interfere with the $R_s \downarrow$ measurements. Both sensors were recalibrated as the instrument had been damaged

during the passage of cyclone Sina. The upward facing sensor was recalibrated against the pyranometer from January 30 until February 18. Reflected radiation measurements were made until April 9 when the albedometer was inverted until April 12 for calibration of the $R_s \uparrow$ sensor against the pyranometer.

The **soil heat flux** (G) was measured with a soil heat flux plate (Middleton & Co. Pty. Ltd.) placed 2 cm below the soil surface. Care was taken not to disturb the vegetation above the flux plate during installation. The accuracy of the plate was 5%. However, as the soil heat flux is spatially very variable, soil heat flux values may be in error of up to 100%.

Air temperature and **relative humidity** were measured at a height of 4.7 m with a Rotronic temperature and humidity sensor (Rotronic A.G., MP100F) equipped with a dust filter. The probe was placed in a Gill radiation screen (model 41004-5) and extended some 60 cm from the mast. The temperature was measured with a platinum resistance thermometer (PRT) with a measuring range of -40 to 60°C and an accuracy better than 0.2 °C. The long-term stable precision of the PRT was 0.1 °C. The humidity sensor had a range of 0–100% with an accuracy better than 1% and a long term stable precision of 0.5% of the relative humidity. However, at relative humidities above 97% very small changes in temperature could cause condensation on the humidity sensor and readings would not have the normal accuracy. Apparent relative humidities in excess of 100% were experienced during rainfall and at night. When this occurred the relative humidity was set at 100%.

Wind speed was measured at 5.0 m with a cup anemometer (Vector Instruments, A101M/L) mounted on a support arm pointing towards the main wind direction (SE). The anemometer has a stalling speed of 0.15 m s^{-1} and could measure wind speeds of up to 75 m s^{-1}. The accuracy was 1–2% of the wind speed according to calibration graphs. No corrections were made for overspeeding or stalling.

Wind direction was measured with a potentiometer type windvane (Vector Instruments, W200P) placed on top of the mast (5.2 m) from February 18 onwards. The fin movement of the windvane had a treshold at 0.6 m s^{-1} and an accuracy of $\pm 1°$. The resolution was 0.3°. As it was difficult to align the arrow on the windvane exactly to the true North, a systematic error of some 5° might have been introduced.

Soil temperatures were measured close to the heat flux plate with two thermistors (Campbell Scientific Ltd. 107B) placed at 2 cm and 10 cm below the soil surface. The accuracy of the thermistors was typically better than 0.2 °C.

All instruments were connected to a Campbell 21X micrologger (Campbell Scientific, Inc.). Measurements were made every 15 seconds and averaged over 15 minutes. The 15-minute averages and standard deviations were temporarily stored on a Campbell Scientific SM726 storage module and later transferred to floppy disk.

Dry season micro-meteorological and hydrological measurements were made in the grassland plot near Nabou station from May 10, 1991, when the grass started to die off, until September 21 when most of the grass had died.

Short-wave radiation was measured by an actinograph (SIAP, type SO-2870), which had been calibrated against the pyranometer, placed at a height of 5.5 m above the soil surface. However, as the calibration of the actinograph proved to be troublesome, the measurements of the Skye pyranometer, which in the meantime had been installed above a mature pine forest 4 km SW of the grassland (Koromani forest plot), were used in the calculations of evapotranspiration. Data from the actinograph were used for the period August 23–26 when all micro-meteorological data were lost in the Koromani forest plot due to a power failure. The 30-minute averages of $R_s \downarrow$ as

measured with the pyranometer were averaged to obtain 2-hourly averages.

The **net radiation** (R_n)is defined as the sum of incoming long-wave and short-wave radiation minus the sum of outgoing long-wave and short-wave radiation (Section 7.5.2, Equation 7.8). The net radiation is usually positive during the day when the solar radiation component dominates, and negative at night (no short-wave radiation) when the terrestrial long wave radiation is dominating (Brutsaert, 1982). R_n was measured above the grass on four days in June and July with a portable net radiation indicator (C.W. Thornthwaite Associates, model 603), which was calibrated against the net radiometer (Radiation and Energy Balance Systems) mounted next to the pyranometer at the forest site. Manual readings of R_n in the grassland were taken every 15 minutes from 9:00 h until 18:00 h at a height of 2.2 m.

Temperature and **relative humidity** were measured at a height of 5.5 m with a thermo-hygrograph (Lambrecht, type 252-Ua) housed in a Stevenson screen. The weekly temperature and relative humidity charts were processed to obtain two-hourly averages. Temperatures given by the thermo-hygrograph were calibrated against a station thermometer and against minimum and maximum thermometers (Lambrecht) housed in the same screen. The relative humidity readings of the instrument had been calibrated earlier against humidity measurements by the Rotronics in the Tulasewa forest plot.

Wind speed and **direction** were measured at a height of 5.9 m with a mechanical wind recorder (Lambrecht GmbH). Hourly averages of wind speed and direction were averaged to two-hourly means.

An automatic porometer (Delta T Instruments, model MK3) was used to determine half hourly values of **stomatal resistance** (r_{st}) of water stressed grass leaves at three levels in the canopy. Measurements were made on four days between June 18 and July 23, 1991 from 9:00–10:00 h until 19:00 h. No early morning measurements could be made due to the presence of dew on the grass leaves. The grass canopy was divided into three levels, a lower level from 0–0.7 m, a middle level from 0.7–1.4 m and an upper level from 1.4–1.8 m. The stomatal resistances of five marked leaves within each level were measured at 30–60 minute intervals. Water stress causes a gradual increase in the daytime stomatal resistance up to a point where all stomata are closed as the soil moisture status approaches wilting point (Rutter, 1975). The grass had experienced severe water stress before June 18 and was dying as indicated by the presence of many yellow leaves on the plants. Most remaining green leaves above a level of 1.4 m in the canopy had yellow tips. The vegetation deteriorated fast as the dry season progressed and on July 23 it was very difficult to find any fresh leaves at all above a height of 1 m, whereas most of the leaves below this level had turned yellow or were dead. No attempts were therefore made to measure r_{st} after this date.

The porometer was calibrated at the beginning of each measurement cycle using a calibration plate with known diffusion resistances. The relative humidity range of the porometer was set as close to the actual relative humidity as possible. Stomatal resistances were calculated from the porometer transit times (counts) following the procedure described by Monteith (1988). However, the constants for the extremes of the calibration plate as used by Monteith (1988) were not included in the regressions of transit time on diffusion resistance as they often deviated considerably from the measured values. The actually measured transit times for these extremes were used instead.

The surface resistance (r_s) characterizes the physiological control of water loss by the vegetation and depends on the bulk stomatal resistances of the individual leaves and on the area of the transpiring surface as represented by the leaf area index (LAI)

Table 5.1: *Long-term average monthly rainfall totals (1980–1991) and monthly rainfall totals (mm) for the dry season of 1991 recorded at Nabou station.*

	Mar	Apr	May	Jun	Jul	Aug	Sep	Oct	Total
Nabou, 1991	183	108	27	25	56	60	152	80	691
Nabou, 1980-1991									
Average	240	162	78	72	57	67	74	80	830
Std.Dev.	164	133	107	61	38	48	53	50	

with r_s approximately equal to r_{st}/LAI (Rutter, 1975) . The stomatal resistance depends on several meteorological parameters (*e.g.* radiation, vapour pressure deficit) as well as on the availability of moisture in the soil. When the vegetation is wet, evaporation occurs directly from the leaf surfaces and r_s is zero (Monteith, 1965). When soil moisture is not limiting, stomatal resistances exhibit a diurnal pattern with high nighttime resistances (stomata closed) and low daytime resistances (stomata opened) with a minimum around noon.

5.3 Grassland Hydrology

Monthly rainfall totals for the dry season of 1991 and long-term monthly averages and standard deviations (1980–1991) for Nabou station are shown in Table 5.1. Rainfall totals in 1991 were below the long-term means from April until June and very close to those for July and August. September experienced much higher rainfall than the long-term mean, but all rainfall occurred in the second week of the month (Figure 5.2). Total rainfall between March 29 and October 4 amounted to 428 mm which was 16% below the long-term mean for this period (510 mm).

Estimates of grassland evapotranspiration for selected periods during the dry season were obtained from repeated measurements of soil moisture profiles (ET_{sm}). Three soil moisture profiles, as measured with the capacitance probe in access tubes G1 and G2 on July 8, August 12 and August 19, are shown in Figure 5.1. Similar profiles were observed throughout the study. The July 8 profile was measured two days after a rainy period during which 52.3 mm of rainfall was recorded. The soil moisture tension at a depth of 20 cm was 64 cm H_2O (pF= 1.8). Only little rainfall (3.4 mm on July 27) was recorded until August 17 and the soil dried out accordingly as shown by the profile measured on August 12. The tension in the topsoil increased to values above 1000 cm H_2O (pF= 3) after July 29. Another 59.9 mm of rainfall was recorded between August 17 and 19 resulting in increased θ levels as illustrated by the August 19 profile. The corresponding tension at this date was 56 cm H_2O (pF= 1.7). It is clear from Figure 5.1 that soil moisture fluctuations in the root zone (0–65 cm), where moisture is removed by both evapotranspiration and drainage, are much larger than those below the root zone where moisture is removed by drainage only. Figure 5.2 shows the time series of the average moisture content within and below (65–110 cm) the root zone for access tubes G1 and G2 and the corresponding daily rainfall amounts. The average range in θ was 0.056($\pm$0.030) m^3 m^{-3} in the root zone and 0.037($\pm$0.007) m^3 m^{-3}

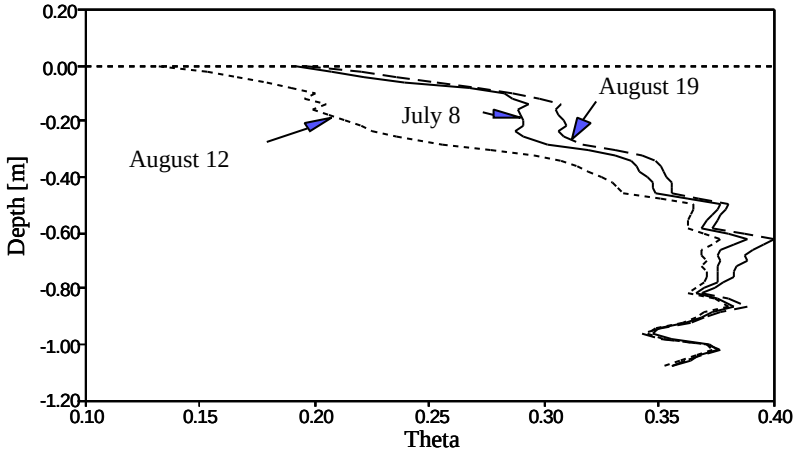

Figure 5.1: *Changes in grassland soil moisture profiles at Nabou during the dry season of 1991 in response to rainfall and drought.*

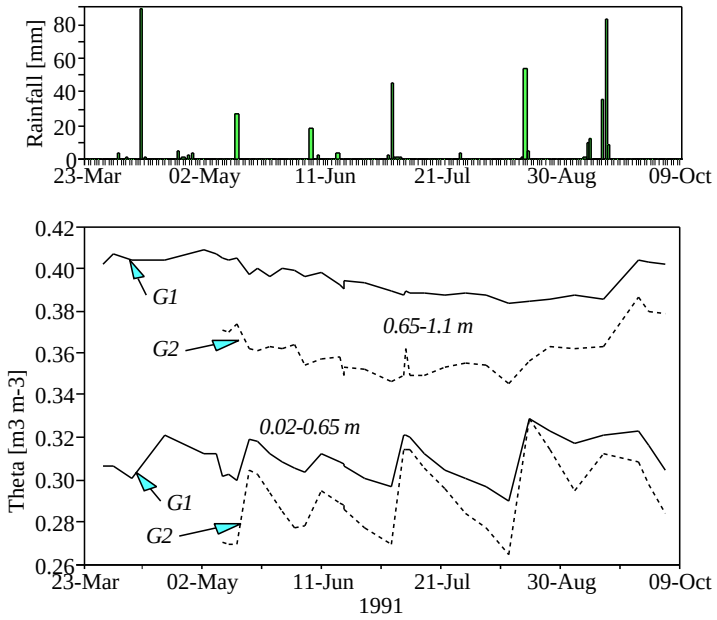

Figure 5.2: *Daily rainfall amounts and changes in θ with time as measured within (2–65 cm) and below the root zone (65–110 cm) in the Nabou grassland plot during the dry season of 1991.*

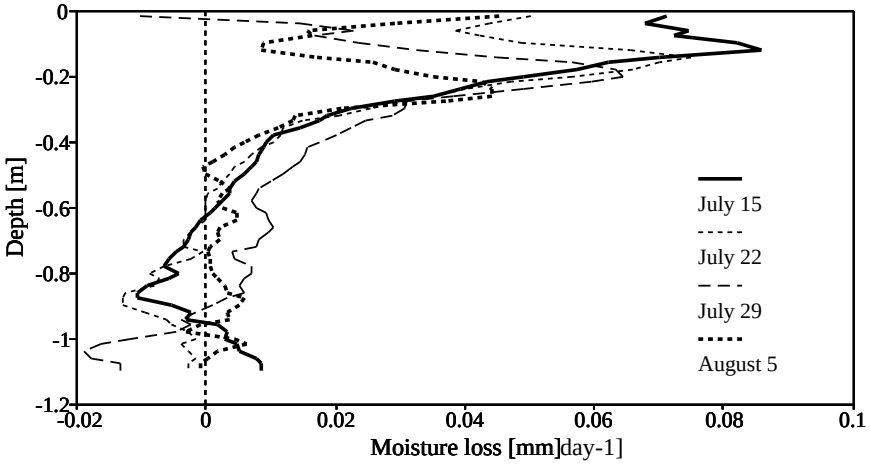

Figure 5.3: *Profiles of moisture loss from the Nabou grassland soil during four consecutive dry weeks in the dry season of 1991.*

below the root zone. The range in θ was largest in the upper 25 cm of the soil where the largest concentration of roots occurred. Soil moisture levels below the root zone showed a gradual decrease from May until August with only small fluctuations in response to rainfall, and increased again to wet season levels after large showers occurred in August and September. The slow changes observed in the moisture profiles below the root zone were consistent with the low unsaturated hydraulic conductivity of this zone (Section 4.3.3).

Soil moisture depletion profiles were calculated from the change in θ between consecutive measurements for each 2 cm depth interval. The change in θ was converted to depths of water (mm) by multiplication with the length of each interval (20 mm) and dividing by the time (in days) between measurements to obtain a moisture loss in mm day^{-1}. The loss was considered positive when moisture was removed and negative when moisture was added. Figure 5.3 shows several moisture loss profiles for the dry period between July 10, shortly after rainfall occurred, and August 5. As indicated earlier, the only rainfall (3.4 mm) within this period occurred on July 27. Throughout the study period similar profiles were observed during dry weather. Moisture losses were close to zero between 50 and 70 cm and a zero flux plane was considered to have developed around a depth of 65 cm. Whenever such a zero flux plane was present all moisture transport above this level was considered upwards as a result of evapotranspiration. Fluxes of moisture below this level were considered downwards as a result of drainage (Cooper, 1979; Wellings and Bell, 1980. The total amount of moisture removed by evapotranspiration (ET_{sm}) was calculated as the sum of the losses for each 2 cm interval above the zero flux plane. As the soil dried the level at which the maximum loss occurred moved downwards from 14 cm on July 15 to 26 cm on August 5. The loss from the upper few cm of soil became negative on July 29 in response to rainfall on July 27. The resulting increase in θ caused a higher moisture loss at this depth during the following week (August 5).

Divergent zero flux planes developed on 59 days around access tube G1 and on 91 days around access tube G2. The resulting average ET_{sm} rates were 0.7($\pm$0.2)

mm day^{-1} and 1.1(±0.3) mm day^{-1} respectively. The average ET_{sm} rate for both tubes therefore amounted to 0.9(±0.2) mm (n=59).

It is not known to what extent the removal of grass on one side of the access tubes has influenced the rates of ET_{sm}. However, the depth of the observed zero flux planes corresponded well with the rooting depth of the grass and the root system surrounding the tubes may not have been affected too much. The high spatial variability of the measured ET_{sm} rates indicated that the presently obtained values may well be several tenths of mm's in error.

5.4 Grassland Micro-meteorology

The temporal resolution of evaporation estimates via hydrological methods is often low, ranging from about 1 day when in the case of soil moisture measurements to a season or year for catchment water balance studies (Ward and Robinson, 1990). The zero flux plane method gave ET_{sm} values for selected dry periods only and the temporal resolution depends therefore on the time elapsed between consecutive soil moisture measurements, which was in the order of a week during the present study. The resolution of micro-meteorological methods is much higher and depends largely on the sample frequency of the necessary meteorological parameters. However, micro-meteorological methods have their own flaws as their use is more or less restricted by the underlying theory which applies for "ideal terrain" only (*e.g.* flat, homogeneous terrain with a large fetch; Thom, 1975). In addition, it is difficult to derive surface dependent parameters as roughness length, displacement length, aerodynamic resistance and surface resistance without an elaborate micro-meteorological set-up (Shuttleworth, 1988). As such a set-up was not feasible for the grassland study, several assumptions had to be made with respect to surface characteristics to calculate daily evapotranspiration rates with the Penman-Monteith model.

5.4.1 Radiation and Soil Heat Fluxes

Daily short-wave radiation totals at the Oleolega catchment site averaged 20.10 (±4.26) MJ m^{-2} day^{-1} in February and 18.58 (±4.98) MJ m^{-2} day^{-1} in March, with corresponding reflected radiation totals of 3.61 (±0.74) MJ m^{-2} day^{-1} and 3.47 (±0.92) MJ m^{-2} day^{-1}. The mean diurnal variations in incoming and reflected short-wave radiation in March are shown in Figure 5.4. Similar patterns were observed in February.

Daily average values of wet season albedo were 0.180 (±0.008) and 0.187 (±0.007) for February and March, respectively. These values are similar to reflection coefficients derived for Amazonian pasture (0.163; Bastable *et al.*, 1993) and various West African savannas (0.17–0.22: Oguntoyinbo, 1970; 0.17–0.20: Montény and Gosse, 1976). The diurnal variation in albedo was calculated from 15-minute daytime averages ($R_s \downarrow$>100 W m^{-2}, n= 2730) of $R_s \downarrow$ and $R_s \uparrow$ and is shown in Figure 5.5. The treshold value of 100 W m^{-2} coincided with an average solar altitude of 16°, whereas elevation of the sun at noon ranged from 90° on January 30 to 67° on April 4. The albedo averaged 0.181(±0.006) between 9 am and 5 pm and had a noon minimum of 0.175(±0.006). Early morning values of the albedo were very low, with a minimum of 0.13(±0.05) (n= 43) at 7:15 h, and increased to a maximum of 0.20(±0.08) (n= 65) at 8:30 h (Figure 5.5). The diurnal pattern showed a typical dish shape from 8:30 h onwards. Similar early morning variations were observed by Oguntoyinbo (1970) for grasslands

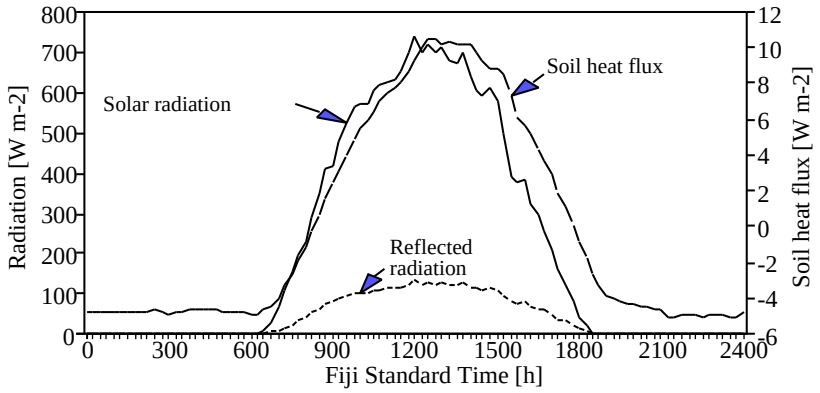

Figure 5.4: *Mean diurnal patterns of solar radiation, reflected short-wave radiation and soil heat flux at the Oleolega catchment in March 1991.*

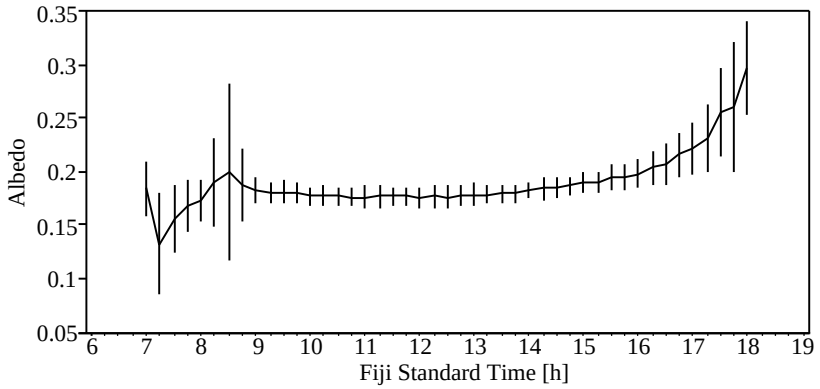

Figure 5.5: *Diurnal course of the albedo for grassland at the Oleolega catchment during the wet season of 1991.*

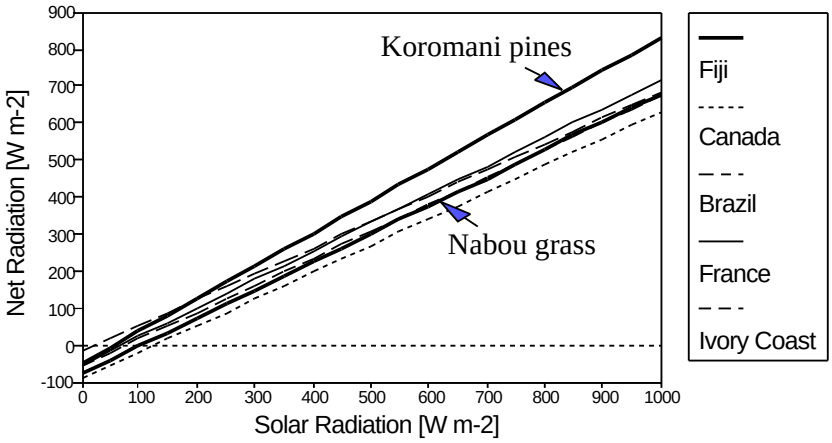

Figure 5.6: *Regressions of daytime* $R_s \downarrow$ versus *on* R_n *for grasslands in the temperate zone and in the humid tropics. The regression line calculated for the Koromani pine forest is shown for comparison.*

in Nigeria, who suggested that dew deposition on the leaf surfaces might reduce the reflectivity by trapping radiation. The grasslands in Nabou were often wet in the early morning due to the deposition of dew and the relatively large standard deviations observed between 8:15 h and 8:45 h could therefore be explained by the changes resulting from the transition from a wet surface to a dry grass surface.

An empirical relation (Equation 5.1) was established between daytime R_n measurements made above grass and corresponding $R_s \downarrow$ measurements near the Koromani forest plot using linear regression analysis. The data set consisted of 26 half-hourly radiation averages collected under clear sky conditions with $R_s \downarrow$ ranging from 86 W m^{-2} to 760 W m^{-2}. The corresponding R_n values ranged from -19 W m^{-2} to 474 W m^{-2}.

$$R_n = -77.7(\pm 27.2) + 0.76(\pm 0.03) R_s \downarrow \qquad \text{n= 26, } r^2 = 0.98 \tag{5.1}$$

The regression line is shown in Figure 5.6 together with those published for other tropical grasslands in Ivory coast (Montény & Gosse, 1976), Central Amazonia (Bastable *et al.*, 1993) and temperate sites in Canada (Ripley & Redman, 1976) and Southern France (Pers. comm. N.J. Bink), despite the fact that observations at the other sites pertained to much shorter grass, and although the presently obtained regression constants were calculated from relatively few clear sky measurements of R_n and $R_s \downarrow$, they fall within the range of those published for the other grassland sites adding confidence to the results. Equation 5.1 was therefore used to calculate R_n for grassland at Nabou during the dry season of 1991 from half-hourly averages of $R_s \downarrow$ measured above Koromani forest. The regression line for a nearby mature pine forest (Koromani forest, Section 7.5.2) is shown in Figure 5.6 to illustrate the difference between the two vegetation types.

Daily totals of the heat flux into the soil (G) amounted to 0.02($\pm$0.10) MJ m^{-2} day^{-1} and -0.00$\pm$0.10 MJ m^{-2} day^{-1} in February and March, 1991, respectively, with

Table 5.2: *Ranges and averages (standard deviation between brackets) of minimum and maximum temperature (°C) and relative humidity (%) measured above the Nabou grassland plot during the dry season of 1991 (n is the number of days).*

	T	Tmin	Tmax	n	RH	RHmin	RHmax	n
Range	19.0-25.9	11.7-24.9	20.9-32.9	127	61-98	42-90	61-100	124
Average	22.5 (1.6)	17.9 (3.0)	28.2 (1.9)	127	83 (6)	59 (9)	98 (6)	124

a minimum value of -0.25 MJ m^{-2} day^{-1} and a maximum of 0.22 MJ m^{-2} day^{-1}. The soil heat flux was low compared to the radiation inputs and the positive value in February indicated a net warming up of the soil. The observed minimum and maximum values of G were -13.9 W m^{-2} and 19.1 W m^{-2}. It was not possible to measure G during the dry season (because the instruments were in use at the Koromani site by then), and a relationship was established between 15-minute averages of daytime solar radiation ($R_s \downarrow > 50$ W m^{-2}) and corresponding values for G, measured in February and March:

$$G = -1.24(\pm 3.15) + 0.015(\pm 0.002) R_s \downarrow \quad \text{n= 2802, } r^2 = 0.65 \tag{5.2}$$

Although it is very likely that the regression constants will show a seasonal variation with positive monthly soil heat flux totals during the wet season (warming up of the soil) and negative totals during the dry season (cooling down of the soil), the variation will presumably be small in densely vegetated grassland areas where there is no direct radiation on the soil. Hence Equation 5.2 was used to calculate dry season values of G.

5.4.2 Temperature and Humidity

Diurnal patterns in temperature and humidity above the Nabou grassland plot were similar to those shown in Section 2.4.2 for Nadi. As the establishment of forest plantations is likely to alter the temperature and humidity regimes average dry season minimum and maximum temperatures and relative humidities will be presented in this section, whereas those measured above Koromani forest during the same period are presented in Section 7.4. The averages and ranges of the temperature and relative humidity at the Nabou grassland site are given in Table 5.2

5.4.3 Wind speed and Direction

Windspeeds during the dry season were low with a mean of 2.1(±0.9) m s^{-1}. The maximum 2-hourly average of recorded wind speed was 7.2 m s^{-1}. Wind speeds were usually even lower at night (1.2(±0.8) m s^{-1} between 18:00 h and 6:00 h) and increased during daytime (2.9(±1.1) m s^{-1} between 6:00 h and 18:00 h). The wind direction was predominantly southeast.

5.4.4 Surface Resistance and Derived Estimates of Evapotranspiration

To derive daily ET rates for the grassland, use was made of the Penman-Monteith equation (Monteith, 1965):

$$\lambda ET = \frac{\Delta(R_n - G) + \rho c_p \, \delta e / r_a}{\Delta + \gamma(1 + r_s/r_a)} \tag{5.3}$$

where ρ and c_p represent the density and the specific heat of air, respectively, δe the vapour pressure deficit, Δ the change of the saturation vapour pressure with temperature and γ the psychrometric constant. Formulas for their calculation have been presented in Appendix 22.2. ET_{sm} was taken as a reference to derive representative values for the surface (or canopy) resistance r_s, which was thought to increase with the progress of the dry season as a result of the dying off of the grassland vegetation.

The aerodynamic resistance (r_a, in s m^{-1}) was calculated from wind speed measurements using Equation 5.4 (Thom, 1975) which holds under neutral atmospheric conditions.

$$r_a = \frac{\left(\ln \frac{z-d}{z_0}\right)^2}{k^2 \cdot u_z} \tag{5.4}$$

In this equation z represents the heigth of the wind speed measurements (5.9 m), z_0 and d are surface roughness parameters, k is the von Karman constant (taken as 0.4) and u_z is the wind speed as measured at height z. The surface roughness parameters (z_0 and d) depend on the height, density and flexibility of the vegetation and are usually obtained from above-canopy wind profiles (Thom, 1975). However, these were not available for the grassland during the present study and the roughness length (z_0) and the displacement length (d) were estimated using empirical expressions relating z_0 and d to the average height of the vegetation (h). The ratio of z_0 to h ranges from 0.02 to 0.2 (Garratt, 1977) and was taken as 0.12, whereas the ratio of d to h averages between 0.7 and 0.8 for most vegetative canopies (Arya, 1988) and was taken as 0.75. The average grass height decreased from 1.9 m in May to 1.2 m in September and z_0 and d decreased correspondingly from 0.23 m and 1.43 m to 0.14 m and 0.9 m respectively.

Daily averages of r_{st} for the various levels in the canopy are shown in Table 5.3 together with the corresponding soil moisture tension. Although soil moisture was not really limiting on the days of measurement, as indicated by the pF values, mean daytime r_{st} values were high at 170–330 s m^{-1} above a height of 0.7 m and 1001–1522 s m^{-1} between ground level and 0.7 m. The stomatal resistances above a height of 0.7 m were relatively low on July 10, possibly in response to increased soil moisture levels (pF= 2.0) as a result of rainfall during the first week of July. The stomatal resistance varied considerably during the day (Figure 5.7) but showed no correlation (r^2= 0.01) with irradiance, as illustrated in Figure 5.8, nor with any other micro-meteorological parameter (*e.g.* vapour pressure deficit). This inability of the stomata to respond to changes in microclimate is not surprising in view of the poor condition of the dying vegetation.

With little variation in daily means of r_{st}, LAI became the single most important factor determining the change in the magnitude of r_s during the dry season. The LAI decreased from 1.3 m^2 m^{-2} in May to 0.2 m^2 m^{-2} in September (Section 10.3) and daily LAI values were calculated with Equation 5.5, which was obtained by linear

Table 5.3: *Average stomatal resistances (s m^{-1}) of grass blades at various heights in the grass cover and those measured on needles of a nearby isolated pine tree. The pF represents the soil moisture tension at the time of the measurements, SD is the standard deviation.*

Date	June 18		June 25		July 10		July 23	
Time	9:30-17:30		10:30-18:30		10:30-18:00		11:30-18:00	
pF(20 cm)	2.6		3.0		2.0		2.6	
Grass	Avg	SD	Avg	SD	Avg	SD	Avg	SD
1.4-1.8 m	214	76	211	33	187	28	239	55
0.7-1.4 m	330	156	312	80	197	33	242	72
0.0-0.7 m	1246	553	1585	548	1674	1150	1239	443
Time			11:00-17:00		11:00-17:00		12:00-17:00	
Isolated pine tree			225	30	231	29	258	54

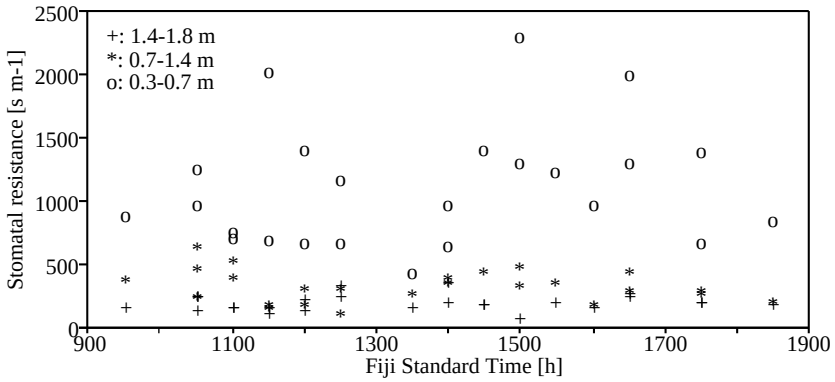

Figure 5.7: *Diurnal variation of r_{st} of grass leaves at different heights in the Nabou grassland plot during the dry season of 1991.*

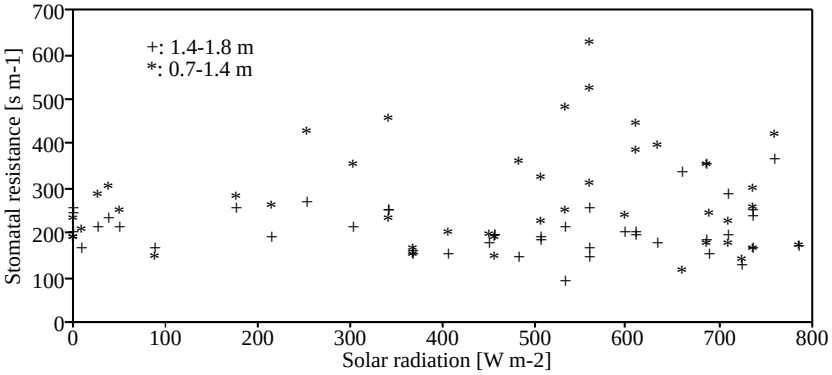

Figure 5.8: *Variation of r_{st} with solar radiation at the Nabou grassland plot during the dry season of 1991.*

regression analysis of the LAI data (n= 3) against julian day (JD).

$$\begin{aligned} \text{LAI} &= 2.5 - 0.009 * \text{JD} \\ \text{r}^2 &= 0.98,\ 130 < \text{JD} < 263 \end{aligned} \tag{5.5}$$

To smooth the transition from daytime (8:00–18:00 h) to nighttime (18:00–8:00 h) conditions (stomatal closure), nocturnal values for r_s were arbitrarily set at $1000 * e/e_{sat}$ and ranged from 500 to 1000 s m^{-1}. During rainfall events and shortly thereafter r_s was set to zero (Monteith, 1965).

Due to the difference in time resolution between the Penman-Monteith equation used in the present study (2 hours) and the soil water depletion method (several days) daytime values for r_s had to be derived by trial and error. Estimates of daytime r_s were inserted in the Penman-Monteith formula and the sum of the resulting 2-hourly ET_{pm} values over seven selected periods spanning 48 days were compared with the corresponding ET_{sm} values. The fitted r_s was low in May (79 s m^{-1} for the period May 20–24) and increased to values between 300 s m^{-1} and 400 s m^{-1} for August and September. Linear regression analysis using data on r_s and LAI for the selected periods resulted in Equation 5.6 which describes the relation between LAI and r_s for daytime conditions.

$$\begin{aligned} r_s &= 441(\pm 79) - 282(\pm 112) * \text{LAI} \\ \text{n= 7, r}^2 &= 0.56 \end{aligned} \tag{5.6}$$

Daytime r_s values for the dry season calculated with Equation 5.6 ranged from 76 s m^{-1} in May to 390 s m^{-1} in September.

Daytime r_s values for May and June, when the grass started to die off, were within the general range for grass (60–200 s m^{-1}) given by Rowntree (1990) and similar to the values reported by Wright *et al.* (1993) for Amazonian ranchland (160–330 s m^{-1} at LAI= 1.2). De Bruin *et al.* (1991) observed r_s values between 30 and 100 s m^{-1} for short (40 cm) irrigated grass in the South of France, whereas much higher values were observed in an adjacent non-irrigated area which was sparsely vegetated with herbs.

The high values presently derived for August and September are not unrealistic in view of the fact that most of the vegetation had died by then. The fit between ET_{sm}

and ET_{pm} for the selected periods was good with a difference of only 0.6% between total ET_{sm} and total ET_{pm} over 47 days. Daily ET_{pm} values were subsequently calculated for the period of May 11 until September 19 (131 days) using Equation 5.6. As the wind speed record was slightly shorter than that for the other meteorological parameters, wind speeds measured above Koromani forest were used for the missing period (6 days). The error introduced in this way was assumed negligible as wind speeds measured above grassland and forest were comparable. Total ET_{pm} for the 131-day period amounted to 127.7 mm (40% of total rainfall) and averaged 0.97(±0.34) mm day^{-1}.

The Penman open water evaporation (E_0, Appendix 22.2) was calculated from daily radiation totals and averages of temperature, relative humidity and wind speed. The ratio of actual sunshine hours to the day length (n/N) was calculated from the radiation record using the relations given in Section 2.4.3. E_0 amounted to 485 mm for the period under consideration (n= 131), with a daily mean of 3.7(±1.0) mm day^{-1}. Daily rainfall totals as well as changes in E_0, ET_{pm} (24-h totals) and ET_{sm} with time are given in Figure 5.9. The ratio of ET_{pm} to E_0 was low and decreased from 0.32±0.11 in May to 0.25(±0.12) in September with a minimum of 0.21(±0.09) in August. The decrease in ET_{pm}/E_0 was attributed to the gradual dying of the grass as the dry season progressed. The evapotranspiration rates presently found for grassland will be compared with those of the pine forests in Chapter 9.

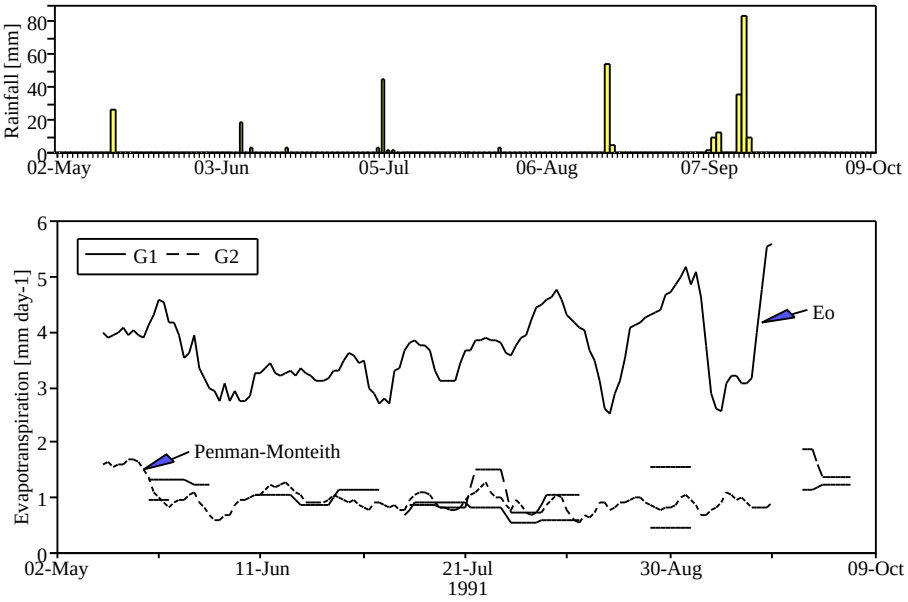

Figure 5.9: *Daily rainfall totals and the course of evapotranspiration in Nabou grassland with time during the dry season as based on soil water depletion rates, and the Penman-Monteith model. The Penman open water evaporation has been added for comparison (ET_{pm} and E_0 smoothed using 5-days moving averages).*

5.5 Modelling of Grassland Interception Loss

Like transpiration, interception of rainfall by grass and litter is likely to show a seasonal variation as well in correspondence with the seasonal changes in grass biomass and litter mass. An attempt was made to quantify the interception loss during the dry season of 1991 (May–October) from daily rainfall totals using the models described in Sections 6.4.1 (Gash analytical model; Gash, 1979) and 6.4.2 (This study).

The free throughfall coefficient (p) for grass was determined from gap fraction measurements (Section 10.3) and amounted to 0.79 (as measured 1 m above the soil surface). The grassland canopy storage (S) was assumed to be slightly lower than the post-cyclone value found for for Tulasewa forest (0.3, Section 6.4.1) which was heavily dominated by mission grass by then with only occasional trees remaining, and was set to 0.2 mm. 'Trunk' storage and the proportion of rainfall going to 'trunks' was set to zero. The evaporation rate from a saturated canopy was determined from the micro-meteorological measurements during rainfall using the Penman-Monteith equation (Equation 5.3) with r_s set to zero and amounted to 0.06($\pm$0.03) mm h^{-1}. The mean rainfall rate onto the saturated grass cover was determined using hourly rainfall data collected at Koromani forest and amounted to 2.13 mm h^{-1} implying an $\bar{E}/\bar{R}$ value of 0.03.

An estimate of the water holding capacity of the litter layer was obtained from litter samples collected in February 1991. The gravimetric moisture content of the litter was equal to the air-dry moisture content (14% of dry weight) on February 21, after 16 days without significant rainfall. At this stage the litter layer contained 0.1 mm of moisture. The gravimetric moisture content had increased to 161% on February 28, some 10 hours after rainfall had ceased. Since no visible drainage occurred from the litter upon sampling, this moisture content may have been close to the field capacity value with a storage equivalent of 1.7 mm. As such, a minimum of 1.6 mm of water may be available for evaporation after rainfall ceases during the wet season. Applying the above percentages of the maximum and residual moisture contents to the litter biomass observed in May resulted in maximum and minimum moisture contents of 1.0 and 0.1 mm respectively. The May values were used to represent the moisture storage characteristics of the litter layer during the dry season. Evaporation rates from the grassland litter layer were assumed to be equal to those in the forest (Section 6.4.2).

Total rainfall during the period of May 2 until October 1, 1991 amounted to 319 mm. Gash's analytical model predicted a throughfall of 306 mm resulting in an interception loss of 13 mm or 4% of total rainfall for the grass canopy. We have been unable to find comparative information on the interception of rainfall by grass in the tropics. However, the presently obtained value compares well with that measured for sugar cane (which, after all, is a domesticated form of a tall grass species) in Brazil (4.1 % of rainfall; Leopoldo *et al.*, 1981). Derived interception losses from the litter layer were higher than those for the live crop, amounting to 21 mm or 7% of total rainfall. The estimated combined interception loss therefore amounted to 34 mm or 11% of total rainfall. A discussion of the differences in interception losses from grassland and forest will be given in Chapter 9.

Chapter 6

Forest Hydrology

6.1 Introduction

A review of the literature dealing with hydrological effects of the the conversion of grassland to plantation forest has already been presented in the previous chapter. This chapter deals with the quantification of the fluxes of water through several pine plantations within the Nabou forest estate. Quantification of these fluxes is a prerequisite for the determination of the nutrient cycle (Chapter 13), as water forms a prime transport medium in this respect (Likens *et al.*, 1977). Considerable attention will be given to the estimation of interception losses, both from the canopy and from the litter layer. Furthermore, an attempt will be made to obtain forest evapotranspiration rates from changes in volumetric soil moisture contents.

6.2 Field Procedures and Methods

Hydrological measurements were made in the Tulasewa, Korokula and Koromani forest plots. The hydrological instrumentation was similar in each plot and the methods and instruments used are discussed below.

Rainfall stations were located in clearings or grassland close to each of the forest plots. Each station consisted of three manual gauges and a pluviograph, positioned such that there were no obstructions above a maximum angle of 30°. Any surrounding grass was kept short. The dates of installation and removal of the equipment are shown in Table 6.1. A standard rainfall gauge (Lambrecht) with an orifice of 100 cm^2 and a capacity of 150 mm was used as a reference for the calibration of the other gauges. The gauge was mounted on a standard at a height of 1.3 m above the soil surface. Rainfall intensity and duration were measured with a tipping bucket rainfall recorder (SIAP, UM- 8100) with a resolution of 0.4 mm (orifice 607 cm^2) and a temporal resolution of one hour. The pluviographs were placed at a height of 1–1.5 m above the soil surface. A custom-made rain gauge (100 cm^2 orifice) with a capacity of 410 mm was placed close to each standard gauge for calibration purposes. A small piece of filter wool in the outlet of the funnel prevented entering of organic debris and insects. The standard raingauge and the custom-made gauge were emptied at least once a week. The fourth rain gauge was used to collect rainwater samples for chemical analysis and consisted of a plastic funnel (orifice 471 cm^2, height 0.7 m) placed on top of a white PVC cylinder

Table 6.1: *Installation and removal dates of rainfall gauges, throughfall gauges and litter percolation trays in Tulasewa, Korokula and Koromani forests.*

Plot	Code	Rainfall		Throughfall		Litter percolate	
		Start	**End**	**Start**	**End**	**Start**	**End**
Tulasewa Forest	PU 20-2	28-Nov-89	30-Sep-91	30-Nov-89	30-Aug-91	22-Dec-89	30-Aug-91
Korokula Forest	PU 09-5	06-Jan-90	01-Oct-91	08-Jan-90	01-Oct-91	16-Jan-90	01-Oct-91
Koromani Forest	PU 09-4	18-Dec-89	02-Oct-91	23-Jul-90	02-Oct-91	24-Dec-89	02-Oct-91

acting as a radiation shield. The funnel drained into a second container of chemically inert plastic with a capacity of 210 mm of rainfall. The light conditions within the PVC container were low to diminish biological activity (*e.g.* growth of algea) in the collected rainwater. Contamination by insects or organic debris was avoided by a chemically inert 2 mm wire mesh on top of the funnel (coarse material) and a piece of filter wool in the funnel outlet (fine material). The funnel, the inner container and the wire mesh were rinsed with rainwater after samples were collected and the filter wool was renewed.

Throughfall was measured with twenty sharp-rimmed standard gauges in each plot. Their dates of installation and removal are shown in Table 6.1. All gauges were placed on the soil surface with the funnel at a height of 35 cm. The gauges were initially placed at randomly selected gridpoints within a 10 m by 10 m grid and were relocated randomly within a 5 m radius of a gridpoint after each measurement to optimize the representativity of the data (Lloyd and Marques-Filho, 1988). On several occasions not all throughfall gauges could be read due to disturbance by children, stray animals or wind (*e.g.* cyclones), and the average of the remaining gauges was then taken to represent the average throughfall.

Stemflow was measured from October 1990 until August 1991 in the Tulasewa forest plot only. Five trees were equipped with a spiral type PVC gutter after the bark had been removed locally. The gutter was connected to a 4.1 l plastic container. Stemflow volumes (ml) were converted to depths (mm) by dividing by the surface area occupied by each tree on the basis of the initial planting density (9 m^2). Due to the small size of the containers (4.1 l) overflow occurred when rainfall exceeded 16 mm and therefore no reliable estimates were obtained for larger storms.

Litter percolate was measured with four litter percolation trays in each plot. Dates of installation and removal are again given in Table 6.1. Each tray consisted of a shallow (3 cm deep) rectangular hard PVC box (area 2090 cm^2) covered with chemically inert wire mesh (1 mm mesh). Three openings on one side were connected at the downslope end of the plate by PVC tubing to a 4.1 l plastic container, placed in a hole dug into the soil. The trays were carefully inserted below the litter layer (L+F) at a low angle so that percolating water flowed into the container. Filter wool was placed underneath the wire mesh in front of the openings to prevent organic material from entering the container or blocking the tubing. Measurements were made at least once a week. Due to the small size of the container overflow occurred whenever rainfall amounts exceeded 30 mm.

The rainfall, throughfall, as well as small amounts of stemflow and litter percolate were determined with plastic measuring cylinders with a volume of 250 ml or 500 ml. The cylinders could be read with an accuracy of 2 ml (or 0.2 mm for rainfall

and throughfall). Larger amounts of litter percolate and stemflow (*e.g.* >2 l) were measured with a 2000 ml plastic measuring cylinder with an accuracy of 10 ml.

The Didcot capacitance soil moisture probe referred to in Section 5.2 was used to measure profiles of **volumetric soil moisture**. Five access tubes were installed in each plot during the dry season of 1990. Depths ranged from 68–118 cm in the Tulasewa forest plot, via 36–70 cm (on bedrock) in the Korokula forest plot to 70–110 cm in the Koromani forest plot. Details on the calibration and measurement procedures are given in Appendix 24.

Ceramic cup tensiometers were used to monitor **soil moisture tensions** in the respective soil horizons. In Tulasewa forest 10 tensiometers were installed around access tube 1 in May 1990 at 10–20 cm depth intervals up to a depth of 1.4 m. At two other locations tensiometer nests consisting of three tensiometers each were installed in June in the A- and B-horizons down to depths of 0.8 m. In Korokula forest six tensiometers were installed close to access tube 1 in June 1990 at 10 cm depth intervals down to 54 cm (bedrock). In Koromani forest six tensiometers were installed in August 1990. The tensiometers were placed close to access tube 4 (midslope) at 15 cm depth intervals down to 80 cm. Soil moisture tensions were read regularly with a custom-made electronic pressure transducer connected to a hypodermic needle which was inserted into the tensiometers through a rubber septum. Soil moisture tensions could be measured up to a tension of 900 cm H_2O (pF= 2.9) and to the nearest cm of tension.

In the Tulasewa forest plot a Scanivalve system (Burt, 1978) has been in operation from June until November 1990 to measure soil moisture tensions on a daily basis. The system consisted of a Scanivalve fluid switch wafer (Scanivalve Corp., model W02 1P-24T) connected to a pressure transducer (Pressure Sensors Ltd. Model MPT-117) and a control unit and datalogger, developed at FES-VUA. The Scanivalve switch was connected to the control unit and all 24 input channels were scanned twice a day within a 60-minute period, allowing 2.5 minute equilibration time for each input channel. The pressure transducer was connected to the datalogger and the data recorded on an audio cassette. The data were later transferred to floppy disc. The system was powered by a 12 V car battery. Two input channels of the Scanivalve were connected to water filled plastic bottles of which the water levels differed by 1.00 m, which were used as a reference (Burt, 1978). Seventeen input channels were connected via copper tubing to tensiometers at various depths. The remaining five channels were not used.

6.3 Rainfall Amounts and Characteristics

The amounts of rainfall recorded at each of the forest plots and at Nabou station during the 21-month period are given in Table 6.2, together with long-term averages for Nabou station (17 years of data). There was no distinct dry season in 1990 as rainfall amounts in June, August and November were well above their long-term averages. The high rainfall amounts recorded during these months were compensated by below average rainfall in April, May and October, resulting in an annual rainfall total close to the long-term average.

During the wet season of 1991 monthly rainfall amounts were close to the long-term average, but lower than average rainfall totals were recorded during the dry season, with the exception of September. Rainfall amounts remained below average until the end of the year and the annual total for 1991 was therefore much lower than average, amounting to 1339 mm at Nabou station (Table 6.2).

Table 6.2: *Monthly rainfall totals (mm) for Tulasewa, Korokula and Koromani forests and for Nabou Station as recorded during the present study, and long-term rainfall totals for Nabou Station (1973–1992).*

Station	Tulasewa Forest		Korokula Forest		Koromani Forest		Nabou station		Nabou 1973-1992	
Year	1990	1991	1990	1991	1990	1991	1990	1991	Average	SD
Jan	254.1	354.2	257.3	231.2	346.8	184.3	250.4	305.8	250.7	*135.5*
Feb	131.1	280.4	145.7	134.8	122.5	147.0	129.0	215.9	281.2	*139.7*
Mar	440.7	370.8	429.2	237.2	468.9	297.8	282.1	187.7	258.6	*185.1*
Apr	91.1	177.1	23.3	117.8	21.1	109.1	41.1	112.3	156.5	*136.8*
May	11.9	20.3	62.0	22.0	56.3	21.8	4.8	29.4	75.7	*93.7*
June	140.0	34.9	148.3	25.3	143.9	37.1	155.8	27.3	73.2	*61.7*
July	54.1	66.7	60.8	49.8	52.4	42.1	72.6	58.7	57.8	*34.3*
August	195.4	56.9	202.4	55.7	196.8	72.7	169.6	63.0	77.8	*67.5*
September	102.0	171.9	104.2	153.3	97.2	147.0	82.4	156.2	78.4	*59.0*
October*	55.3		34.3		49.0		35.7	75.0	108.0	*69.1*
November	437.7		218.7		252.6		213.1	52.6	119.4	*98.9*
December*	199.1		109.8		96.8		87.2	54.6	158.1	*109.8*
Total	**2112.5**	**1533.2**	**1796.0**	**1027.1**	**1904.3**	**1058.9**	**1523.8**	**1156.3**	**1695.4**	*408.9*

*: Underlined values excluded from the total.

The rainfall data presented in Table 6.2 reveal a clear trend with respect to the distance from the coast, with relatively low rainfall near the coast (*e.g.* Korokula site) and increasingly higher amounts more inland (*e.g.* Tulasewa site). However, rainfall also showed a large spatial variation, as shown by the different amounts recorded at Korokula and Koromani rainfall stations, which were less than 4 km apart and both situated close to the coast (Figure 2.2). The temporal variation of rainfall in the tropics is often high where rainfall is convective (Riehl, 1979), resulting in large standard deviations for long-term averages. This is illustrated by the annual totals recorded at Nabou station, which ranged from 826 mm in 1987 to 2498 mm in 1989. Similarly, wet season (November–April) monthly rainfall totals ranged from 4 mm in April 1983 to 658 mm in March 1985, whereas dry season monthly totals ranged from 0 mm in October 1986 and August 1988 to 400 mm in May 1989 (Table 6.2).

Rainfall totals recorded by the pluviograph, the standard gauge, the custom-made gauge and the above-canopy raingauge in the meteorological tower (if present) corresponded very well. Therefore errors in annual rainfall totals for the forest stations are thought to be within 5%. Errors were probably larger for rainfall collected during the passage of cyclone Sina, due to disturbances in the wind fields caused by the hurricane force winds. The low rainfall total recorded at Nabou station in November 1990 (when cyclone Sina passed) compared to those measured at the forest sites may have been caused by the sheltering of the Nabou gauge by nearby buildings located upwind from the gauge.

Short-duration rainfall intensities were obtained from 5-minute above canopy rainfall totals recorded by the micro-meteorological set-ups in the Tulasewa (1990) and near the Koromani forest (1991) plots. The overall maximum intensity (9.9 mm in 5 minutes) was observed above Tulasewa forest on February 16, 1990, during a single

Table 6.3: *Maximum rainfall amounts and intensities for different time intervals as measured above the canopy of Tulasewa forest on February 16, 1990.*

Time interval (minutes)	5	10	15	20	25	30	60
Rainfall amount (mm)	9.9	18.5	25.1	31.2	34.6	36.4	43.2
Rainfall intensity (mm/h)	118.2	110.9	100.5	93.5	83.0	72.8	43.2

afternoon shower which lasted for less than an hour (Table 6.3). The observed rainfall intensities for time periods ranging from 5 minutes to 1 hour are shown in Table 6.3. Extreme rainfall intensities of these magnitude are common in Fiji with return periods of 2 years for the 10-minute and 20-minute intensities and less than 2 years for the 30-minute and 60-minute intensities (Reddy, 1989c). The maximum rainfall intensities observed at Nadi Airport (1951–1988) were 40 mm, 61 mm and 162 mm for durations of 10, 30 and 60 minutes respectively (Reddy, 1989c).

The absolute maximum amount of rainfall recorded in a single hour during the study was 61.2 mm at Koromani forest in the evening of March 6, 1990, with a return period of 2 years (Reddy, 1989c). The storm lasted for 5.5 hours, producing a total of 66.8 mm of rain. The same storm produced 36.8 mm of rain in Korokula forest, with a maximum intensity of 26.8 mm h^{-1}, and 20.8 mm in Tulasewa forest. This again illustrates the high spatial variation of convective tropical rainfall. This storm also produced the maximum observed 2-hour rainfall intensity of 65.4 mm at Koromani forest.

The number of rain days (defined as a day on which rainfall exceeds 0.2 mm) was highest at Tulasewa forest where rainfall was recorded on 169 days in 1990 and 115 days in 1991 (January – September), and lowest at Korokula forest at 134 and 83 rain days days in 1990 and 1991 (January – September), respectively. The number of rain days at Koromani forest totalled 148 in 1990 and 96 in 1991 (January– September). Rainfall in excess of 0.2 mm was recorded at the latter on 51% of the days during the wet season and on 27% of the days during the dry season. The number of rain storms amounted to 171 in 1990 and 107 in 1991 (January–September) at the Koromani forest plot, where a rainstorm was somewhat arbitrarily defined as a period of rainfall separated from other periods of rainfall by at least four dry hours. The average number of storms per rain day amounted to 1.16 for the wet season and 1.10 for the dry season.

6.4 Rainfall Interception

The amount of rainfall intercepted by a forest, and subsequently lost by evaporation depends on the distribution, surface characteristics and amount of intercepting material (*e.g.* foliage), on the vegetation structure (branching patterns, stocking), on the rainfall duration and intensity as well as on several meteorological variables controlling the evaporation (*e.g.* net radiation, temperature, wind and humidity) (Leonard, 1967).

Under similar climatic conditions, the increase in foliar biomass with forest age should result in an increase in the interception of rainfall, until canopy closure is completed, after which the fraction of rainfall intercepted by the canopy should become fairly constant as the increase in the foliar biomass levels off. A sudden decrease in

foliar biomass as a result thinning, cyclone damage, fire, drought, disease or insect attack may result in a temporary decrease in interception loss until the canopy is fully recovered (Rogerson, 1967). This may take from several months to more than a year, depending on the amount of damage inflicted.

The seasonal variation in foliar biomass of pines in Fiji was negligible as these relatively young forests seemed to increase their biomass steadily throughout the rotation period, which excludes this factor as a cause for seasonal variation of interception loss. However, such a variation could be caused by variations in rainfall characteristics (*e.g.* storm size, duration and intensity; Jackson, 1975) or micro-meteorological conditions controlling evaporation (Rowe, 1983). Therefore a distinction was made between wet and dry season interception losses.

Interception and subsequent evaporation of rainfall (E_i) can be calculated from measurements of incident rainfall (P_g), throughfall (Tf) and stemflow (Sf) according to:

$$E_i = P_g - Tf - Sf \tag{6.1}$$

Throughfall amounts were measured at a level of 35 cm above the soil surface, which is well below the maximum height of the undergrowth (1–6 m), and interception losses calculated with Equation 6.1 therefore include those by the undergrowth.

Measured rainfall and throughfall totals for selected periods during the study are summarized in Table 6.4, together with the number of storms (as defined in Section 6.3) in each period, and the resulting mean rainfall amounts. Throughfall amounted to 77% of incident precipitation in both the Tulasewa and Korokula forest plots during the wet season and part of the dry season of 1990 (December/January – July). No throughfall measurements were made in Koromani forest during this period. During the following part of the dry season (July – November) throughfall increased to 84% and 79% of incident rainfall at the Tulasewa and Korokula forest plots respectively. An intermediate value (82% of dry season rainfall) was observed in the Koromani forest plot.

Cyclone Sina afflicted severe damage to Tulasewa forest at the end of November 1990, whereas most trees in the Korokula and Koromani forests were only defoliated. The sudden reduction in foliar biomass caused an increase in throughfall from 77% of incident rainfall during the wet season of 1990 (December/January – July) to 86% and 88% during the wet season of 1991 (December – April) for the Tulasewa and Korokula forest plots respectively. A similar increase may have occurred in Koromani forest where the post-cyclone throughfall amounted to 84% of incident rainfall.

The slightly lower percentage of throughfall in the Tulasewa forest plot, which suffered much higher cyclone damage than Korokula forest, could be caused by the vigorous response of the undergrowth (mainly mission grass) to the opening up of the forest. By the end of the wet season in 1991 the grass had reached heights of 2.5 m. Some rainfall intercepted by the grass presumably reached the forest floor as stemflow rather than as throughfall and post-cyclone amounts of throughfall and stemflow may therefore have been underestimated somewhat. As discussed in Section 5.5 rainfall interception by *Pennisetum polystachyon* grassland may be in the order of 5% of incident rainfall.

The ratio of throughfall to incident precipitation decreased to 78% at the Koromani forest plot, and to 81% at the Tulasewa and Korokula forest plots during the dry season of 1991, which is lower than those observed for the dry season of 1990. This must be due to the difference in rainfall between the dry season of 1990 (420–546 mm) and that of 1991 (150–173 mm; Table 6.4).

Table 6.4: *Observed wet and dry season amounts of rainfall, and observed and predicted amounts of throughfall, stemflow and interception loss for the Tulasewa, Korokula and Koromani forest plots for the pre- and post-cyclone periods. Cyclone Sina occurred on November 28, 1990.*

Period	**P**	**n**	**P-avg**	**Tf**		**Sf**	**Interception loss**					
				Obs.	Pred.	Pred.	Obs.	Pred.	Iwet	Isat	Idry	Istem
	(mm)		(mm)	(mm)	(mm)	(mm)	(mm)	(mm)	(mm)	(mm)	(mm)	(mm)
Tulasewa Forest												
30/11/89 - 05/01/90	155.6	9	17.3	124.6	126.5	2.0	29.0	27.1	3.0	17.3	6.5	0.3
06/01/90 - 18/07/90	1107.2	98	11.3	849.1	899.1	14.8	243.3	193.2	25.6	123.5	42.0	2.1
19/07/90 - 15/11/90	545.6	50	10.9	459.2	442.2	7.2	79.2	96.2	13.2	60.9	20.8	1.2
16/11/90 - 18/12/90	266.3	18	14.8	220.7	211.1	3.8	41.8	51.5	2.8	45.2	2.9	0.6
19/12/90 - 30/04/91	1378.6	99	13.9	1178.6	1090.6	19.6	180.4	268.3	16.6	230.1	17.5	4.0
01/05/91 - 30/08/91	173.4	30	5.8	141.1	135.9	2.0	30.3	35.6	5.6	25.5	3.8	0.8
30/11/89 - 30/08/91	**3626.7**	**304**	**11.9**	**2973.3**	**2905.3**	**49.4**	**604.0**	**671.9**	**66.8**	**502.5**	**93.5**	**9.0**
Korokula Forest												
08/01/90 - 16/07/90	1047.7	81	12.9	802.9	812.9	14.8	230.0	220.1	30.4	131.7	54.2	3.7
17/07/90 - 19/11/90	422.3	51	8.3	333.6	318.2	5.6	83.1	98.6	20.1	48.0	28.7	1.9
20/11/90 - 24/12/90	246.0	20	12.3	218.1	189.8	3.3	24.6	52.8	4.0	42.4	6.2	0.2
25/12/90 - 29/04/91	761.2	66	11.5	668.0	587.0	10.5	82.7	163.8	12.1	130.0	20.2	1.5
30/04/91 - 02/09/91	150.4	35	4.3	121.2	112.5	1.8	27.4	36.2	7.8	22.7	4.9	0.7
08/01/90 - 02/09/91	**2627.6**	**253**	**10.4**	**2143.8**	**2020.5**	**36.0**	**447.8**	**571.4**	**74.5**	**374.9**	**114.2**	**7.9**
Koromani forest												
08/01/90 - 22/07/90	*1165.1*	*98*	*11.9*	n.d.	*951.1*	*16.3*	n.d.	*197.7*	*26.8*	*114.5*	*51.6*	*4.8*
23/07/90 - 21/11/90	419.7	44	9.5	342.9	335.7	5.5	71.3	78.6	13.2	38.6	24.6	2.2
22/11/90 - 24/12/90	*242.6*	*21*	*11.6*	n.d.	*192.9*	*3.6*	n.d.	*46.1*	*4.0*	*36.2*	*5.4*	*0.5*
25/12/90 - 29/04/91	774.5	79	9.8	650.5	608.7	9.9	114.1	155.9	15.1	109.4	27.8	3.6
30/04/91 - 02/09/91	170.6	33	5.2	132.9	131.3	1.9	35.8	37.5	7.8	21.8	7.1	0.9
23/07/90 - 02/09/91*	**1364.8**	**156**	**8.7**	**1126.3**	**1075.7**	**17.3**	**221.2**	**272.0**	**36.1**	**169.7**	**59.4**	**6.7**

P= Rainfall, n = Number of storms, P-avg = Average rainfall during n storms, Tf = Throughfall, Sf = Stemflow.
Obs.= Field observations, Pred.= Predicted by the Gash model, n.d.= Not determined.
Iwet, Isat, Idry = Interception loss during wetting up, saturation and drying of canopy respectively (Gash model).
Istem = Interception loss from the drying of the trunks (predicted by the Gash model).
*: Values in italics have not been included in totals and averages.

As stemflow was considered to be a small component of the water balance (generally only a few % of P_g in tropical pine forests; Bruijnzeel, 1988) no attempts were made to measure stemflow in the Korokula and Koromani forest plots. Reliable estimates were obtained in the Tulasewa forest plot for small storms only ($P_g < 16$ mm) due to overflow of one or more stemflow collectors during larger storms. The between-tree variation of stemflow was very high with maximum amounts up to 40 times the minimum amount collected during a storm. No stemflow was observed for storms smaller than 3 mm. Gash's analytical model (Gash, 1979), which will be described in Section 6.4.1, was used to predict the stemflow amounts given in Table 6.4. The predicted stemflow amounted to 1.4% of incident rainfall which is in accordance with values found for other tropical pine forests (Bruijnzeel, 1988).

The interception losses (E_i) calculated from Equation 6.1 for the various periods are given in Table 6.4. Pre-cyclone interception losses in the Tulasewa and Korokula forest plots during the wet season of 1990 (December/January – July), expressed as a fraction of P_g, were similar at 22% (Table 6.7). Relative losses decreased in the dry season of 1990 (July – November), although mean rainfall amounts were similar to those in the wet season, and ranged from 14.5% in Tulasewa forest to 19.7% in Korokula forest (Table 6.7). This probably reflects seasonal variations in climate (*e.g.* net radiation, temperature), resulting in lower evaporation rates.

The damage afflicted to the forests by cyclone Sina reduced the interception loss by some 40–50% during the early months season of 1991 as compared to that during the wet season of 1990, with E_i ranging from 10.9% of P_g in the Korokula forest plot to 14.7% in the Koromani forest plot (Table 6.7). Dry season values of E_i, expressed as a fraction of P_g, were slightly lower (18.2% in the Korokula forest plot) or higher (18% and 21% in the Tulasewa and Koromani forest plots, respectively) than those obtained for the dry season of 1990.

Interception losses over the whole period (Table 6.4) did not differ much between the sites, ranging from 16.2% to 17.0% of P_g for the Koromani and Korokula forest plots, respectively, with an intermediate value of 16.7 % for the Tulasewa forest plot. Hence the interception characteristics of these forests seem to be fairly constant after age 6, implying that the largest changes occur during the early years of the plantation.

6.4.1 Modelling of Throughfall, Stemflow and Interception Losses

An analytical model, of which the derivation has been given in detail by Gash (1979), was used to obtain daily estimates of E_i, Tf and Sf from daily rainfall totals. The Gash model has been developed as an attempt to combine the simple features of the empirical regression approach (Helvey and Patrick, 1965; Jackson, 1975; Leonard, 1967; Zinke, 1967) with the conceptual basis of the Rutter model (Rutter *et al.*, 1971, 1975) and has been tested on coniferous and broadleaf forests in temperate climates (Gash, 1979; Gash *et al.* 1980; Pearce and Rowe, 1981; Rowe, 1983) and in tropical climates (Bruijnzeel and Wiersum, 1987; Lloyd *et al.*, 1988; Hutjes *et al.* 1990) with fairly good agreement between observed and predicted interception losses over a large range of precipitation totals (600–2800 mm).

The model is based on the assumption that the actual rainfall pattern can be represented by a series of discrete (*e.g.* daily) storms, separated by periods during which the canopy dries completely. This is a reasonable assumption for SW Viti Levu where rain typically falls in short, intense convective storms, as indicated by the

averages (1.1–1.2) for the number of storms on a rain day given in Section 6.3 for Koromani forest. A running water balance is calculated for the canopy and trunks using daily values of incident rainfall as input. The incident rainfall is apportioned into the fraction of rainfall reaching the forest floor without hitting the canopy (free throughfall, p) and the fraction of rainfall diverted to the tree trunks (p_t), with the remaining fraction of P_g assigned to the canopy ($1-p-p_t$). Gash (1979) assumed that no drip occurred from the canopy until the canopy storage (S) was completely filled, implying that the interception loss from the canopy (E_i) equals $P_g(1-p-p_t)$ if rainfall amounts are insufficient to fill the canopy storage. The amount of rain necessary to fill the canopy storage (P'_g) is calculated from Equation 6.2 (Gash, 1979):

$$P'_g = (-\bar{R}S/\bar{E}) \ln 1 - (\bar{E}/\bar{R})(1-p-p_t)^{-1}) \tag{6.2}$$

For storms larger than P'_g the interception loss is the sum of the losses during the period of wetting up (I_{wet}), the period of saturation (I_{sat}) and the period of drying up of the canopy (I_{dry}) as shown in Equation 6.3:

$$E_i = \underbrace{P'_g(1-p-p_t) - S}_{I_{wet}} + \underbrace{\bar{E}/\bar{R}(P_g - P'_g)}_{I_{sat}} + \underbrace{S}_{I_{dry}} \tag{6.3}$$

Gash (1980) further assumed that evaporation from the trunks occurred after rainfall had ceased, which is valid if rainfall durations are short and stemflow fractions low. As such the interception loss from the trunks (E_{it}) is equal to the trunk storage (S_t) for a storm filling the trunk storage completely or to $p_t * P_g$ if rainfall is insufficient to fill the trunk storage.

The evaporation rate from the saturated canopy during rainfall is assumed to be constant and equal to the average rate ($\bar{E}$) for all storms. Gash (1979) has shown that the slope (a) in a linear regression equation ($E_i = a \cdot P_g + b$) of observed interception losses (E_i) on P_g is given by the ratio of $\bar{E}$ to $\bar{R}$, where $\bar{R}$ is the mean rainfall rate onto a saturated canopy. $\bar{E}$ can be determined from the slope (a) of the regression when $\bar{R}$ is known, or alternatively from above-canopy micro-meteorological data using the Penman-Monteith equation with r_s set to zero (Gash, 1979; Gash *et al.* 1980).

The free throughfall coefficient was determined from the coefficient of a regression of Tf on P_g for small storms insufficient to saturate the canopy (Gash and Morton, 1978). Single storm rainfall and throughfall data with rainfall amounts of less than 2.7 mm were used to determine p for the pre- and post-cyclone periods. The pre-cyclone free throughfall coefficients ranged from 0.54 (n= 6) and 0.56 (n= 4) for Korokula and Koromani forests respectively, to 0.60 (n= 6) for Tulasewa forest (Figure 6.1A), where n represents the number of storms used in the regression. The regression equations used for the derivation of the various Gash model parameters for each of the forests are given in Table 6.5. The post-cyclone values of p were even higher ranging from 0.58 (n= 3) for the Korokula forest plot to 0.69 (n= 6) and 0.71 (n= 6) for the Koromani and Tulasewa forest plots, respectively. However, due to the limited number of single storms used in the regressions the errors in p may be considerable.

Shuttleworth (1989) found average values of about 0.1 for p in a comparison of interception studies in temperate and tropical forests. In Java, Bruinzeel and Wiersum (1987) obtained estimates of 0.34–0.38 in a 4–5-year-old *Acacia auriculiformis* plantation, whereas Bons (pers. comm.) obtained a value of 0.26 for p for a 35-year-old *Pinus merkusii* plantation forest. The relatively high values of p found in the present study are consistent with the rather open character of the pine forests in Fiji and were

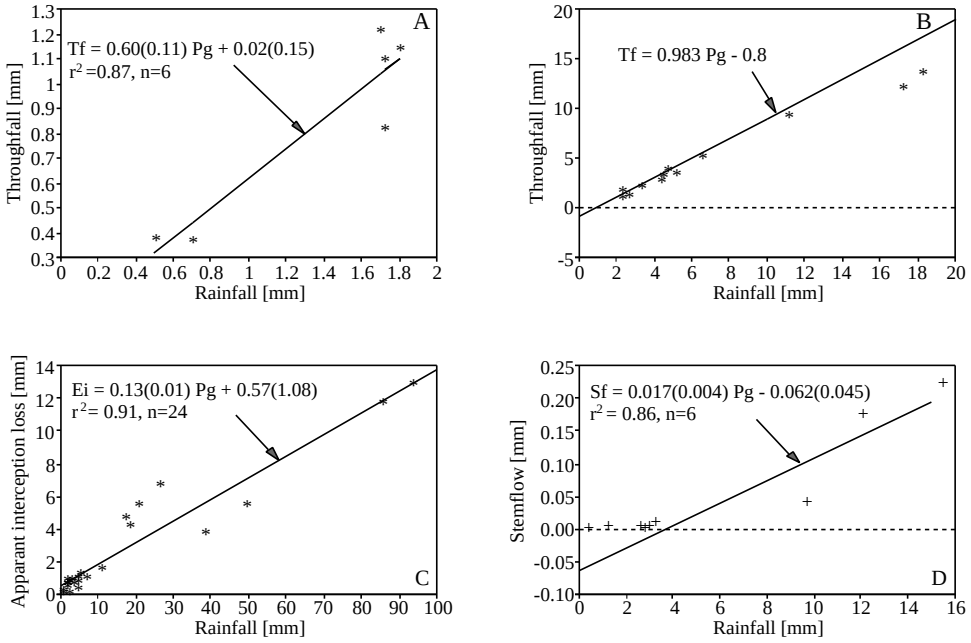

Figure 6.1: *Determination of pre-cyclone free throughfall coefficient (A), canopy storage capacity (B) $\bar{E}/\bar{R}$ (C) as well as stemflow fraction and trunk storage capacity (D) for the Tulasewa forest plot.*

Table 6.5: *Regression coefficients and statistics of linear regressions ($Y = a \cdot X + b$) of throughfall (Tf), interception loss (E_i) and stemflow (Sf) on incident rainfall (P_g) for the Tulasewa, Korokula and Koromani forest plots.*

Location	Equation	r^2	n	Storm size
Tulasewa				
Pre-cyclone	$Tf = 0.604(0.116)P_g + 0.015(0.153)$	0.87	6	< 2.7 mm
	$E_i = 0.132(0.008)P_g + 0.571(1.083)$	0.91	24	all storms
Post-cyclone	$Tf = 0.714(0.108)P_g + 0.048(0.100)$	0.92	6	< 2.7 mm
	$E_i = 0.183(0.051)P_g - 0.020(0.794)$	0.68	8	all storms
Whole period	$Sf = 0.017(0.004)P_g - 0.062(0.045)$	0.86	5	< 16.0 mm
Korokula				
Pre-cyclone	$Tf = 0.539(0.074)P_g + 0.235(0.109)$	0.93	6	< 2.7 mm
	$E_i = 0.154(0.044)P_g + 0.408(0.639)$	0.58	11	all storms
Post-cyclone	$Tf = 0.581(0.082)P_g + 0.390(0.079)$	0.98	3	< 2.7 mm
	$E_i = 0.194(0.040)P_g - 0.269(1.226)$	0.86	6	all storms
Koromani				
Pre-cyclone	$Tf = 0.556(0.115)P_g + 0.047(0.125)$	0.92	4	< 2.7 mm
	$E_i = 0.117(0.017)P_g + 0.826(1.643)$	0.79	14	all storms
Post-cyclone	$Tf = 0.685(0.097)P_g - 0.052(0.238)$	0.93	6	< 2.7 mm
	$E_i = 0.166(0.004)P_g - 0.307(0.355)$	0.99	12	all storms

confirmed by canopy gap fraction measurements using a ceptometer, as well as by measurements of projected crown area in the Koromani forest plot (Opdam, 1993). In the Tulasewa forest plot the pre-cyclone canopy gap fraction, as measured in June 1990, was 0.47(±0.14) which had increased slightly, but not significantly, to 0.50(±0.26) by July 1991. Post-cyclone gap fractions in the Korokula and Koromani forest plots were 0.28(±0.23) and 0.46(±0.26), respectively. The gap fractions were measured at 1.3 m, which is just below the upper levels of the undergrowth, and slightly lower values may be expected at the level where throughfall was collected (0.4 m).

The canopy storage capacity (S) was determined by the method of Leyton *et al.* (1967) using data for single storms larger then 2.7 mm. A straight line with a slope of $(1 - p_t)$ was drawn through the points such that the line passed through those points representing conditions with minimum evaporation (*e.g.* Figure 6.1B). S was then given by the intercept of that line with the throughfall axis. Pre-cyclone values of S were 0.8 mm (n= 18), 1.4 mm (n= 5) and 1.2 mm (n= 10) found in the Tulasewa, Korokula and Koromani forest plots, respectively (Table 6.6). Post-cyclone values of S were lower, reflecting the loss of foliage, amounting to 0.3 mm (n= 6), 0.5 mm (n= 3) and 0.6 mm (n= 6), respectively. Typical values of S for lowland tropical rainforest are 0.8–0.9 mm (Jackson, 1975; Lloyd *et al.*, 1988) whereas values similar to the presently found pre-cyclone figures have been reported for 4—5-year-old *Acacia auriculiformis* (S= 0.5–0.6 mm; Bruijnzeel and Wiersum, 1987) and 35-year-old *Pinus merkusii* plantations (S= 0.6–1.0; Mr. C.A. Bons, pers. comm.) in Java.

$\bar{E}/\bar{R}$ values for the pre- and post-cyclone periods were calculated from the slopes of regressions of interception loss E_i (approximated by $P_g - Tf$), on P_g for all single storms (*e.g.* Figure 6.1C). The pre-cyclone values were 0.132 (n= 24), 0.154 (n= 11) and 0.117 (n= 14) for the Tulasewa, Korokula and Koromani forest plots, respectively

Table 6.6: *Vegetation parameters and adjusted $\bar{E}/\bar{R}$ values used in the Gash model to predict daily throughfall and stemflow.*

Period	S	p	S_t	p_t	E/R	E/R adjusted
Tulasewa						
Pre-cyclone	0.8	0.60	0.062	0.017	0.132	0.147
Post-cyclone	0.3	0.71	0.062	0.017	0.184	0.125
Korokula						
Pre-cyclone	1.4	0.54	0.062	0.017	0.154	0.160
Post-cyclone	0.5	0.58	0.062	0.017	0.193	0.087
Koromani						
Pre-cyclone	1.2	0.56	0.062	0.017	0.117	0.123
Post-cyclone	0.6	0.61	0.062	0.017	0.166	0.114

(Tables 6.5 and 6.6). The low value of $\bar{E}/\bar{R}$ for the Koromani forest plot compared to that for the Korokula forest plot may be caused by the lack of wet season measurements for the former, during which evaporation rates were presumably higher as a result of higher temperatures and radiation. Post-cyclone $\bar{E}/\bar{R}$ values were higher at 0.183 (n= 8), 0.194 (n= 6) and 0.166 (n= 12) for the Tulasewa, Korokula and Koromani forest plots, respectively. As one would expect a lower $\bar{E}$ after defoliation whereas large changes in $\bar{R}$ were not observed as shown below, this is believed to reflect the limited number of single storms (particularly larger storms) sampled during this fairly dry period, rather then an actual increase in $\bar{E}/\bar{R}$. Bruijnzeel and Wiersum (1987) and Bons (pers. comm.) obtained respective values of 0.07–0.14 and 0.20–0.22 for $\bar{E}/\bar{R}$ in their forests discussed earlier in this section.

The average rainfall rate onto a saturated canopy was calculated from half-hourly pre-cyclone rainfall totals and amounted to 5.5 mm h^{-1} at Tulasewa forest in 1990, with a dry season average of 5.0 mm h^{-1}. This would result in apparent pre-cyclone $\bar{E}$ values of 0.72 mm h^{-1}, 0.85 mm h^{-1} and 0.59 mm h^{-1} for the Tulasewa, Korokula and Koromani forest plots, respectively. A post-cyclone value for $\bar{R}$ of 4.7 mm h^{-1} was obtained from data collected at Koromani forest, resulting in post-cyclone $\bar{E}$ values of 0.86 mm h^{-1}, 0.91 mm^{-1} and 0.78 mm h^{-1} for the Tulasewa, Korokula and Koromani forest plots, respectively. These values are much higher than the ones calculated on the basis of above canopy weather data (Section 7.7, Table 7.6). Possible reasons for this discrepancy are given later in this section.

The trunk storage capacity (S_t) and the fraction of rainfall going to the trunks were determined from the regression of stemflow (Sf) on incident rainfall (Gash and Morton, 1978) as measured in the Tulasewa forest plot (Figure 6.1D, Table 6.5). This suggested values for S_t and p_t of 0.062 and 0.017, respectively, and these were used to calculate the stemflow component for Tulasewa forest, as well as for Korokula and Koromani forests (Table 6.6). These values compare rather well to those obtained by Bons (pers. comm.) from measurements of stemflow in a 35-year-old *Pinus merkusii* plantation in Java (S_t= 0.026 and p_t= 0.028). The pre- and post-cyclone values of S,

p, S_t, p_t and $\bar{E}/\bar{R}$ found for the various sites have been summarized in Table 6.6.

The Gash model was run on daily rainfall data using the appropriate model parameters for each period. The observed and the predicted throughfall and stemflow amounts and interception losses are compared in Table 6.4. Predicted throughfall amounts were only 2% (Tulasewa forest plot) to 6% (Korokula forest plot) lower than the observed totals over the whole period. This resulted in an overestimation of interception losses, ranging from 11% at the Tulasewa forest plot to 28% at the Korokula forest plot, whereas that at the Koromani forest plot was overestimated by 23%.

The predicted throughfall amounts for the pre-cyclone period on the other hand were very close to the observed values with absolute deviations of less than 2.5% from observed amounts for all forests. Predicted interception losses were therefore much closer to observed losses for this period with absolute deviations of less than 11% from the observed values. These deviations are similar to those obtained by Bruijnzeel and Wiersum (1987) in an Indonesian *Acacia auriculiformis* plantation and smaller than those found in applications of the model in tropical rain forests (−35%, Hutjes *et al.*, 1990; +27%, Lloyd *et al.*, 1988) .

Much larger deviations from observed throughfall amounts were found for the post-cyclone period, ranging from -5.5% for Koromani forest to -11.7% for Korokula forest. As such interception losses were overestimated, with deviations ranging from +29% in the Koromani forest plot, to +88% in the Korukola forest plot. This is not very surprising as the post-cyclone model parameters were based on only very few single storms which, in addition, were collected in a period when the canopy was not in a steady state due to rapidly regenerating foliage. The obtained post-cyclone values for S and p nevertheless seemed reasonable considering the damage afflicted to the forests. However, the much larger post-cyclone values of $\bar{E}/\bar{R}$ compared to the pre-cyclone values (0.117–0.154) seem unrealistic as meteorological conditions were broadly similar during both periods.

Alternatively, evaporation rates during rainfall may be calculated from above canopy micro-meteorological data using the Penman-Monteith formula (Monteith, 1965, Equation 5.3) with r_s set to zero for the time that the canopy is wet (Section 7.7, Table 7.6). The $\bar{E}/\bar{R}$ values obtained with the Penman-Monteith method were several times smaller than those obtained from the above mentioned regression analysis on rainfall and throughfall data. There may be several explanations for these discrepancies. The estimates obtained with the Penman-Monteith equation are likely to be underestimated as advective energy inputs were not taken into account (Stewart, 1977). Sources of advective energy can easily be identified in the study area, where the forests were close to the Pacific Ocean and surrounded by grassland. The mean daily temperature of days with rainfall exceeding 10 mm was 24.2(±1.8) °C, whereas the mean sea surface temperature varied between 25 °C and 28 °C (Basher, 1986b). Therefore a horizontal temperature gradient followed by a downward sensible heat flux (Pearce *et al.*, 1980) is likely to exist when the temperature over land drops below that of the seawater (*e.g.* at night, during periods with rainfall). Because r_s for a dry canopy is high during nighttime, such an extra advective energy input will not result in transpiration. However, when the canopy is wet the extra energy input may be used for evaporation of moisture from the canopy, and the rates derived with the Penman-Monteith equation may therefore be considered underestimates under such conditions.

The lack of stemflow data for large storms may also have resulted in errors in the estimated $\bar{E}/\bar{R}$ values obtained from regressions of E_i on P_g, because the interception loss was approximated by $P_g - Tf$, neglecting the contribution of stemflow.

This approximation may be valid for small storms, during which the branches and stems are not thoroughly wetted. However, the structure of the tree crowns was such (Section 11.3) that the proportion of rainfall going to the trunks may have become much higher when branches and stems were saturated, as large amounts of water intercepted by needles and branches pointing upwards at angles of more than 45° may have been conducted towards the trunk. Interception losses for large storms may have been overestimated, therefore resulting in the obtained high $\bar{E}/\bar{R}$ values.

6.4.2 Modelling Moisture Fluxes through the Litter Layer

Accurate estimates of the amounts of water percolating through the litter and fermentation layers could not be obtained for storms exceeding 25–30 mm due to overflow of the collectors. A simple model was developed therefore to obtain daily estimates of litter percolate volumes (D_{lf}) and rainfall interception by the litter layer (E_{il}) using daily throughfall and stemflow amounts as predicted by the Gash model as input. A description of the model and the assumptions made during its derivation are given below.

Interception of rainfall by the litter layer is a function of the micro-meteorological conditions within the forest, as well as the moisture content (MC_l), and thus the storage capacity (S_l) of the litter layer. Amounts of radiation reaching the forest floor depend on the areal distribution of pine foliage and undergrowth. Fractions of photosynthetically active radiation (PAR) reaching the undergrowth level (1.3 m) ranged from 21% of incoming PAR in the Korokula forest plot to 36% and 39% in the Koromani and Tulasewa forest plots, respectively (see Section 11.3.6). Tannai and Hattori (1993) observed that the influence of $R_s \downarrow$ on evaporation from the forest floor (E_l) was small during the growing season of a deciduous broad-leaved forest in Japan and that E_l was basically constant under the prevailing climatic conditions. Because below canopy wind speeds in the forests in Fiji are low it is safe to assume that the evaporative demand at the forest floor will not be high and that temporal variations in micro-meteorological conditions just above the forest floor will be relatively small. As such the moisture status of the litter layer may be identified as the main factor determining E_l.

A general relationship between the moisture content of the litter layer, obtained from samples collected at regular time intervals during the study (see Section 11.2), and the time passed since the last rainfall event (t) is shown in Figure 6.2. The moisture content of each sample was corrected for differences in litter mass at the time of sampling by normalizing it to that of the average pre-cyclone mass. There were no significant differences between the forest sites, despite differences in the mass and composition of the litter layer. Therefore a single exponential curve was fitted through the combined data set. Litter samples which contained less than 1.5 mm of water within 20 hours or less than 1 mm within 80 hours after sampling were excluded as the amount of rainfall may not have been sufficient to saturate the litter layer completely. When t exceeded 200 hours the moisture content remained essentially constant at 0.2–0.3 mm. The decrease in moisture content (MC) as a function of time t could be described accurately by Equations 6.4 and 6.5.

$$0 \leq t \leq 200: \quad MC_l = 2.43 \exp^{-0.0135t} \qquad \text{n= 18, } r^2 = 0.94 \tag{6.4}$$

$$t > 200: \quad MC_l = 0.2 \tag{6.5}$$

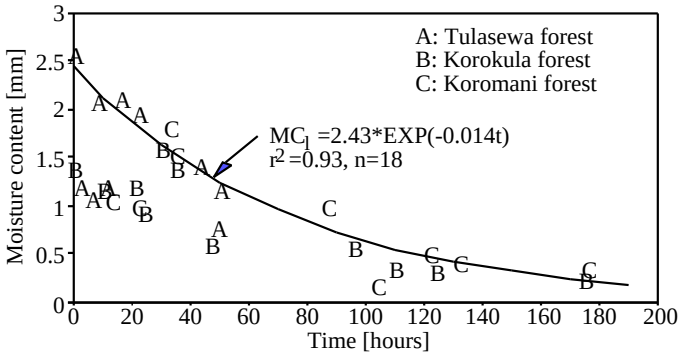

Figure 6.2: *Relationship between litter layer moisture contents and time since the last rainfall event for the three study plots.*

The maximum pre-cyclone moisture content of the litter layer (MC_{lmax}) was assumed to be equal to the moisture content at time t= 0 and amounted to 2.4 mm (Equation 6.4). Therefore moisture storage (S_l) was allowed to vary between 0.0 (air dry) and 2.2 mm (saturated, S_{lmax}). The pre-cyclone maximum was multiplied by the average ratio of the post- to pre-cyclone mass (1.67) which gave a value of 4.0 mm for the maximum post-cyclone moisture content.

For any MC_l value a corresponding t value could be calculated using an exponential regression equation (Equation 6.6) of t on $MC_l(t)$.

$$t = 220.9 \exp^{-1.251 MC_l}$$
$$\text{n= } 18,\ r^2 = 0.93 \tag{6.6}$$

The rate of removal of moisture from the litter layer by evaporation (E_l) is described by Equations 6.7 and 6.8, which represent the first order derivatives of Equations 6.4 and 6.5.

$$0 \leq t \leq 200 :\ E_l = 0.034 \exp^{-0.0135t} \tag{6.7}$$

$$t > 200 :\ E_l = 0 \tag{6.8}$$

Equation 6.7 implies an evaporation rate of 0.034 mm h^{-1} at t= 0 or 0.79 mm day^{-1}, for a saturated litter layer (E_{lsat}). The actual evaporation from the litter layer during rainfall may have been even higher as additional energy for evaporation may have been provided by cooling of the air within the forest.

Stemflow was assumed to reach the soil without interception by the litter layer, as the flow is concentrated in a small area around the trunk of the tree. Depending on the amount of throughfall the model selected one out of four possible options to calculate the interception by the litter layer (E_{il} and the flux of water through the litter layer (D_{lf}):

1. If Tf= 0 the moisture content of the litter layer decreases from $MC_l(t)$ to $MC_l(t + 24)$ according to Equation 6.4. Both E_{il} and D_{lf} are zero.
2. For $0 < Tf < S_l(t)$ all throughfall is used to increase the MC_l and a corresponding t_{new} is calculated from Equation 6.6. MC_l then becomes $MC_l(t_{new} + 24)$; E_{il} equals Tf and D_{lf} is zero.

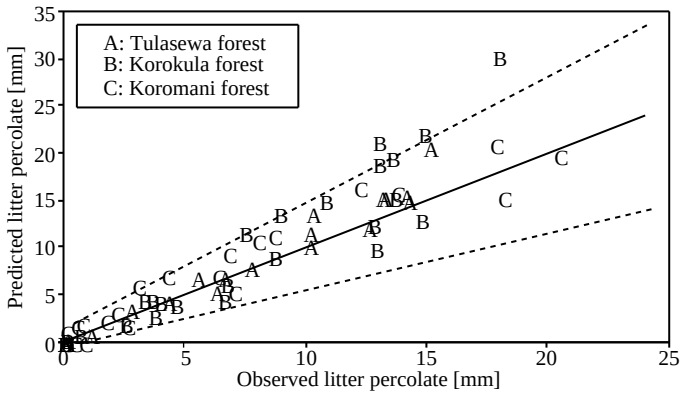

Figure 6.3: *Observed and predicted moisture fluxes through the litter layers of Tulasewa, Korokula and Koromani forests. The solid line is a line of unit slope whereas the dotted lines represent the range of standard deviations of the observed fluxes.*

3. For $S_l(t) < Tf < S_{lmax} + E_{lsat}$, MC_l is set to MC_{lmax} and t is set to zero. E_{il} equals Tf and D_{lf} is zero.
4. For $Tf > S_{lmax} + E_{lsat}$, MC_l is set to MC_{lmax}, t is set to zero, E_{il} is set to $S_{lmax} - S_l(t) + E_{lsat}$ and D_{lf} equals $Tf - E_{il}$.

As indicated earlier, the Gash model was used to obtain daily values of throughfall and stemflow to be used as inputs to the litter layer interception model. The $\bar{E}/\bar{R}$ values to be used were adjusted by trial and error until the predicted throughfall totals were equal to the observed totals given in Table 6.4. The vegetation parameters and the adjusted $\bar{E}/\bar{R}$ values are shown in Table 6.6. The empirical $\bar{E}/\bar{R}$ values were similar to the adjusted ones for the pre-cyclone period, whereas the adjusted post-cyclone values were much lower than the empirical ones, and approached pre-cyclone values (with the exception of that of the Korokula forest plot, Table 6.6).

To test the model a comparison was made between observed and predicted amounts of litter percolate for daily rainfall totals smaller than 20 mm (Figure 6.3). The model seems to overestimate the moisture fluxes through the litter layer because the sum of the predicted totals was 9% (Tulasewa forest) to 21% (Korokula forest) higher than the sum of the observed totals. However, no corrections were made as the predicted values were generally within the range of the standard deviations of the measured volumes.

Predicted fluxes of moisture through the litter layer for various periods during the study are given in Table 6.7 together with observed rainfall and throughfall amounts, and predicted stemflow amounts. The interception loss from the litter layer was calculated from Equation 6.9 and ranged from 9.5% of total rainfall in Tulasewa forest to 11.0% in Korokula forest.

$$E_{il} = (Tf + Sf) - D_{lf} \tag{6.9}$$

As shown in Table 6.7 interception losses from the litter layer were relatively low during the wet season (4–10% of rainfall) as the time between consecutive rainfall events was

Table 6.7: *Observed amounts of rainfall and throughfall, and predicted amounts of stemflow and litter percolate for Tulasewa, Korokula and Koromani forests. Interception losses from the canopy and litter layer are expressed both as depths of water and as a percentage of total rainfall.*

Period	**Rainfall**	**Throughfall**	**Stemflow**	**Litter Percolate**	**Interception loss**			
					Canopy		**Litter layer**	
	(mm)	(mm)	(mm)	(mm)	(mm)	% Rainfall	(mm)	% Rainfall
Tulasewa Forest								
30/11/89 - 05/01/90	155.6	124.6	*2.0*	*106.7*	29.0	18.6	19.9	12.8
06/01/90 - 18/07/90	1107.2	849.1	*14.8*	*789.6*	243.3	22.0	74.3	6.7
19/07/90 - 15/11/90	545.6	459.2	*7.2*	*388.1*	79.2	14.5	78.3	14.4
16/11/90 - 18/12/90	266.3	220.7	*3.8*	*214.5*	41.8	15.7	10.0	3.8
19/12/90 - 30/04/91	1378.6	1178.6	*19.6*	*1064.0*	180.4	13.1	134.2	9.7
01/05/91 - 30/08/91	173.4	141.1	*2.0*	*115.1*	30.3	17.5	28.0	16.1
30/11/89 - 30/08/91	**3626.7**	**2973.3**	**49.4**	**2678.0**	**604.0**	**16.7**	**344.7**	**9.5**
Korokula Forest								
08/01/90 - 16/07/90	1047.7	802.9	*14.8*	*735.1*	230.0	22.0	82.6	7.9
17/07/90 - 19/11/90	422.3	333.6	*5.6*	*276.2*	83.1	19.7	63.0	14.9
20/11/90 - 24/12/90	246.0	218.1	*3.3*	*184.5*	24.6	10.0	36.9	15.0
25/12/90 - 29/04/91	761.2	668.0	*10.5*	*598.5*	82.7	10.9	80.0	10.5
30/04/91 - 02/09/91	150.4	121.2	*1.8*	*97.7*	27.4	18.2	25.3	16.8
08/01/90 - 02/09/91	**2627.6**	**2143.8**	**36.0**	**1892.0**	**447.8**	**17.0**	**287.8**	**11.0**
Koromani forest								
08/01/90 - 22/07/90	1165.1	*945.2*	*16.3*	*867.0*	203.6	17.5	94.5	8.1
23/07/90 - 21/11/90	419.7	342.9	*5.5*	*294.7*	71.3	17.0	53.7	12.8
22/11/90 - 24/12/90	242.6	*204.7*	*3.6*	*185.1*	34.3	14.1	23.2	9.6
25/12/90 - 29/04/91	774.5	650.5	*9.9*	*560.4*	114.1	14.7	100.0	12.9
30/04/91 - 02/09/91	170.6	132.9	*1.9*	*103.5*	35.8	21.0	31.3	18.3
23/07/90 - 02/09/91	**2772.5**	**2276.2**	**37.2**	**2010.7**	**459.1**	**16.6**	**302.7**	**10.9**

Values predicted by the Gash and litter layer interception models shown in italics

too short to deplete the storage of moisture completely. Dry season interception losses from the litter layer were relatively high and comparable to those in the canopy, ranging from 13–18% of total rainfall. The combined interception losses from the canopy and litter layer ranged from 26% of total rainfall for Tulasewa forest to 28% for Korokula forest. This would imply a total interception loss of 444–475 mm for a year with average rainfall (Table 6.2).

An overview of estimates of E_i including some obtained in coniferous plantation forests in the humid tropics has been presented by Bruijnzeel (1988). E_i was found to vary between 7% of rainfall for a 4–6 year old *Pinus caribaea* forest in Brazil (Shuttleworth, 1988) and 23% for a *Pinus merkusii* plantation forest in West Java (Bruijnzeel, 1988), whereas a value of 17% was found for an 18-year-old *Pinus caribaea* forest in Jamaica (Richardson, 1982). Interception losses from the litter layer are usually neglected in rainfall interception studies, and we have not been able to find any information for comparison with the values presently obtained.

6.5 Forest Evapotranspiration as derived from Soil Moisture Depletion

Soil moisture profiles (θ) were determined regularly throughout the dry season of 1990 and 1991 using a capacitance probe (*cf.* Appendix 24). The average depths of the θ profiles sampled were 1.0 m, 0.6 m and 0.8 m in the Tulasewa, Korokula and Koromani forest plots, respectively. Although the largest concentration of roots was observed in the upper 0.5 m of the soil, roots were also observed penetrating the bedrock at depths between 0.8 and 1.6 m. Because the pine root network extended beyond the maximum depth of the access tubes, and therefore of the moisture measurements, the zero flux plane approach (Cooper, 1979; *cf.* Section 5.2) could not be used to distinguish between moisture removed by evapotranspiration (ET_{sm}) and by drainage. The importance of drainage (D in mm day^{-1}) during periods without rainfall was therefore evaluated from the Darcy equation for unsaturated flow (Equation 6.10), assuming stationary flow conditions and using modelled values of K_{unsat} (or K_θ, see Appendix 25 and Section 4.3.4) in combination with pressure gradients ($\frac{\partial H}{\partial z}$) as obtained from tensiometer readings at various depths in the soil (Hanks and Ashcroft, 1980).

$$D = -K_{unsat} \cdot \frac{\partial H}{\partial z} \tag{6.10}$$

Variations with time of the soil moisture tension (with reference to the soil surface) for two depths in the soil at each of the forest sites are shown in Figure 6.4. The pressure gradients were usually low ranging from -7 to 15 cm H_2O cm^{-1} during dry periods. The modelled unsaturated hydaulic conductivities were low as well for tension values drier than field capacity (pF= 2.0; Appendix 25). Hence the contribution of drainage to the removal of moisture from the soil could safely be neglected after 3–5 days since a major rainfall event during the dry season.

The loss of moisture during such rainless periods without drainage were therefore nevertheless (even though it is recognised that the results must represent underestimates due to the fact that some roots extended beyond the depth of moisture observations) calculated from consecutive measurements of θ profiles. Time series of θ measured at several depths in access tubes A1, B1 and C1 (for which the longest records were available) in the respective forest plots are shown in Figure 6.5. The soil

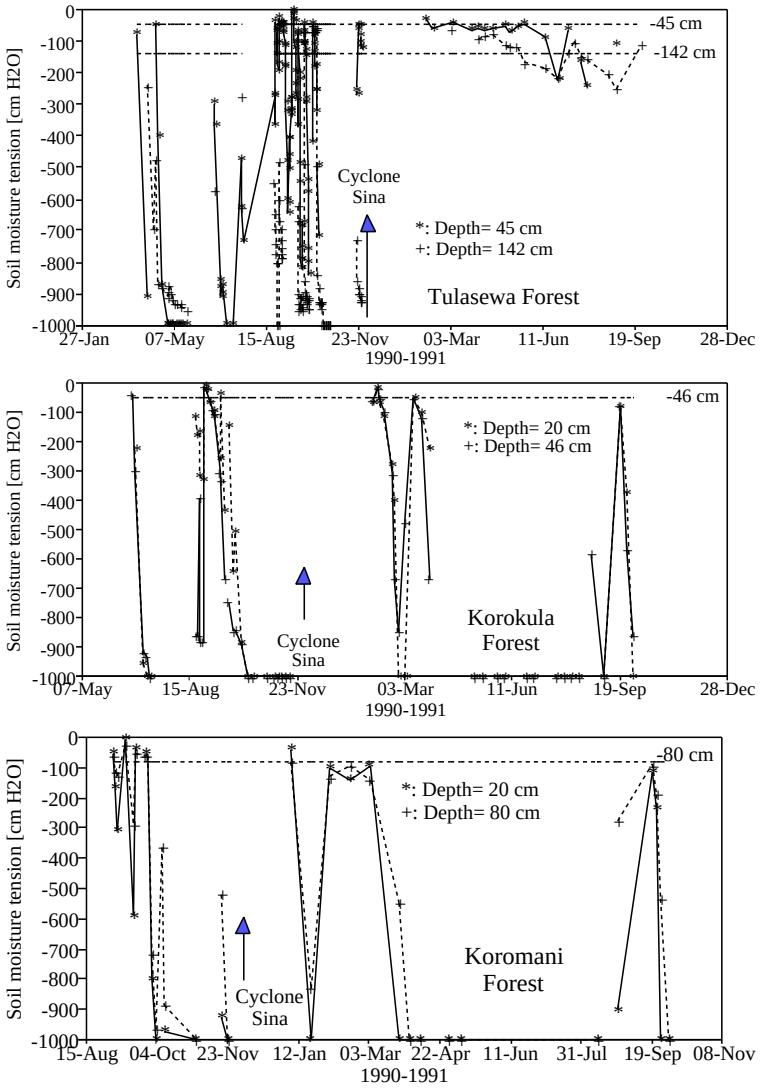

Figure 6.4: *Time series of soil moisture tension at two depths in the Tulasewa, Korokula and Koromani forest plots. Dry periods during which the soil moisture tension was higher than -1000 cm H_2O are indicated by the respective labels on the X-axis. Saturated conditions occurred whenever values exceeded the dashed lines indicating the depth of the respective observations.*

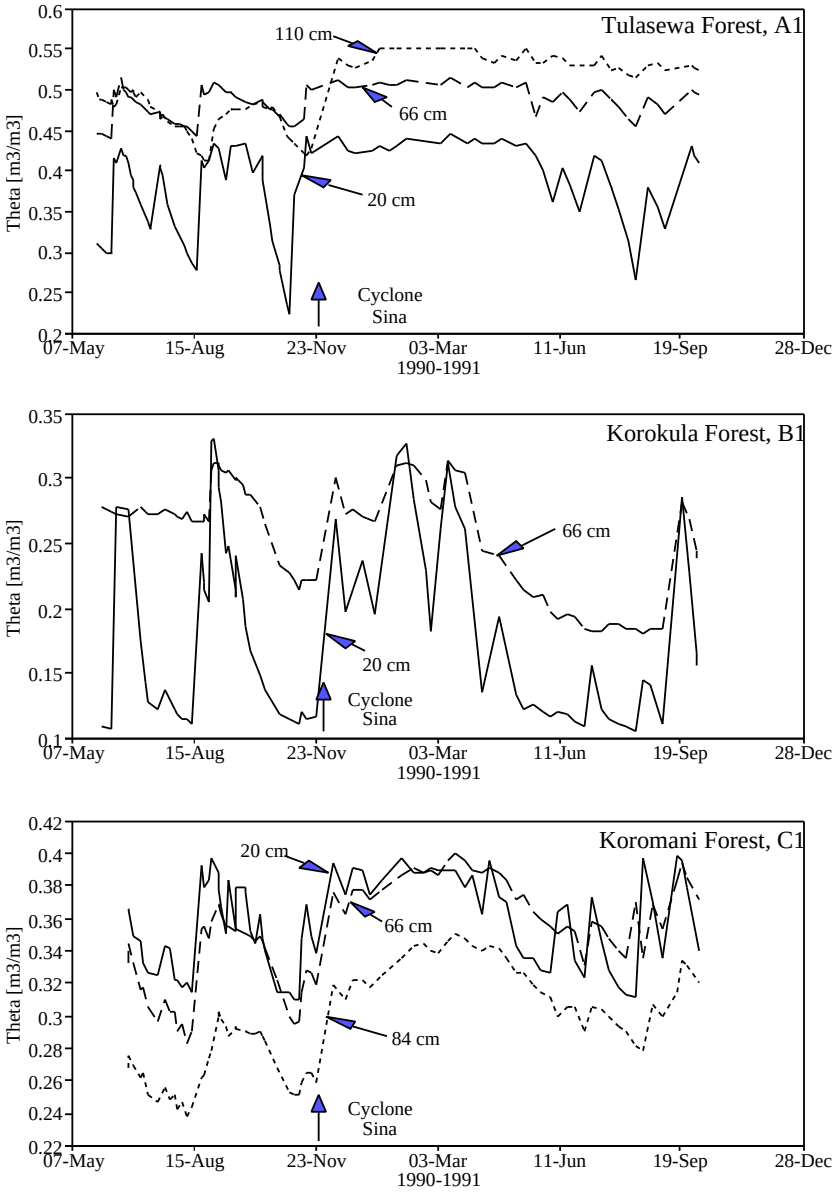

Figure 6.5: *Time series of θ at various depths in the Tulasewa, Korokula and Koromani forest plots as measured in capacitance probe access tubes A1, B1 and C1, respectively.*

Table 6.8: *Average ET_{sm} rates (mm day^{-1}) for Tulasewa, Korokula and Koromani forests during the dry seasons of 1990 and 1991 and interception losses E_i (including interception by the litter layer) observed over the periods for which ET_{sm} was calculated. Total ET (mm day^{-1}) was calculated as the sum of ET_{sm} and the average daily interception loss. The number of days was variable in 1990 depending on the number of access tubes installed at the time.*

Location	Tulasewa forest		Korokula forest		Koromani forest	
Year	1990	1991	1990	1991	1990	1991
ET-sm	3.27	2.23	1.41	0.90	1.81	1.67
Standard deviation	0.61	0.49	0.40	0.20	0.27	0.19
Number of days	86-16	69	85-48	86	98-50	89
Interception loss	23.4	8.4	38.3	8.8	45.5	10.1
Total ET	3.54	2.35	1.86	1.00	2.27	1.78

moisture content showed a clear seasonal trend with large fluctuations of θ, both in the topsoil and in the subsoil, during the dry seasons, and much smaller fluctuations during the wet season when the whole soil profile remained near field capacity. The large fluctuations in the subsoil of the forest plots, in contrast to those observed below the root zone in the Nabou grassland plot (*cf.* Section 5.3), constitute further evidence of water extraction by the pine roots beyond the depths of observations.

Cyclone Sina destroyed 42% of all trees in the Tulasewa forest plot, including those surrounding access tube A1, and defoliated the surviving trees. This was followed by vigourous regrowth of grass during the wet season of 1991. The damage to the forest resulted presumably in lower ET rates during the dry season of 1991 as compared to those in 1990. As a result soil moisture levels in the dry season of 1991 did not drop to the low levels observed during the dry season of 1990, despite lower rainfall inputs during the former (503 mm *versus* 351 mm). This is evident in the time series of the soil moisture tension (Figure 6.4) as well as in those for θ (Figure 6.5). Soil moisture profiles measured in the other access tubes in the Tulasewa forest plot (A2–A5) confirmed the pattern shown for access tube A1 in Figure 6.5.

The damage to the older forests was mainly confined to a reduction of the amount of foliage on the trees as less than 5% of the trees had been destroyed, and regrowth of needles was rapid. This, and the fact that the dry season of 1991 was much drier than that of 1990, may explain why there were no pronounced differences between dry season minimum soil moisture levels in 1990 and 1991. An exception must be made for access tube C1 in the Koromani forest plot, where a tree close to the access tube had been destroyed, and where dry season soil moisture levels in showed a similar trend, although not as pronounced, to those measured in access tube A1 in the Tulasewa forest plot (Figure 6.5). This suggests that cyclone Sina increased the spatial variation in soil moisture considerably in 1991 due to local disturbances to the forest (*e.g.* tree fall).

The average daily ET_{sm} rates for the Tulasewa, Korokula and Koromani forest plots are given in Table 6.8. As the access tubes were installed during the dry season of 1990 the ET_{sm} rates for that season represent the average obtained from a steadily increasing number of tubes. There were large differences between the ET_{sm} rates

obtained for the various plots with the highest rates observed in Tulasewa forest and the lowest in Korokula forest. However, as explained earlier, the rates presented in Table 6.8 must be considered underestimates as only the upper part of the soil profile containing roots could be sampled. The results of various micro-meteorological approaches to the evaluation of forest ET will be presented in Chapter 7.

The effect of cyclone Sina on rates of ET_{sm} was evident in Tulasewa forest where a reduction of 32% was observed for the dry season of 1991 compared to that of 1990. This reduction could not have been caused by differences in rainfall between the seasons as moisture was not limiting in 1991 (Figure 6.4). The lower ET_{sm} rates observed in Korokula and Koromani forests (36% and 8% respectively) in 1991 compared to those in 1990 may reflect a combination of reductions in the LAI of these forests (*cf.* Section 11.3.6) and, in the case of Korokula forest, also the relatively low plant available water capacity of the soil (Section 4.3.4).

6.6 Moisture Fluxes through the Soil

As explained in the previous section, amounts of water draining to deep groundwater (D) during the wet season were not measured directly. These were therefore estimated from a simple water balance equation (Ward and Robinson, 1990):

$$Q + D = P - ET \pm \Delta S \tag{6.11}$$

Similarly, ET was not measured continuously at all plots either and several assumptions were therefore needed to obtain estimates of D for both pre- and post-cyclone periods. As a result, the errors in these estimates may be considerable.

Pre-cyclone estimates of ET for the young forest at the Tulasewa forest plot (4.85 mm day^{-1}) were obtained by micro-meteorological techniques (Section 7.7), and at Oleolega for the mature forest (4.3 mm day^{-1}) by means of the catchment water balance method (Chapter 8). Because age and tree density of Koromani forest were roughly similar to those of the Oleolega forest, the pre-cyclone ET of Koromani forest was assumed to equal that of Oleolega forest. For want of actual observations ET at the Korokula forest plot was also assumed to be equal to that of Oleolega forest, in spite of the higher tree density in the former, because occasional water stress during dry periods is likely to have reduced ET to some extent at the Korokula forest plot (*cf.* Table 6.8). Pre-cyclone rainfall inputs, estimated ET totals and derived amounts of D are presented in Table 6.9. The runoff coefficients (D/P) calculated for the Tulasewa and Korokula forest plots were lower, whereas that for the Koromani forest plot was slightly higher than that calculated for the Oleolega catchment (0.16, Chapter 8). The relatively low values calculated for the former plots seem reasonable in view of the higher tree density in these sites compared to the other sites (Chapter 3).

Post-cyclone measurements of forest ET were limited to Koromani forest during the dry season of 1991. Because the wet season rainfall totals at the Korokula (831 mm) and Koromani forest plots (835 mm) were quite similar to that at Oleolega forest (904 mm), drainage losses during the 1990/1991 wet season and for September, 1991 (a wet month; Table 6.2), were approximated using the wet season runoff coefficient obtained for the Oleolega catchment (0.23; Chapter 8). The 1991 dry season rainfall was low and the soils at the Korokula and Koromani forest plots were relatively dry from April until September (Figures 6.4 and6.5) and drainage during this period may safely be neglected. The overall post-cyclone estimates of drainage rates for the two forest plots are presented in Table 6.9. The apparent post-cyclone ET value obtained

Table 6.9: *Components of the water balance for the pre- and post-cyclone periods at Tulasewa, Korokula and Koromani forests, n is the number of days in each period. Note that the pre-cyclone estimates for Tulasewa pertain to a different period than those of Korokula and Koromani forests. The mean daily drainage (D) and rainfall (P) rates and their ratio has been added for comparison.*

Component	Pre-cyclone			Post-cyclone		
	Tulasewa	Korokula	Koromani	Tulasewa	Korokula	Koromani
P [mm]	1932	1617	1745	1858	1190	1224
ET [mm]	1765	1423	1423	981	979	983
D [mm]	167	194	322	877	211	241
n [days]	364	331	331	306	306	306
Average P [mm day-1]	5.3	4.9	5.3	6.1	3.9	4.0
Average D [mm day-1]	0.5	0.6	1.0	2.9	0.7	0.8
D/P	0.09	0.12	0.18	0.47	0.18	0.20

by inserting the values of P and D in Equation 6.11 for Koromani forest was only slightly higher (3.2 mm day^{-1}) than the dry season ET_{pm} (3.0 mm day^{-1}) as derived from micro-meteorological measurements above Koromani forest for the period May – September 1991, lending some confidence to the D values for the Korokula and Koromani forest plots.

Wet season rainfall at Tulasewa forest was some 500 mm higher than that measured at Oleolega, and it was therefore not realistic to use the runoff coefficient obtained at the latter site to calculate D at the Tulasewa forest plot. Furthermore, the soil at Tulasewa forest remained wet throughout the 1991 dry season (Figures 6.4 and 6.5), since the tree density of the forest had been reduced considerably after the passage of cyclone Sina. As such drainage will have occurred throughout the post-cyclone period. To calculate D from Equation 6.11, estimates of post-cyclone ET were obtained from the pre-cyclone value of ET_{pm}, using a reduction factor (0.66) obtained from a comparison of post-cyclone and pre-cyclone ET_{sm} values (Table 6.8). This factor may have been too high since the pre-cyclone ET_{sm} was underestimated due to the presence of roots below the measurement depth, whereas the 1991 value may have been fairly accurate due to the reduced tree density (no water stress in top soil at any time). A summary of the results is presented in Table 6.9.

Chapter 7

Forest Micro-meteorology

7.1 Introduction

The chief advantage of micro-meteorological methods over the soil moisture and catchment water balance methods is that the magnitudes of the various components of the forest energy balance, and therefore evapotranspiration, may be established from relatively simple above and within canopy measurements of meteorological parameters (*e.g* radiation, temperature, humidity and wind speed) over short periods of time (*e.g.* 30-minute intervals).

The methods discussed in this chapter include the Bowen Ratio Energy Balance method (BREB method; Angus and Watts, 1984), the Temperature Fluctuation Energy Balance method (TFEB method; Tillman, 1972; De Bruin, 1982) and the more empirical Penman-Monteith method, which has already been discussed briefly in Chapter 5. The Penman open water evaporation (E_0) was used as a reference, because long-term E_0 values could be obtained from routine measurements of climatic variables by the Fiji Meteorological Service.

There are several restrictions to the application of the energy balance methods. Both the BREB and the TFEB methods assume that all the energy fluxes act in the vertical (no advection) and that wind, temperature and humidity profiles are in equilibrium with the underlying surface. As such the research area should be flat and a large fetch is required in the upwind direction, and preferably in the downwind direction as well (Angus and Watts, 1984). This severely restricts the general application of such methods as forests in Fiji (and elsewhere) tend to be planted in patches in more or less steeply dissected terrain. However, the vegetation around the sites selected for micro-meteorological measurements within the present framework (Tulasewa and Koromani) was thought to be sufficiently homogeneous for the application of the BREB and TFEB methods, but the topography was not entirely flat, which will have influenced the results to some extent.

Several working papers were prepared by MSc students from FES-VUA on the determination of surface roughness characteristics, energy balance components and evapotranspiration rates for both the Tulasewa (Beekman, 1992; Frumau, 1993) and the Koromani forest (Harkema, 1994; Opdam, 1993; Van Well, 1993a). The results presented in this chapter rely partly on their work (*e.g.* calibration of instruments), but also include new data (*e.g.* wet season evapotranspiration rates for Tulasewa Forest).

To limit the size of this chapter the theory underlying the various methods will be discussed only briefly and the reader is referred to the work of Thom (1975), Monteith (1976), De Bruin (1982), Brutsaert (1982) and Frumau (1993) for more comprehensive discussions.

7.2 Methods and Procedures

Above and within canopy micro-meteorological measurements were made in the Tulasewa forest plot from November 29, 1989 until November 28, 1990, when the micro-meteorological set-up and the forest were destroyed by cyclone Sina, and at the meteo site near the Koromani forest plot from April 27, 1991 until September 20, 1991. The instrumentation of the meteorological towers was similar in both forests and the configurations of the instruments are given in Table 7.1. Details on the instruments are given below.

Short-wave solar radiation and **reflected radiation** were measured with the types of pyranometer and albedometer which have already been discussed in Section 5.2.

Net radiation was measured with a net radiometer (Radiation and Energy balance Systems Inc., Model Q*5) placed level within 1° on a support arm extending 1.5 m from the mast. The position of the radiometer was such that the shadow of the mast could not interfere with the measurements. The calibration given by the manufacturer (13.7 W m^{-2} mV^{-1}) was used throughout the measurement period. The instrument was supplied with heavy duty polyethylene windshields, which were replaced in June 1990. Recalibration of the instrument after replacement of the domes was not possible and a small error (up to 3%) could have been introduced. The net radiometer was damaged during the passage of cyclone Sina and a new instrument was used for the measurements in Koromani forest.

The **soil heat flux** was measured with soil heat flux plates placed at a depth of 2 cm below the soil surface. Care was taken not to disturb the litterlayer above the flux plates during installation. Details on the plates were provided in Section 5.2.

Air temperatures and **relative humidities** were measured at three levels above the canopy and at one level within the canopy using the following instruments. Three pairs of fast response thermocouples (chromium–constantane) were used to measure wet and dry bulb temperatures above the canopy whereas one thermocouple (dry) was placed within the canopy. The wet bulb temperature was measured with a thermocouple of which the junction was kept moist by a thin cotton wire connected to a reservoir filled with rain water (electrical conductivity ≈ 2 μS cm^{-1}). Profiles of air temperature and relative humidity were also measured with non-aspirated Rotronic temperature and humidity probes (Section 5.2). All instruments were calibrated before installation at their respective levels within and above the canopy, followed by recalibrations during the measurement period by shifting the position of one of the instruments (*e.g.* within canopy rotronic) to higher levels for periods of several days at a time. As a back-up system, wet and dry bulb temperatures were measured with aspirated psychrometers equipped with radiation shields made at the FES-VUA. The temperatures were measured using Negative Temperature Coefficient (NTC) resistors. The wet and dry bulb sensors were placed in separate tubes to avoid interference between sensors, and the wet bulb sensor was kept moist by a cotton wick immersed in a reservoir filled with rain water. Aspiration was provided by a miniature electric fan. Details on the calibration of the instruments in Tulasewa Forest have been provided in

Table 7.1: *Configuration of instruments in the meteorological masts in the Tulasewa forest plot between ([a]) November 1989 – April 1990 and ([b]) April – November 1990, and in that at the Koromani meteo site between April – September 1991.*

Level	**Instruments**	**Tulasewa[a]** *Height*	**Tulasewa[b]** *Height*	**Koromani** *Height*
Tree height		*11.5 m*	*12.5 m*	*17.5 m*
High, z_3	Wind vane	12.5 m	21.9 m	32.3 m
	Anemometer	12.5 m	21.1 m	32.1 m
	Rotronic	12.5 m	21.1 m	32.1 m
	Psychrometer	12.5 m	21.2 m	31.8 m
	Thermocouples (dry-wet)		21.2 m	31.9 m
Mid, z_2	Anemometer	11.0 m	17.0 m	27.0 m
	Rotronic		17.0 m	27.0 m
	Psychrometer		17.0 m	27.0 m
	Thermocouples (dry-wet)		17.0 m	26.9 m
Low, z_1	Anemometer	9.5 m	13.0 m	24.1 m
	Rotronic	9.5 m	13.0 m	24.1 m
	Psychrometer	9.5 m	13.0 m	24.1 m
	Thermocouples (dry-wet)		13.0 m	24.0 m
	Pyranometer	11.0 m	12.8 m	21.9 m
	Albedometer		12.6 m	21.9 m
	Net radiometer	11.0 m	12.5 m	21.9 m
	Rain gauge	8.7 m	11.8 m	22.0 m
Forest, z_f	Rotronic		6.0 m	12.8 m
	Psychrometer		6.1 m	12.8 m
	Thermocouple (dry)		6.1 m	12.8 m
Tree	Thermistor		1.5 m	2.0 m
Litter	Thermistor	0.0 m		
Soil	Flux plates	-2 cm (1)	-2 cm (2)	-2 cm (2)
	Thermistor	-2 cm	-2 cm	-2 cm
	Thermistor		-10 cm	

the working papers by Beekman (1992) and Frumau (1993), whereas those for the Koromani forest have been provided by Opdam (1993), Van Well (1993a) and Harkema (1994).

Profiles of above canopy **wind speed** were obtained using 3 anemometers (see Section 5.2 for instrument details) mounted on 0.8 m support arms pointing towards the main wind direction (SE). No corrections were made for overspeeding or stalling. **Wind direction** was measured with a potentiometer windvane (see Section 5.2 for details) placed on top of the mast. As it was difficult to align the arrow on the windvane exactly to the true North, measurements may again have a systematic error of about 5°.

Litter and **soil temperatures** were measured with thermistors (Campbell Scientific Ltd. 107B) placed at 0 cm, 2 cm and 10 cm (in Tulasewa forest only) below the soil surface. A fourth thermistor was implanted in the bole of a tree with near average dimensions at a depth of 4–5 cm with reference to the bark surface. In each forest the sensor was implanted in the bole of a tree with near average dimensions (Tree no. 57 and 219 in Tulasewa (Frumau, 1993) and Koromani forests (Opdam, 1993), respectively). The accuracy of the thermistors was typically better than 0.2 °C.

Above canopy **rainfall** was measured with a Campbell Scientific tipping bucket raingauge (model ARG100) with a resolution of 0.2 mm and a funnel diameter of 25.5 cm. As explained in Section 6.2 additional rainfall measurements were made in nearby clearings using manual gauges and mechanical recorders.

All instruments were connected to a Campbell 21X micrologger in combination with a multiplexer system (Campbell Scientific Inc., USA). Half-hourly averages, standard deviations and correlation coefficients between the various thermocouple temperatures were determined from 5-minute means of temperature measurements, obtained at a sampling frequency of 2 seconds, to minimize the influence of trends on the standard deviations (De Bruin *et al.*, 1993). The other instruments were sampled with a 30-second interval to obtain 30-minute averages and standard deviations. Total rainfall was recorded every five minutes as the sum of 30-second measurements. The data were temporarily stored on a Campbell Scientific SM716 storage module and later transferred to floppy disk.

Additional **tree bole temperatures** were measured using pre-calibrated NTC resistors, implanted at various heights and depths in the bole. The sensors were connected to a datalogger developed at FES-VUA. The measurements were made at a 30-minute interval and started on May 2, 1990, and May 7, 1991, in the Tulasewa forest plot and at the Koromani meteo site, respectively. Measurements were made on tree no. 57 at heights of 1.5 m (implantation depths: 2 and 8.5 cm with reference to the bark surface) and 7.0 m (implantation depths: 2 and 5 cm) in the Tulasewa forest plot, and on tree no. 219 at heights of 2.0 m and 6.5 m (implantation depths: 0, 3 and 7 cm) and 15.5 m (implantation depths: 0 and 2 cm, from July 17 onwards) at the Koromani meteo site.

An automatic porometer (see also Section 5.2) was used to determine half-hourly values of the **stomatal resistance** of pine needles from a single young tree (age 3–4 years) in the grassland and from a tree in Koromani forest at heights of 12.7 m, 15.7 m and 19.0 m. No such measurements were made in the Tulasewa forest plot since the instrument only became available after the forest had been destroyed by cyclone Sina. Access to the canopy of Koromani forest was provided by a scaffolding tower with a height of 20.6 m, which was also used for the micro-meteorological measurements. Measurements were made on nine days between July 2 and September 20, 1991, with the earliest measurement at 5:55 h and the latest at 21:45 h. The stomatal resistances

of five needle sets within each level were measured at 30–60 minute intervals. The porometer cup was designed to be used on broad leaved species. Measurements could therefore not be made on single needles as leakage would occur along the edges. However, the stomatal resistance could be measured by aligning several needles in such a way that a smooth surface was formed on which the cup of the porometer could be placed. To test whether leakage occurred a set of dead needles was aligned in a similar way and the cup was placed on the needles after which the relative humidity in the cup was lowered to a much lower level than that of the ambient air. Because the dead needles were very dry, a rise in humidity within the cup would indicate leakage. Leakage was not observed at low wind speeds, but occurred when wind speeds within the canopy exceeded 3–4 m s^{-1} and measurements were stopped accordingly.

7.3 Forest Aerodynamic Characteristics

7.3.1 Theory

Near the earth surface vertical fluxes of mass and heat are mainly transported by turbulence produced by the friction between horizontal winds and the surface (Thom, 1975). In a neutral surface layer, characterized by the absence of buoyant eddies, where the Coriolis effect can be ignored and the momentum flux may be considered independent of height, the vertical distribution of the wind speed over a uniform, flat surface can be described by the logarithmic wind profile equation (Thom, 1975):

$$u(z) = \frac{u_*}{k} \cdot \ln \frac{z}{z_0} \tag{7.1}$$

where $u(z)$ is the horizontal wind speed at height z above the surface, u_* is the friction velocity, k is the Von Karman's constant and z_0 is the roughness length, which depends on the average height, spatial distribution, shape, flexibility and mobility of the roughness elements and ranges from $2 \cdot 10^{-4}$ m for ice and mud flats to several metres for tall forests and urban areas (Arya, 1988). For a surface covered with tall vegetation, the logarithmic wind profile is lifted to a new reference level, lying somewhere between the surface and the height of the vegetation h. The height of this level is called the zero plane displacement length (d) and, for tall vegetation, Equation 7.1 needs to be modified (Thom, 1975) to:

$$u(z) = \frac{u_*}{k} \cdot \ln \frac{z-d}{z_0} \tag{7.2}$$

The zero plane displacement length for a given vegetation type depends on the height and areal density of the elements, being low for scattered vegetation (*e.g.* savanna) and approaching h for very dense canopies (Arya, 1988). It is unrealistic to assume zero wind velocity below the level $d + z_0$, as momentum is absorbed gradually over the height of the vegetation and the logarithmic wind profile, as described by Equation 7.2, does develop not immediately above the level $d + z_0$, but at a certain distance from the canopy (Hicks, 1985) where the influence of individual roughness elements can be discarded. Wind profile measurements should therefore be made at sufficient height above the canopy, but within the layer of constant flux (Thom, 1975).

It is common to express z_0 and d in relation to the mean or median vegetation height and Stanhill (1969) and Szeicz *et al* (1969) derived the following empirical relations:

$$\log(d) = 0.979 \log(h) - 0.154 \tag{7.3}$$

$$\log(z_0) = 0.997 \log(h) - 0.883 \tag{7.4}$$

Jarvis *et al.* (1976) gave an overview of the aerodynamic characteristics for temperate coniferous forests with median tree heights ranging from 4.5 to 28.0 m and observed that the ratio of z_0/h ranged from 0.02 to 0.14, whereas d/h ranged from 0.61 to 0.92 over a fairly wide range of stable and unstable atmospheric conditions.

The Richardson number (Ri) is the ratio of the buoyancy energy production term to the windshear energy production term in the turbulent kinetic energy budget. It is dimensionless and provides a good indication of the local turbulent structure of the air. As such it may be used as a criterium to select wind data close to neutral atmospheric conditions for the determination of z_0 and d. If temperatures T_1 and T_2 and wind speeds u_1 and u_2 are measured at levels z_1 and z_2 above the surface, Ri for the intermediate layer can be calculated from the following equation (Thom, 1975):

$$Ri = \frac{g}{T} \cdot \frac{(T_2 - T_1 + \Gamma \cdot (z_2 - z_1))(z_2 - z_1)}{(u_2 - u_1)^2} \tag{7.5}$$

where g is the gravitational acceleration, T is the mean temperature of the layer and Γ is the adiabatic lapse rate (0.01 K m^{-1}). Ri is close to zero under near-neutral conditions as the buoyant energy production term approaches zero, whereas Ri is negative for stable atmospheric conditions and positive for unstable conditions (Thom, 1975).

There are several methods for the estimation of z_0 and d. The graphical and analytical methods, which are basically similar, require knowledge of the above canopy wind speed distribution and are based on the following assumptions (Thom, 1975):

- All momentum is absorbed at the level $d + z_0$; hence wind speeds are assumed zero below this level.
- The wind profile immediately above the level $d + z_0$ is logarithmic under neutral atmospheric conditions.

With the **graphical method** proposed by Thom (1975), the level $d + z_0$ can be found by plotting averages of $u(z)$, measured under neutral atmospheric conditions at a minimum of three levels above the canopy, against z and drawing a logaritmic curve through the data points. The intercept of this line with the z-axis ($u(z) = 0$) represents the value of $d + z_0$ (Thom, 1975). As the drawing of the curve is done by eye, this method is somewhat subjective. Estimates of z_0 and d can then be obtained by elimination of the unknown u_* in Equation 7.2 using ratios of $u(z)$ measured at two levels according to:

$$\frac{u(z_2)}{u(z_1)} = \ln \frac{\frac{z_2 - d}{z_0}}{\frac{z_1 - d}{z_0}} \tag{7.6}$$

A matrix of $u(z_2)/u(z_1)$ can be prepared for various combinations of z_0 and d and because $d + z_0$ is derived from the graphical method, fairly accurate values of d, and therefore also z_0, may be obtained by searching for the combination of z_0 and d in the matrix, that equals the ratio of measured wind speeds at levels z_2 and z_1.

With the **analytical method** proposed by Robinson (1962) Equation 7.2 is solved numerically for d, z_0 and u_* by minimizing the square of the vector of errors with the condition that the partial derivatives with respect to u_*/k, d and z_0 are zero.

Another method involves the fitting of a straight line through a semi-logarithmic plot of $u(z)$ against $\ln(z - d)$ for various values of d. The optimum value of d is that for which the Pearson product-moment correlation coefficient is highest, and $\ln z_0$ is

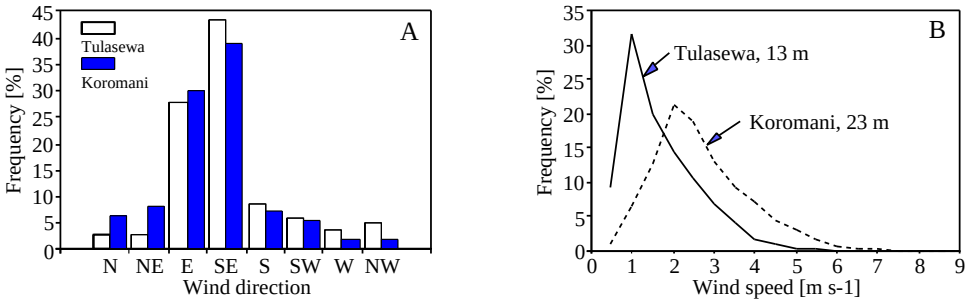

Figure 7.1: *Frequency distributions of 30-minute average wind directions (A) and wind speeds (B) for Tulasewa (n= 16817) and Koromani (n= 6771) forests.*

then found as the intercept of that line with the $\ln(z-d)$ axis (Thom, 1975; Frumau, 1993).

Mass conservation methods (*e.g.* Molion and Moore, 1983; De Bruin and Moore, 1985) require knowledge of both above and within canopy wind speed distributions. In the present case the latter were not available and these methods could therefore not be applied without introducing uncertainties caused by the assumption of a within canopy wind speed distribution (Frumau, 1993).

7.3.2 Wind Speed and Direction

Frequency distributions of wind directions and speeds, measured just above the forest canopies at Tulasewa and Koromani forests, are shown in Figure 7.1A and 7.1B, respectively. The wind direction was predominantly east to southeast and wind speeds were low, seldomly exceeding 5 m s^{-1} (Figure 7.1B). The wind speed as measured at 24.1 m at the Koromani forest meteo site averaged 3.0($\pm$0.8) m. The diurnal cycles of wind speeds were similar to those observed at Nadi Airport (Section 2.4.4) with low values at night and higher values during daytime with a maximum shortly after noon.

7.3.3 Quantification of Aerodynamic Characteristics of Study Forests

Above canopy wind speeds were measured at or at less than the minimum number of levels required for the determination of z_0 and d with most of the previously discussed any methods, and the use of the more sophisticated models (*e.g.* mass conservation methods of Molion and Moore (1983), De Bruin and Moore (1985)) to obtain the surface roughness parameters for Tulasewa and Koromani forests was not justified therefore. As such, d and z_0 were determined using the graphical method. The Richardson number was calculated for each half-hour period and wind profiles were selected for neutral conditions ($-0.01 < Ri < 0.01$). Profiles having wind speeds of less than 1 m s^{-1} at the lowest level (z_1) were excluded, since these may have been influenced by the proximity to the canopy (Frumau, 1993; Opdam, 1993). In view of the undulating topography of the areas surrounding the masts (both masts were on SE facing slopes), local inhomogeneities in the forest canopies (small gaps, roads and stream valleys) and fetch limitations, a dependency of z_0 and d on wind direction was

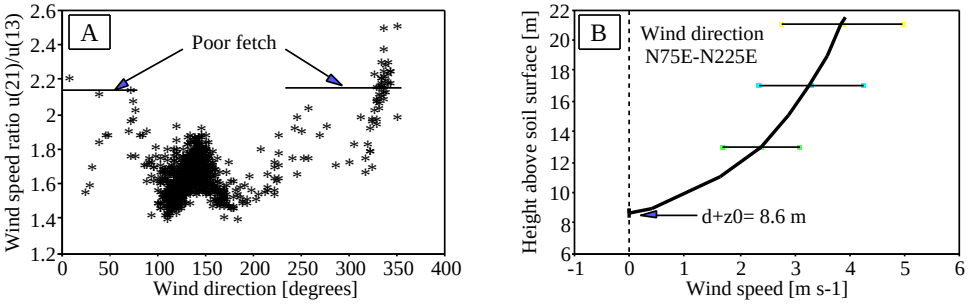

Figure 7.2: *Ratio of* $u(21.1)/u(13.0)$ versus *the wind direction (A), and the curve fitted through the mean wind profile (B; standard deviations represented by vertical and horizontal bars) to determine the level of* $d+z_0$ *(B) for Tulasewa forest according to the graphical method.*

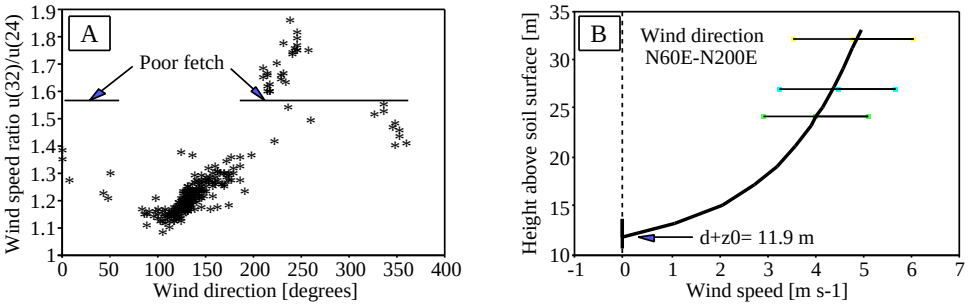

Figure 7.3: *Ratio of* $u(32.1)/u(24.1)$ versus *the wind direction (A), and the curve fitted through the mean wind profile (B; standard deviations represented by horizontal bars) to determine the level of* $d+z_0$ *(B) for Koromani forest according to the graphical method.*

expected. To test this the ratios of $u(z_3)/u(z_1)$ (a measure of the shape of the wind profile) were plotted against wind direction as shown in Figures 7.2A and 7.3A for the Tulasewa and Koromani sites, respectively. These diagrams clearly show that the shape of the profiles, and therefore the magnitudes of z_0 and d, varied with wind direction, with large changes in the ratios observed for those wind directions where the fetch changed from sufficient to poor. A further selection was made therefore, selecting only those wind profiles for which the wind direction was such that the fetch was sufficient. Hence wind profiles for wind directions between N225E–N75E at Tulasewa forest, and N200E–N60E at Koromani forest were excluded, resulting in 971 and 244 variable wind profiles, respectively. The average wind speeds and standard deviations measured at levels z_1, z_2 and z_3 at Tulasewa and Koromani forests have been plotted against height to determine the levels of $d+z_0$ in Figures 7.2B and 7.3B, respectively. Logarithmic curves were fitted by trial and error and the intercepts with the Y-axis provided information on the mean levels and range of $d+z_0$. This resulted in average values of $8.6(\pm 0.5)$ m and $11.9(\pm 1.5)$ m for $d+z_0$ in Tulasewa and Koromani

Table 7.2: *Matrix of* $u(21.1)/u(13.0)$ *values calculated for various combinations of* d *and* z_0*. Ratios close to the average ratio of measured wind speeds at Tulasewa forest are shown in bold typeface, whereas the most likely combination of* z_0 *and* d *is shadowed.*

	Displacement length d, [m]													
z0 [m]	5.7	5.9	6.1	6.3	6.5	6.7	6.9	7.1	7.3	7.5	7.7	7.9	8.1	8.3
0.8	1.335	1.346	1.357	1.370	1.383	1.397	1.412	1.429	1.447	1.466	1.487	1.509	1.534	1.561
0.9	1.354	1.365	1.378	1.391	1.406	1.421	1.438	1.456	1.475	1.496	1.519	1.544	1.571	**1.601**
1	1.372	1.385	1.399	1.413	1.429	1.445	1.463	1.483	1.504	1.527	1.552	1.579	**1.609**	**1.642**
1.1	1.391	1.405	1.419	1.435	1.452	1.470	1.489	1.510	1.533	1.558	1.585	**1.615**	**1.648**	1.684
1.2	1.410	1.424	1.440	1.457	1.475	1.494	1.515	1.538	1.563	1.590	**1.619**	**1.652**	1.688	1.728
1.3	1.429	1.444	1.461	1.479	1.499	1.519	1.542	1.567	1.593	**1.623**	**1.655**	1.690	1.730	1.773
1.4	1.448	1.465	1.483	1.502	1.523	1.545	1.569	1.596	**1.625**	1.656	1.691	1.730	1.773	1.821
1.5	1.468	1.485	1.504	1.525	1.547	1.571	1.597	**1.626**	1.657	1.691	1.729	1.771	1.818	1.870
1.6	1.488	1.506	1.527	1.549	1.572	1.598	**1.626**	1.657	1.690	1.727	1.768	1.814	1.865	1.922
1.7	1.508	1.528	1.550	1.573	1.598	**1.626**	1.656	1.689	1.725	1.765	1.809	1.859	1.914	1.977
1.8	1.529	1.550	1.573	1.598	**1.625**	1.654	1.687	1.722	1.761	1.804	1.852	1.906	1.967	2.036

Theoretical ratio of wind speeds measured at 21.0 m and 13.0 m

forests, respectively.

To obtain individual estimates of d and z_0, the ratios of average wind speeds at the upper, middle and lower levels were calculated and matrices were prepared for each forest using Equation 7.6 to calculate theoretical ratios for various combinations of z_0 and d, keeping in mind that for temperate pine forests z_0 and d are usually in the range of $0.02h$–$0.14h$ and $0.6h$–$0.9h$, repectively (Jarvis *et al.*, 1976). The ratio $u(z_3)/u(z_1)$ averaged $1.625(\pm 0.098)$ and $1.200(\pm 0.060)$ in Tulasewa and Koromani forests, respectively, and using the matrices shown in Tables 7.2 and 7.3 in combination with the previously determined averages of $d + z_0$, resulted in the estimates of d and z_0 given in Table 7.4 for the respective mean wind profiles. The table also includes earlier estimates by Beekman (1992), Frumau (1993), Opdam (1993) and Harkema (1994) for short selected periods from the overall data set.

Even within the reduced data set, for which the fetch was considered sufficient, some dependency of roughness parameters on wind direction existed due to topography and inhomogeneities in the respective forest canopies, with ratios of $u(z_3)/u(z_1)$ ranging from 1.4 to 1.9 at Tulasewa and from 1.1 to 1.4 in Koromani (see Figures 7.2A and 7.3A). Higher than average ratios of $u(z_3)/u(z_1)$, pointing to relatively flat wind profiles, were observed for wind directions around N140E in Tulasewa forest and between N160–180E at Koromani forest. However, the scatter of the wind speed ratios was considerable and, as the resulting variations in z_0 and d were thought to be within 15% of the averages given in table 7.4, no further classification with respect to wind direction was made.

Frumau (1993) also calculated values for d and z_0 for Tulasewa forest using the analytical and mass conservation methods referred to earlier. The analytical methods produced widely varying results, which were sometimes physically unrealistic (*e.g.* negative values of d). However, if the latter were excluded averages of d and z_0 of 7.0 m and 1.5 m, respectively, were obtained which were similar to those presently obtained with the graphical method. Application of the analytical method of Robinson (1962) to various classes of wind speeds and directions indicated that the roughness parameters

Table 7.3: *Matrix of* $u(32.1)/u(24.1)$ *values calculated for various combinations of* d *and* z_0. *Values comparable to the measured* $u(z_3)/u(z_1)$ *ratios at Koromani forest are shown in bold typeface, whereas the most likely combination of* z_0 *and* d *is shadowed.*

	Displacement length d, [m]													
z0 [m]	**9.0**	**9.2**	**9.4**	**9.6**	**9.8**	**10.0**	**10.2**	**10.4**	**10.6**	**10.8**	**11.0**	**11.2**	**11.4**	**11.6**
0.8	1.145	1.147	1.149	1.152	1.154	1.157	1.159	1.162	1.165	1.168	1.170	1.174	1.177	1.180
0.9	1.151	1.153	1.156	1.158	1.161	1.163	1.166	1.169	1.172	1.175	1.178	1.181	1.185	1.188
1.0	1.157	1.159	1.162	1.164	1.167	1.170	1.173	1.176	1.179	1.182	1.185	1.189	1.192	**1.196**
1.1	1.162	1.165	1.168	1.170	1.173	1.176	1.179	1.182	1.186	1.189	1.192	**1.196**	**1.200**	**1.204**
1.2	1.168	1.171	1.173	1.176	1.179	1.182	1.186	1.189	1.192	**1.196**	**1.199**	**1.203**	1.207	1.211
1.3	1.173	1.176	1.179	1.182	1.185	1.189	1.192	**1.195**	**1.199**	**1.203**	1.206	1.210	1.214	1.219
1.4	1.179	1.182	1.185	1.188	1.191	1.195	**1.198**	**1.202**	**1.205**	1.209	1.213	1.217	1.222	1.226
1.5	1.184	1.187	1.190	1.194	**1.197**	**1.201**	**1.204**	1.208	1.212	1.216	1.220	1.224	1.229	1.233
1.6	1.189	1.193	**1.196**	**1.199**	**1.203**	1.207	1.210	1.214	1.218	1.222	1.227	1.231	1.236	1.241
1.7	1.195	**1.198**	**1.201**	**1.205**	1.209	1.212	1.216	1.220	1.225	1.229	1.233	1.238	1.243	1.248
1.8	**1.200**	**1.203**	1.207	1.211	1.214	1.218	1.222	1.227	1.231	1.235	1.240	1.245	1.250	1.255

Theoretical ratio of wind speeds measured at 32.1 m and 24.1 m

were independent of wind speed (range 1–5 m s^{-1}) but confirmed the dependency on wind direction for Tulasewa forest where d dropped sharply from 8.5($\pm$2.0) m for the N110–130E interval to 5.7($\pm$2.0) for the N130–150E interval, with a corresponding increase of z_0 from 0.7($\pm$1.0) m to 2.4$\pm$1.3 m. The results of various mass conservation methods, (using a theoretical function; Cionco, 1965) to simulate the within canopy wind speed distribution) were comparable to those obtained with the graphical and analytical methods (Frumau, 1993). Estimates of 7.0 m for d and of 1.5 m for z_0 for the mean wind profile were obtained with the method of Molion and Moore (1983), whereas the method of De Bruin and Moore (1985) yielded less realistic averages of 5.1 m for d and 1.0 m for z_0 (Frumau, 1993). The mass conservation methods further indicated that d was highest for the N130–150E interval, in contrast to the results obtained with the analytical methods, whereas z_0 remained fairly constant regardless of wind direction. These uncertainties in the dependency of the roughnes parameters on wind direction supported the decision to use averages of d and z_0, rather than to express them as a function of wind direction.

The trees in the Tulasewa forest plot increased some 2.5 m $year^{-1}$ in height during the measurement period and it is therefore not realistic to assume that z_0 and d remained constant over longer periods of time. However, d/h and z_0/h may be considered fairly constant and these, in combination with measured growth rates (Chapter 11), were used in the calculations of the sensible heat flux with the temperature fluctuation energy balance method (Equation 7.24) and of the aerodynamic resistance for the Penman-Monteith method (Equation 5.4). Therefore z_0 increased from 1.3 m in December 1989 to 1.6 m in November 1990, with corresponding values for d increasing from 6.3 m to 7.4 m.

Koromani forest showed no significant increase in height and constant values of z_0 and d were used in the calculations throughout.

Table 7.4: *Summary of forest aerodynamic characteristics as obtained for various selected periods in Tulasewa and Koromani forests under neutral atmospheric conditions.*

Location & method	Wind direction	z0 [m]	d [m]	h [m]	z0/h	d/h	Remarks	Period	Author
TULASEWA FOREST									
Graphical	**N75-225E**	**1.5**	**7.1**	**12.7**	**0.12**	**0.56**	**All weather**	**May-Nov '90**	**Present study**
Graphical	SE	0.8	8.3	12.1	0.07	0.69	Cloudy day	14/5/90	Beekman, 1992
Graphical	SE	0.9	8.1	12.3	0.07	0.66	Sunny day	2/6/90	Beekman, 1992
Graphical	N	1.3	9.4	12.3	0.11	0.76	Rainy day	10/6/90	Beekman, 1992
Graphical	N90-270E	1.3	7.9	12.7	0.10	0.62	All weather	17-22/8/90	Frumau, 1993
Analytical	N90-270E	1.5	7.0	12.7	0.12	0.55	All weather	17-22/8/90	Frumau, 1993
M&M	N90-270E	1.5	7.0	12.7	0.12	0.55	All weather	17-22/8/90	Frumau, 1993
DB&M	N90-270E	1.0	5.1	12.7	0.08	0.40	All weather	17-22/8/90	Frumau, 1993
Empirical		*1.7*		*12.7*	*0.13*				*Szeicz et al., 1969*
Empirical			*8.4*	*12.7*		*0.69*			*Stanhill, 1969*
KOROMANI FOREST									
Graphical	**N60-200E**	**1.4**	**10.4**	**17.8**	**0.08**	**0.58**	**All weather**	**May-Sep '91**	**Present study**
Graphical	SE	0.9	10.2	17.8	0.05	0.58	All weather	Jun-Jul '91	Opdam, 1993
Graphical	SE	1.2	10.2	17.8	0.07	0.57	All weather	May-Jun '91	Harkema, 1993
Empirical		*2.3*		*17.8*	*0.13*				*Szeicz et al., 1969*
Empirical			*11.8*	*17.8*		*0.66*			*Stanhill, 1969*

M&M: Molion and Moore, 1983; DB&M: De Bruin and Moore, 1985.

7.4 Temperature and Relative Humidity

Dry season averages of temperature and relative humidity measured above grassland in the dry season of 1991 were presented in Chapter 5. Corresponding averages measured above Tulasewa (13 m) and Koromani (24 m) forests are presented in Table 7.5. Differences beteween the site were significant. However, these differences may be the result of differences between two seasons themselves as the dry season of 1990 was rather wet and that of 1991 fairly dry (*cf.* Table 6.2). The differences will be discussed in Chapter 9.

7.5 Forest Energy Balance

7.5.1 Introduction

The BREB and TFEB methods use the surface energy balance equation (Equation 7.7) which partitions the incoming energy minus various storage terms (A) between the sensible heat flux H and the latent heat flux λE (Thom, 1975):

$$R_n - D_a - G - J - P_{veg} = A = H + \lambda E \tag{7.7}$$

where R_n is the net radiative input, D_a is the horizontal flux divergence or advective energy flux, G the soil heat flux, J and P_{veg} the fluxes of energy going into aboveground physical and biochemical storages, respectively. Evaporation rates (E,

Table 7.5: *Ranges and averages (standard deviation between brackets) of temperature (°C) and relative humidity (%) measured above Tulasewa and Koromani forests during the dry seasons of 1990 and of 1991, respectively.*

Location	T	Tmin	Tmax	n	RH	RHmin	RHmax	n
Tulasewa Forest, 1990								
Range	18.8-26	13.5-24.5	19.3-30.9	132	67-98	44-98	81-100	132
Average	22.2 (1.4)	18.8 (2.0)	26.5 (2.1)	132	84 (6)	66 (11)	96 (4)	132
Koromani Forest, 1991								
Range	18.4-26.9	16.6-24.8	19.4-31.7	127	53-88	33-88	68-100	124
Average	22.9 (1.5)	20.4 (1.5)	26.1 (1.9)	127	70 (8)	61 (11)	89 (8)	124
Tulasewa <> Koromani	<***	<***	>*		>***	>***	>***	

Significance level: *: 0.10; **: 0.05; ***: 0.01

in mm s^{-1}) can be obtained by dividing the latent heat flux (W m^{-2}) by the latent heat of vaporization of water (λ, in J kg^{-1}) and multiplying by the density of water (1.0 kg l^{-1}). Conventionally, fluxes in the downward direction (incoming) have a positive sign, whereas those in the upward direction (outgoing) are negative (Thom, 1975).

The advective energy flux was neglected in the energy balance as estimates of D_a can only be obtained if horizontal gradients of temperature, humidity and wind speed are known from simultaneous measurements made at a minimum of two sites (Thom, 1975). Under conditions of high R_n the error introduced by neglecting D_a was considered small as the upwind fetches of the Tulasewa and Koromani sites (about 75 and 47 times the height at which R_n was measured, respectively) were thought to be sufficient to limit advective energy inputs from surrounding dry grassland areas to a large extent. However, during periods of rainfall, when R_n is low and the wind direction may differ markedly from the SE, advective energy inputs from surrounding grasslands or the Ocean may play a significant role (*cf.* Section 6.4.1). Neglecting D_a under these circumstances may result in serious errors in H or λE.

The biochemical storage term P_{veg}, representing the use of energy in the production of biomass through photosynthesis, was neglected because it was difficult to measure and because it constitutes generally less than 1% of $R_s \downarrow$ (Brutsaert, 1982).

The magnitudes and the diurnal cycles of the various energy balance components for selected days, representing a range of climatic conditions (*e.g.* sunny, overcast and rainy), at the Tulasewa and Koromani sites will be presented in the following sections.

7.5.2 Net Radiation

The net radiation is the sum of downward and upward fluxes of short-wave and long-wave radiation (Brutsaert, 1982):

$$R_n = \underbrace{R_s \downarrow + \alpha R_s \uparrow}_{shortwave} + \underbrace{R_l \downarrow + R_l \uparrow}_{longwave} \tag{7.8}$$

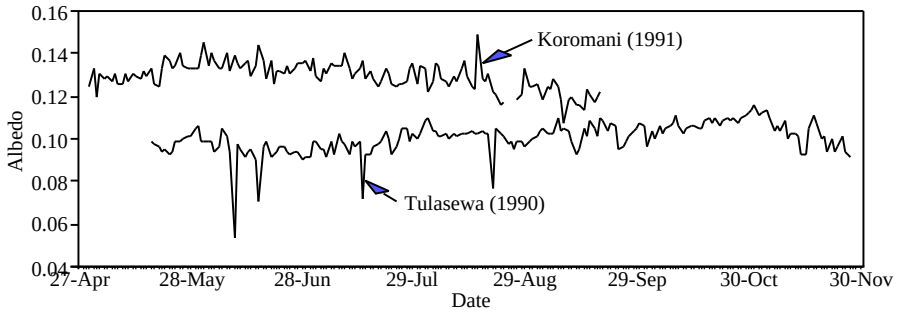

Figure 7.4: *Daily variation in the albedoes at Tulasewa and Koromani forest sites.*

where α represents the surface albedo for short-wave radiation. Incoming radiation consists of direct beam and diffuse short-wave solar radiation and of long-wave sky radiation. Outgoing radiation consists of reflected radiation and terrestrial long-wave radiation. The amount of reflected radiation depends both on the solar radiation intensity and on surface characteristics (*e.g.* albedo, *cf.* Section 5.4.1). The short-wave component of the net radiation is zero at night and the nigthtime R_n is therefore determined by the magnitude of the long-wave components. The opposite is true during daytime when the net short-wave component is much larger than the net long-wave component.

Both downward and upward fluxes of short-wave radiation were measured with the albedometer at Tulasewa and Koromani sites and the average dry-season value for α could therefore be calculated from the ratio of their daily totals. The daily variations in the albedoes of Tulasewa and Koromani forests are shown in Figure 7.4. The average albedo for Tulasewa forest over the period May 17 – November 27, 1990 was $0.100(\pm 0.007)$ (n= 195), whereas that for Koromani forest over the period April 30 – September 19, 1991, was significantly higher at $0.126(\pm 0.008)$ (n= 123). These values are in the range (0.08–0.14) found for temperate pine forests by Jarvis *et al.* (1976). At Tulasewa forest low α-values (down to 0.05) were observed when the canopy was wet, but this was not observed at Koromani forest. Such differences between forests may be caused partly by differences in canopy structure/density between the young and mature forest (Jarvis *et al.*, 1976). Furthermore, the canopy of Koromani forest had been severely damaged by cyclone Sina, which may also have influenced the 1991 value of α to some extent. The diurnal courses of α for Tulasewa and Koromani forests are shown in Figure 7.5.

Because α was fairly constant, R_n may be related to $R_s\downarrow$ empirically using a linear regression equation (Jarvis *et al.* 1976). The resulting expressions for the Tulasewa and Koromani forest sites based on half-hourly data are given by Equations 7.9 and 7.10, respectively.

$$R_n = -21.73(\pm 16.38) + 0.866(\pm 0.001) \cdot R_s\downarrow \qquad \text{n= 7646, } r^2 = 1.00 \tag{7.9}$$

$$R_n = -39.99(\pm 21.01) + 0.846(\pm 0.001) \cdot R_s\downarrow \qquad \text{n= 5938, } r^2 = 0.99 \tag{7.10}$$

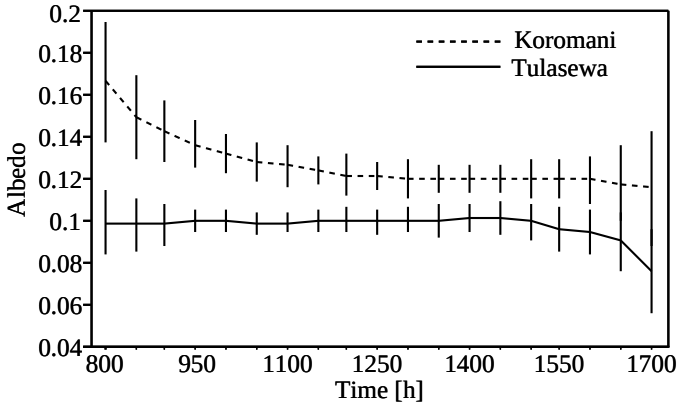

Figure 7.5: *Average diurnal courses and standard deviations (vertical bars) of the albedo at the Tulasewa and Koromani forest sites.*

Due to cracking of the plastic domes moisture entered the net radiometer in Tulasewa forest during a four week period in July and August 1990, and R_n during this period was therefore calculated using Equation 7.9. The net radiometer at the Koromani forest site was installed two weeks later than the other micro-meteorological equipment, and Equation 7.10 was therefore used to calculate R_n for this period.

Not all wavelengths are equally absorbed by vegetation (Ross, 1975). To obtain some insight into these differences, the albedo of photosynthetically active radiation (400–700 nm, α_{par}) for Koromani forest was determined on July 12 (14:00 h) from the ratio of reflected PAR, as measured at seven locations around the tower above the canopy with ceptometer held inverted, to incoming PAR as measured with the instrument above the canopy. This resulted in an α_{par} of 0.04, which is comparable to that given for temperate coniferous forests (0.03) by Ross (1975). The difference between α (300–2500 nm) and α_{par} indicates that reflection occurs mainly at wavelengths higher than 700 nm. Profiles of PAR were measured along the respective meteorological towers as shown in Figure 7.6. The profile for Tulasewa forest represents the average of two profiles measured on June 28, 1990, between 13:00 h and 13:30 h under clear sky conditions, whereas that for Koromani forest was the average of four replications of three profiles measured at different times on July 12, 1991, between 9:00 h and 15:00 h, againd during clear sky conditions. The profiles indicate that a large portion of PAR was absorbed by the foliage in the upper canopy. Vose and Swank (1990) assessed the vertical distribution of leaf area by ceptometer PAR measurements in a 32-year-old *Pinus strobus* plantation forest in North Carolina, USA, with LAI (3.6 m^2 m^{-2}) similar to that of the forests presently studied. The pattern observed was similar to that shown in Figure 7.6, with a sharp decrease of Q_z/Q_0 within the upper canopy from 0.9 at 26 m to less than 0.3 at 20 m. The PAR fraction remained fairly constant at about 0.05 below the canopy.

Diurnal patterns of $R_s \downarrow$, $\alpha R_s \uparrow$, R_n and the long-wave component of R_n for selected days with clear sky, overcast sky, and rainy conditions in Tulasewa and Koromani forests are shown in Figures 7.7 and 7.8, respectively. The net long-wave component was calculated as the difference of R_n and the short-wave component. The long-wave component remained negative throughout the day under all climatic con-

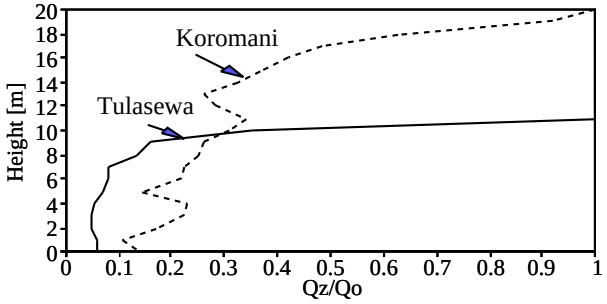

Figure 7.6: *Average profiles of PAR measured along the towers in Tulasewa and Koromani forests, expressed as the ratio of PAR at height z within the canopy (Q_z) to that measured above the canopy (Q_0).*

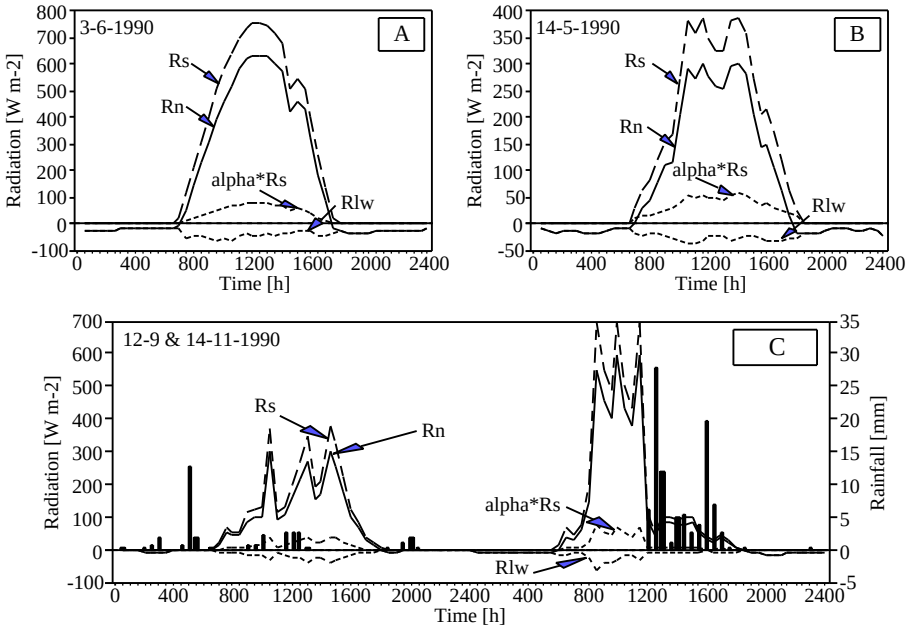

Figure 7.7: *Diurnal patterns of $R_s \downarrow$, $\alpha R_s \uparrow$, R_n and the long-wave component (R_{lw}) of R_n for selected days with clear sky (A), overcast sky (B), and rainy conditions (C) in Tulasewa forest.*

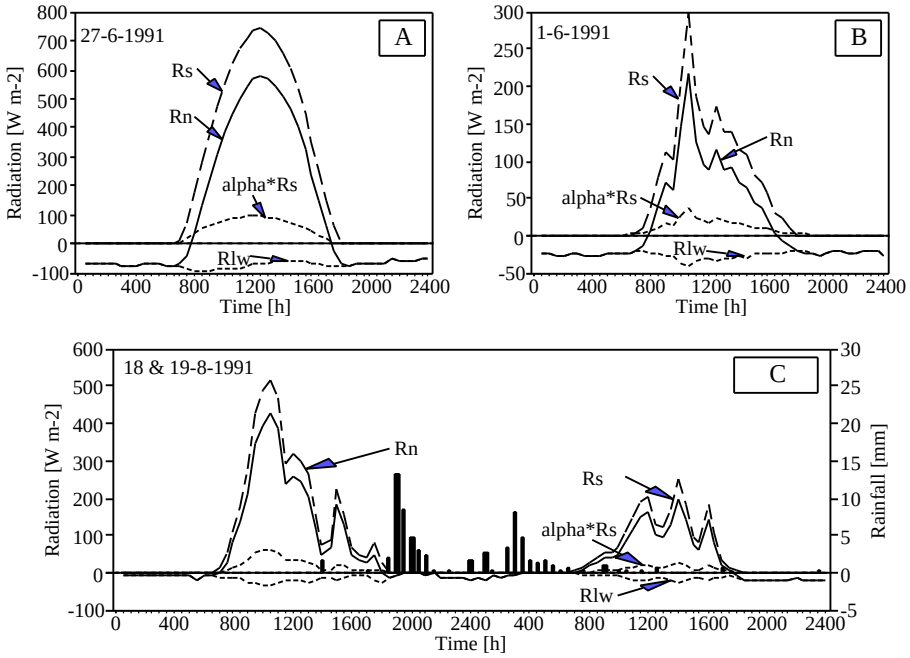

Figure 7.8: *Diurnal patterns of $R_s \downarrow$, $\alpha R_s \uparrow$, R_n and the long-wave component (R_{lw}) of R_n for selected days with clear sky (A), overcast sky (B), and rainy conditions (C) in Koromani forest.*

ditions, with minimum values in the mornings under clear skies. However, downward fluxes of long-wave radiation (emitted by clouds) resulted in less negative values of the net long-wave component, whereas it approached zero during periods of high rainfall (Figures 7.7C and 7.8C).

7.5.3 Physical and Biochemical Storage Terms

The total physical energy storage (J) within a column of unit cross-sectional area extending from the soil surface to the level at which R_n is measured can be separated into three terms:

$$J = J_h + J_w + J_{veg} \tag{7.11}$$

where J_h and J_w are the sensible and latent heat storage in the air within the stand, respectively, and J_{veg} is the rate of change in the heat content of the above-ground part of the vegetation (Thom, 1975). As most of the energy stored in each of these components during daytime will be released again during nighttime, the total energy storage may be negligible on a daily basis. However, on a half-hourly basis the storage in these components cannot be neglected (Stewart and Thom, 1973), especially during periods of low R_n and rapid changes in temperature (*e.g.* sunrise, sunset). The magnitudes of J_h and J_w are described by Equations 7.12 and 7.13, respectively (Thom, 1975):

$$J_h = \int_0^{z_{Rn}} \rho c_p \frac{\partial T}{\partial t} \cdot dz \tag{7.12}$$

$$J_w = \int_0^{z_{Rn}} \rho c_p \frac{\partial q}{\partial t} \cdot dz \tag{7.13}$$

where z is the height above the soil surface, z_{R_n} is the height of the R_n measurement, ρ and c_p are the density and heat capacity of the air, t is the time, and T and q are the temperature and specific humidity of the air, respectively (see Appendix 22.2 for details). Similarly, the amount of heat stored in the vegetation is described by Equation 7.14:

$$J_{veg} = \int_0^{h} \rho_{veg} c_{veg} \frac{\partial T_{veg}}{\partial t} \cdot dz \tag{7.14}$$

where h is the mean vegetation height, ρ_{veg} and c_{veg} are the density and specific heat of the vegetation, and T_{veg} is the temperature of the vegetation.

Assuming that ρ and c_p may be considered constant over the height of the air column, and with t= 1800 s for half-hourly measurements, the expressions for J_h and J_w may be simplified to respectively (Thom, 1975):

$$J_h = \frac{c_p \cdot \rho \cdot z_{R_n}}{1800} \Delta T \tag{7.15}$$

$$J_w = \frac{\lambda \cdot \rho \cdot z_{R_n}}{1800} \Delta q \tag{7.16}$$

and the expression for J_{veg} may be simplified to Equation 7.17 by substitution of the integral of $\rho_{veg} \cdot dz$ from $z = 0$ to $z = h$ by the mass of the vegetation per unit area (fresh biomass, M_{veg}).

$$J_{veg} = \frac{c_{veg} \cdot M_{veg}}{1800} \Delta T_{veg} \tag{7.17}$$

In these expressions ΔT and Δq represent the rates of changes in representative temperature and specific humidity values for the whole column, whereas ΔT_{veg} is the rate of change of the mean temperature of the biomass.

Within-canopy 30-minute averages of T and q were obtained at heights of 6.1 m and 12.8 m in Tulasewa and Koromani forests, respectively. Figure 7.6 has shown that most PAR had already been absorbed above these levels. Therefore the values of T and q measured at these heights were assumed representative for the conditions within the forests and were subsequently used to calculate J_h and J_w.

For the calculation of J_{veg}, data on the biomass, its temperature and c_{veg} are required. Values for the oven-dry standing biomasses of the Tulasewa and Koromani forest plots were taken from Chapter 11 representing estimates of 7.0 kg m^{-2} and 14.6 kg m^{-2}, respectively. The fresh biomass needed in the present calculations was obtained using conversion factors from Section 11.3.2, resulting in values of 14.9 and 28.1 kg m^{-2}, respectively. The heat capacity of fresh *Pinus caribaea* wood was unknown and was taken as 70% of the heat capacity of water, following Thom (1975) and McCaughey (1985). A large part of the forest biomass in the study plots was concentrated in the lower part of the tree stems (Chapter 11) and the tree bole temperatures measured at various heights and depths in the stems were averaged such that the distribution of the biomass with height was taken into account to obtain representative average tree temperatures. Both forests were even-aged monocultures, which will reduce between-tree temperature variation as compared to more complex natural vegetation types (McCaughey and Saxton, 1988) and the calculated temperatures for the single sample trees in each forest were therefore assumed to be representative for the whole stand.

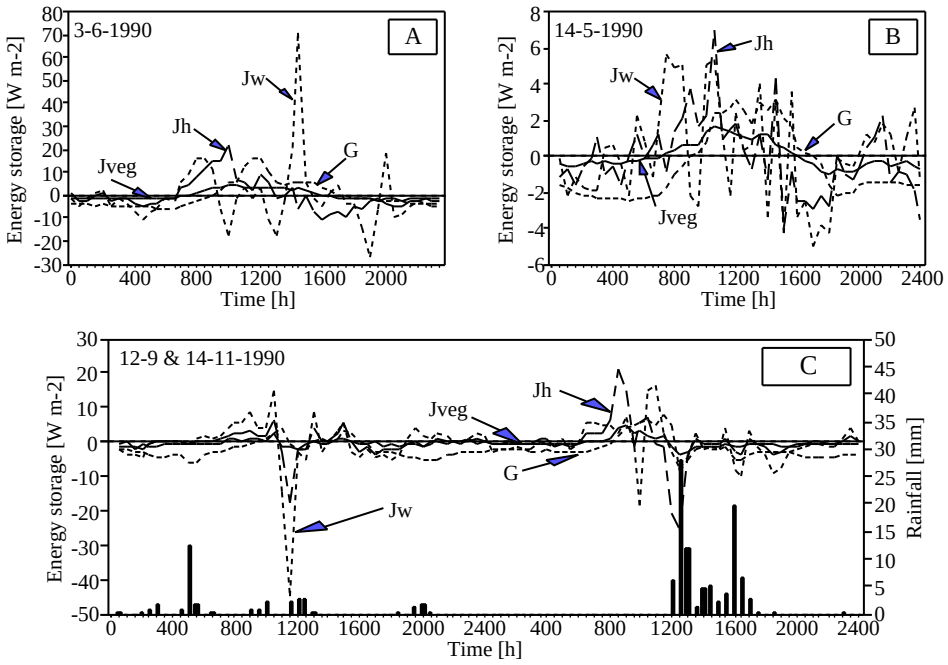

Figure 7.9: *Diurnal patterns of J_h, J_w, J_{veg} and G for selected days with clear sky (A), overcast sky (B), and rainy conditions (C) in Tulasewa forest.*

Finally, energy storage occurs in the soil through changes of its temperature. The

spatial variation in soil heat flux (G) was assumed small as the radiative inputs to the soil surface were relatively low due to interception of the light by the forest canopy (Figure 7.6), the undergrowth and the litter layer. As such averages provided by the two soil heat flux plates were assumed to be representative for the whole stand.

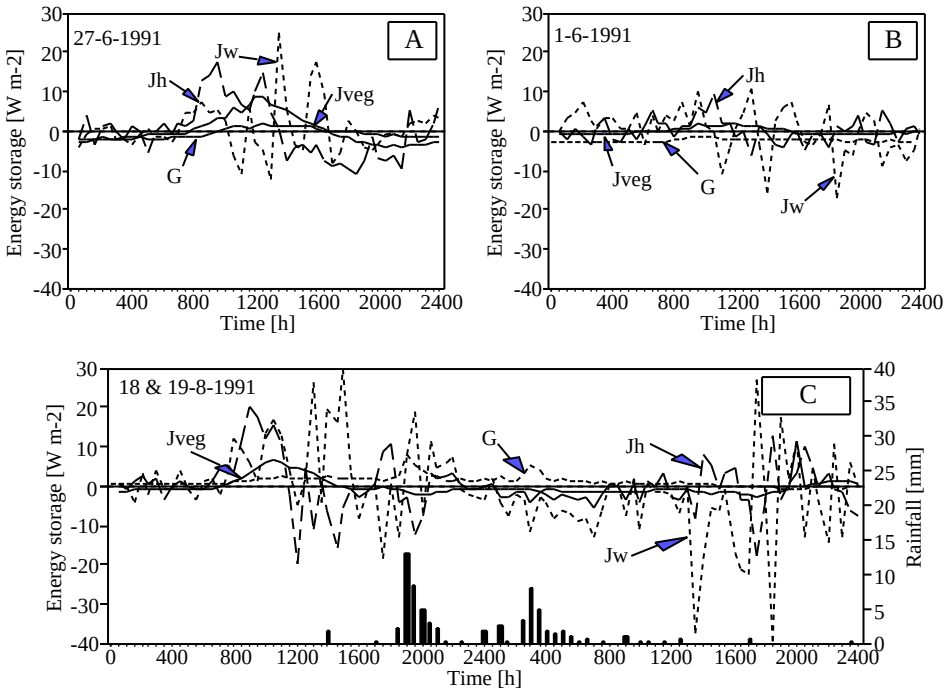

Figure 7.10: *Diurnal patterns of J_h, J_w, J_{veg} and G for days with clear sky (A), overcast sky (B), and rainy conditions (C) in Koromani forest.*

The storage terms were calculated for each 30-minute interval during the respective dry season measurement campaigns. Typical examples of the diurnal patterns of J_h, J_w, J_{veg} and G in Tulasewa and Koromani forests under various climatic conditions are shown in Figures 7.9 and 7.10. On dry days J_h, J_{veg} and G showed distinct diurnal patterns, with energy going into storage (positive values) in the morning and early afternoon, followed by a release of energy (negative values) in the late afternoon and night (Figures 7.9A and 7.10A). The cooling effect of rainfall caused the release of energy, resulting in negative values of J_h, J_{veg} and G. Unlike the other storage terms, J_w did not show a distinct diurnal pattern and under such conditions (Figures 7.9C and 7.10C) fluctuated considerably during daytime with periods of energy going into latent heat storage often being followed by periods of energy release.

Fluxes of J_h, J_{veg} and G were invariably low, remaining within the range -10 to 20 W m^{-2}, whereas the variation of J_w was much larger with extremes ranging from -50 W m^{-2} to 70 W m^{-2} (Figures 7.9 and 7.10). The soil heat flux at Tulasewa forest reached values of up to 20 W m^{-2} on sunny days, whereas that at Koromani forest was in the range of -6 to 7 W m^{-2}. Total daytime energy storage was generally less than 3% of R_n on dry days. On rainy days, however, the total daytime storage could

exceed 10% of R_n, and should therefore not be neglected. The storage terms may thus safely be neglected on dry days but should be taken into account around sunrise and sunset as well as during rainy periods.

7.6 Sensible and Latent Heat Fluxes

7.6.1 The Temperature Fluctuation and Bowen Ratio Energy Balance Methods

One of the conventional methods to determine the sensible and latent heat fluxes H and λE is the Bowen Ratio Energy Balance method (Angus and Watts, 1984). The Bowen ratio (β) is defined as the ratio of the sensible heat flux to the latent heat flux (Thom, 1975):

$$\beta = \frac{H}{\lambda E} \tag{7.18}$$

When both the available energy A (Equation 7.7) and β are known, the magnitudes of H and λE can be determined from Equations 7.19 and 7.20, respectively.

$$H = \frac{A}{1+\beta^{-1}} \tag{7.19}$$

$$\lambda E = \frac{A}{1+\beta} \tag{7.20}$$

The exchanges of sensible and latent heat are turbulent transfer processes which, in the absence of advection and under steady conditions, may be described by (Thom, 1975):

$$H = -\rho c_p \cdot K_H \frac{\partial T}{\partial z} \tag{7.21}$$

$$\lambda E = -\rho c_p \cdot K_E \frac{\partial q}{\partial z} \tag{7.22}$$

where K_H and K_E are eddy diffusivity coefficients for heat and vapour respectively (Thom, 1975). The exact magnitudes of these coefficients are generally unknown and depend on the stability conditions of the atmosphere. K_H may be assumed equal to K_E (Monin and Yaglom, 1971) and as ∂T and ∂q may be approximated by the finite difference of measurements made at two levels within a layer of constant flux above a homogeneous forest canopy, the Bowen ratio becomes (Jarvis *et al.*, 1976):

$$\beta = \frac{c_p}{\lambda} \cdot \frac{T_2 - T_1 + \Gamma \cdot (z_2 - z_1)}{q_2 - q_1} \tag{7.23}$$

The gradients of T and q are generally small above forest canopies, which places heavy demands on the quality of the instruments used for their measurement, especially when these measurements need to be made over longer periods of time.

As an alternative, β may be obtained from standard deviations and correlation coefficients of dry- and wet-bulb temperatures, as measured with fast-response thermocouples at a single level above the canopy (Vugts *et al.*, 1993). With this method the need for expensive equipment for gradient measurements and time consuming calibrations is eliminated. Vugts *et al.* (1993) found good agreement between fluxes of H and λE as determined on the one hand from Bowen ratios based on measured gradients of T and q and values of β obtained with the correlation method for a two-day period

in Tulasewa forest. However, due to problems with the supply of moisture to the wick of the wet-bulb thermocouple sensor the correlation method could be used for the calculation of β for short periods of time (several days) only. The method will therefore not be discussed further, and the reader is referred to the publication by Vugts *et al.* (1993) for more details. Improvements of the wet-bulb sensors are presently being made and tested at FES-VUA, and the usefulness of this promising method depends on whether reliable wet-bulb temperature measurements can be made in future.

Arguably, the best way to determine H and λE is the eddy correlation technique (Shuttleworth *et al.*, 1984), but the costs and delicacy of the instruments (sonic anemometers) are likely to prohibit the day-to-day application of this method in undeveloped tropical countries.

7.6.2 Application of the Temperature Fluctuation and Bowen Ratio Energy Balance Methods

A cheap and reliable alternative to determine H is the temperature fluctuation method (Tillman, 1972; De Bruin, 1982; Lloyd *et al.*, 1991; Vugts *et al.*, 1993; De Bruin *et al.*, 1993). When R_n and energy storage components are also measured, λE may be deduced from the energy balance equation (Equation 7.7) and it is thus referred to as the TFEB method. Turbulent motions of the air near the vegetation canopy are responsible for most of the vertical transfer of heat (Thom, 1975). The standard deviation of the temperature (σ_T, obtained from high frequency measurements of temperature with fast-response thermocouples) may serve as a measure of the intensity of temperature fluctuations caused by turbulence, and is therefore related to H with the term $\frac{\partial T}{\partial z}$ in Equation 7.21 effectively being replaced by $\frac{\sigma_T}{z}$. Tillman (1972) obtained the following expression relating T and σ_T to H under unstable atmospheric conditions ($Ri < -0.05$), where z is replaced by $z - d$ to account for tall vegetation and h_σ is a constant equal to 0.7 (Wijngaard and Cote, 1971):

$$H = h_\sigma \rho c_p \sqrt{(z-d)\frac{g}{T}} \cdot \sigma_T^{1.5} \tag{7.24}$$

Although the formula was developed for application during unstable conditions ($Ri < -0.5$), Frumau (1993) showed that the error in H remained less than 10% if the formula was applied to situations with $-0.5 < Ri < -0.1$ at Tulasewa forest. At near-neutral atmospheric stability ($Ri \approx 0$) errors in H of up to 65% were observed when equation 7.24 was used (Frumau, 1993). However, as H and λE are generally small under such conditions the error in the daily ET total as a result of the error in H remains low. Errors in H resulting from uncertainties in d may be minimized by measuring T and σ_T at sufficient height above the forest canopy (Vugts *et al.*, 1993).

The TFEB method seems to be less sensitive to inhomogeneities in the terrain and vegetation than the BREB method, and has the additional advantage that calibration errors are avoided by measuring at a single level. However, the method cannot be used under stable atmospheric conditions and, if the thermocouples are not shielded, neither during periods of rainfall.

Vugts *et al.* (1993) and Frumau (1993) compared estimates of H and λE as obtained with the **TFEB** method over a two-day period at Tulasewa forest with those obtained with the **BREB** method. Both methods gave comparable results with differences generally being less than 10%. A similar exercise on the data collected at Tulasewa and Koromani forests is presented below, using much larger data sets. The Bowen ratio was calculated for 30-minute intervals over a period of 30 (Tulasewa

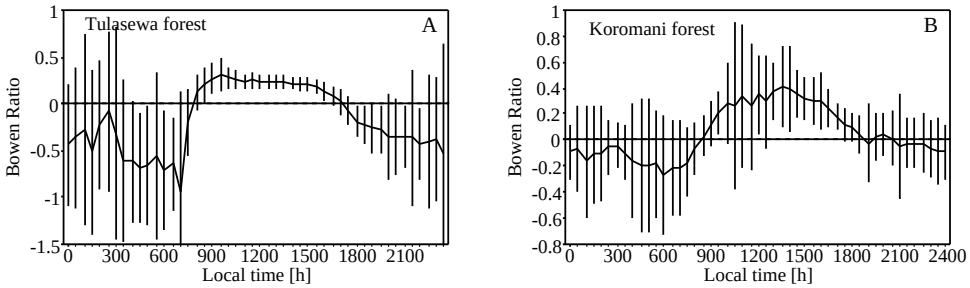

Figure 7.11: *Average diurnal course of β at (A) the Tulasewa (n= 30) and (B) the Koromani forest (n= 34) sites. Standard deviations of the means represented by vertical bars.*

forest) to 34 (Koromani forest) dry days with varying soil moisture deficits. At both forests β was calculated from temperature and humidity data collected at the highest (z_3) and lowest (z_1) levels with the calibrated Rotronic sensors. Half-hourly periods for which the wind direction was such that the fetch was insufficient (Section 7.3.3) were excluded. Estimates of H were obtained from β and the corresponding available energy A using Equation 7.19. The average diurnal patterns of β for each of the forest sites are shown in Figure 7.11 A and B. The Bowen ratio was usually negative at night reaching minimum values of -0.7±0.64 and -0.3±0.46 just before sunrise in Tulasewa and Koromani forests, respectively. After sunrise, β increased sharply to a maximum of 0.3±0.2 in the early morning (9:00–10:00 h) in Tulasewa forest, after which a gradual decrease occurred towards negative values in the late afternoon (18:00 h). The diurnal course of β at Koromani forest differed in that higher daytime values and a maximum of 0.4±0.3 in the early afternoon rather than in the morning. The higher β values observed for Koromani forest may be caused by its age, and possibly also by the damage afflicted to the canopy by cyclone Sina, which may have reduced the potential of the forest to evaporate to the extent that more energy was available for the sensible heat flux (*cf.* Table 6.8). The calculated values of β were well within the range of 0.1 to 1.5 for dry-canopy daytime values for coniferous forests in the temperate zone given by Jarvis *et al.* (1976).

The TFEB method was used to calculated H for half-hourly intervals with unstable conditions ($Ri <$ -0.01) and wind directions such that the fetch was sufficient. The average diurnal courses of the Richardson number at Tulasewa and Koromani forests for the periods under consideration are shown in Figures 7.12A and 7.12B, respectively. Near-neutral to stable conditions ($Ri >$ -0.01) prevailed during the late afternoon and at night, implying that the TFEB method could not be used to calculate H for these periods. The atmosphere generally turned unstable in the early morning (8:00–9:00 h), with the average Ri reaching minimum values of -0.55(±0.87) at 9:00 h in Tulasewa forest and of -0.22(±0.47) around 10:00 h in Koromani forest. In the early afternoon Ri increased to values of around -0.07 and then remained fairly constant until the late afternoon (17:00 h). As such the use of the TFEB method for the determination of H was generally restricted to daytime conditions (8:00–17:00 h).

The sensible heat fluxes for the periods under consideration were calculated using T and σ_T values measured with the thermocouple at the highest level to minimize the effects of errors in d on H (Frumau, 1993; Vugts *et al.*, 1993). Displacement lengths

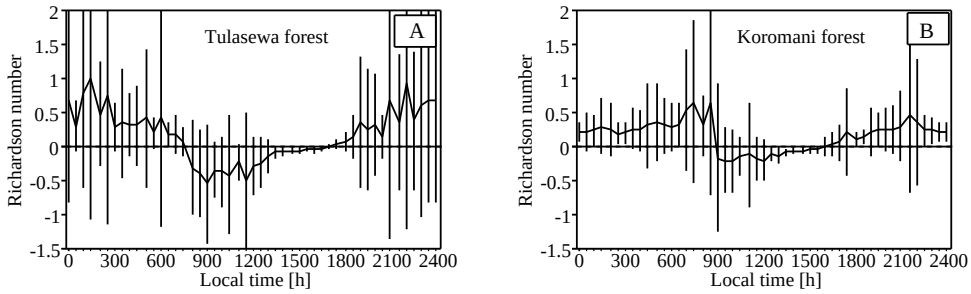

Figure 7.12: *Average diurnal course of the Richardson number at (A) Tulasewa (n= 30) and (B) Koromani forest (n= 34). Standard deviations of the means represented by vertical bars.*

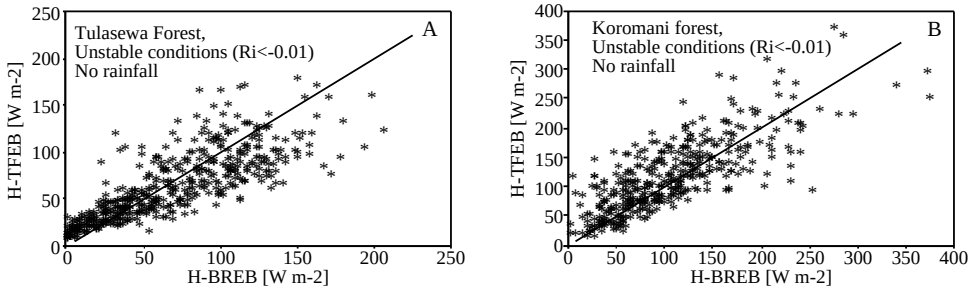

Figure 7.13: *Half-hourly fluxes of sensible heat obtained with the TFEB method* versus *corresponding values obtained with the BREB method for (A) Tulasewa (n= 478) and (B) Koromani (n= 404) forest. The solid line represents equal values.*

of 7.1 m and 10.4 m were used in the calculations for Tulasewa and Koromani forests, respectively (Section 7.3.3). The results of the TFEB method are plotted against those of the BREB method in Figures 7.13A and 7.13B for Tulasewa and Koromani forests, respectively. The methods showed good agreement with no significant differences (α= 0.05) between averages of H, although the average H obtained with the TFEB method was about 8% less than that obtained with the BREB method in Tulasewa forest. On the other hand, the TFEB method overestimated H on average by about 13% at the Koromani forest site.

The agreement between the two methods was less good for the individual half-hourly values as indicated by the large scatter in Figures 7.13A and 7.13B. Some of the scatter will undoubtedly have been caused by errors in H as obtained by the BREB method, because this method is very sensitive to errors in measured gradients of T and q (Angus and Watts, 1984). Measured gradients of T and q were in the ranges of 0.01–0.03 °C m^{-1} and 2–4·10^{-5} kg m^{-1}, respectively. The Rotronic sensors were sufficiently accurate for the measurement of the temperature gradients but failed occasionally in the measurement of q (possibly due to the filter surrounding the sensor), resulting in unrealistic values of β, and therefore of H and λE. This is illustrated in

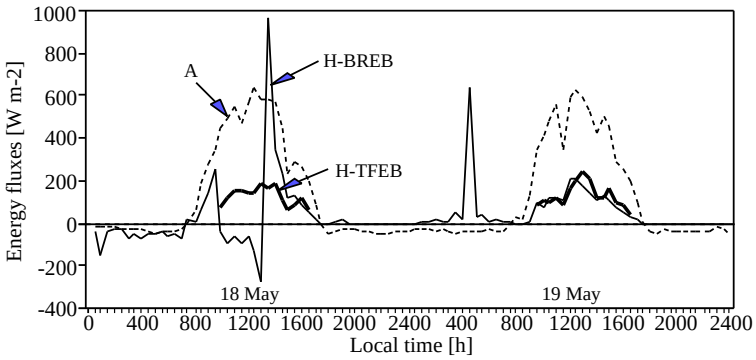

Figure 7.14: *Comparison between fluxes of sensible heat as determined with the BREB and TFEB methods, and available energy on 18–19 May 1991 at the Koromani forest site.*

Figure 7.14 where the sensible heat fluxes over a two-day period at the Koromani forest site are shown. The diurnal courses of the available energy, temperatures and relative humidities were similar on both days, and so were the sensible heat fluxes obtained with the TFEB method. However, the BREB method provided unrealistic values of H during the morning and early afternoon of the first day, whereas both methods compared well on the second day (Figure 7.14).

The standard deviation of temperature is positive by definition and will never be zero due to instrumental noise in the thermocouple – datalogger system. As such the outcome of Equation 7.24 is inherently larger than zero. The influence of instrumental noise on σ_T may be considered negligible if temperature fluctuations (and therefore H) are large, but may cause an overestimation of H if the temperature remains fairly constant ($H \approx 0$ W m^{-2}). In practice a minimum σ_T of 0.05 °C was observed for periods when H-BREB was close to zero. Assuming that the minimum σ_T could be wholly attributed to noise, a minimum offset of about +10 W m^{-2} would be expected. The sensitivity of the TFEB method to errors in d was tested for the Koromani and Tulasewa forest sites using 3121 and 1525 30-minute periods with $Ri < -0.01$, dry conditions and $A > 50$ W m^{-2}. For both data sets a 15% error in d resulted in errors of less than 4% of average values of H and of less than 1.5% in those of λE. As such the use of a constant d, independent of wind direction, to calculate H will not have caused large errors in the determination of λE and is therefore justified.

7.6.3 Penman-Monteith Model

Neither the TFEB method nor the BREB method could provide a continuous time series of H or λE and the Penman-Monteith model (Equation 5.3) was therefore used for the determination of daily evapotranspiration rates throughout the respective observation periods. Application of the model requires knowledge of the surface resistance r_s, which varies both with micro-meteorological and soil moisture conditions (Monteith, 1965; Shuttleworth, 1988). When estimates of λE are available (*e.g.* via the BREB or TFEB methods), the Penman-Monteith formula can be rearranged and used inversely

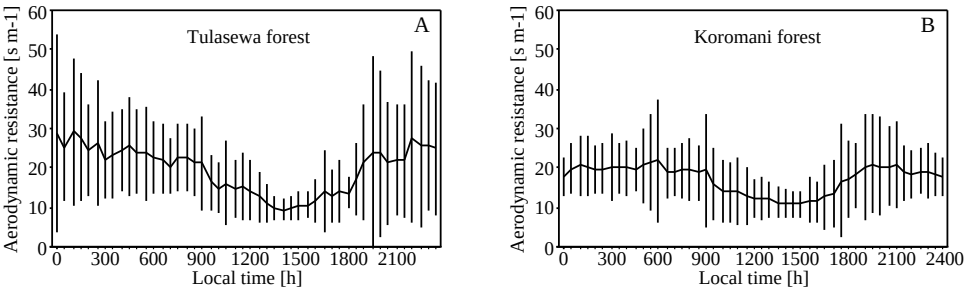

Figure 7.15: *Average diurnal courses of r_a in (A) Tulasewa (n= 31 days) and (B) Koromani (n= 30 days) forests. Standard deviations around the mean are represented by the vertical bars.*

to provide estimates of r_s:

$$r_s = \frac{\rho c_p}{\gamma} \cdot \frac{\delta e}{E} + r_a \cdot \left(\frac{\Delta A}{\gamma E} - \frac{\Delta}{\gamma} - 1 \right) \tag{7.25}$$

where r_a may be obtained from measured wind speeds for known values of z_0 and d (Section 7.3.3) according to Equation 5.4.

Average diurnal patterns of r_a are shown in Figures 7.15A and 7.15B for Tulasewa and Koromani forests, respectively. In spite of the differences in height of the forests the aerodynamic resistances were quite similar, with daytime averages of 14.1(±8.2) s m^{-1} and 13.5(±7.6) s m^{-1} and afternoon minima of 9.4(±2.8) s m^{-1} and 10.7(±3.2) s m^{-1} at Tulasewa and Koromani forests, respectively. The errors in average r_a as a result of errors of 15% in both d and z_0 were less than 23% and 18% in Tulasewa forest and Koromani forests, respectively.

Equation 7.25 was used to calculated r_s for Tulasewa and Koromani forests from estimates of λE, as obtained with the TFEB method, and average diurnal courses of r_s for the two forests are shown in Figures 7.16A and 7.16B, respectively. The surface resistance was high during the night and dropped steeply shortly after sunrise after which it remained low until late in the afternoon. The daytime (8:00-17:00 h) average r_s was 43(±21) s m^{-1} in Tulasewa forest, with a minimum of 35(±11) s m^{-1} in the morning, whereas that in Koromani forest was higher at 113(±126) s m^{-1} with a minimum of 62(±20) s m^{-1}. The sensitivity of the calculated r_s to errors in d and z_0 was low, with errors of 15% in both d and z_0 resulting in errors of less than 3% and 6% in average values of r_s in Tulasewa and Koromani forests, respectively.

Measurements of stomatal resistances with a porometer in the canopy of Koromani forest (Opdam, 1993) indicated that r_{st} followed the diurnal course of r_s, although at higher values. Stomatal resistances above 15000 s cm^{-1} were observed throughout the canopy before sunrise (6:30 h) on July 17, 1991, after which r_{st} dropped sharply to 356(±160) s m^{-1} at 7:20 h and remained fairly constant until about 17:00 h when r_{st} increased again to values wel above 1000 s m^{-1}. There was a distinct decrease in r_{st} with height in the canopy, which was also observed in tropical rainforest in Amazonia by Roberts *et al.* (1990). The daytime average r_{st} in the lower canopy (obtained from 35 measurements on five needle sets at 13 m) amounted to 594(±220) s m^{-1}, and decreased to 512(±225) s m^{-1} at mid canopy level (16 m) and 406(±140) s m^{-1}

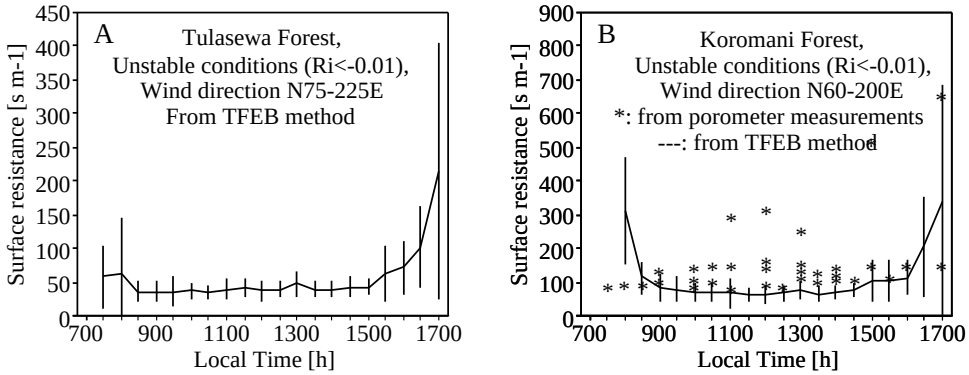

Figure 7.16: *Average diurnal patterns of r_s in (A) Tulasewa (n= 31 days) and (B) Koromani forest (n= 12 days). Estimates of r_s (*) obtained from measurements of r_{st} and LAI (Koromani forest only) added for comparison. Standard deviations around the mean represented by vertical bars.*

near the tree top (19 m). Assuming that the bulk stomatal resistance for the whole canopy could be approximated by the average of the measurements in the upper and middle regions of the crown, where most of the foliage biomass was (*cf.* Roberts *et al.*, 1990), and using a LAI of 3.5 m^2 m^{-2} (Section 11.3.6) an average r_s of 131($\pm$64) s m^{-1} was calculated (see also Section 5.4.4). This is quite comparable to the daytime average obtained with Equation 7.25 from the TFEB method (Figure 7.16B). The good agreement between the two methods for the determination of r_s suggests that the combination of porometer measurements of r_{st} and measurements of the LAI with a ceptometer may provide a good indication of the surface resistance of forests located in terrain that is not suited to the use of micro-meteorological methods.

We were not able to find any information on r_s or r_{st} of other tropical pine plantations for comparison with the values presented above. However, in Japan, Sugita (1987) calculated the surface resistance of a 10–13 m high *Pinus densiflora* forest from a combination of eddy correlation measurements and the Penman-Monteith model and obtained monthly daytime averages ranging from 40 and 120 s m^{-1} over the period of a year. Jarvis *et al.* (1976) provided a list of minimum r_{st} values for coniferous forests in the temperate zone, with r_{st} ranging from 120 to 950 s m^{-1} for current year needles, whereas values up to 2700 s m^{-1} were measured in old growth. This suggested that the values presently found for r_s and r_{st} were within the normal range for (temperate) coniferous forests.

To allow the inclusion of the effect of variations in soil moisture deficit (SMD) on r_s, in addition to those in micro-meteorological conditions, values of SMD were derived for the upper 1 m of soil. Firstly field capacity conditions (drainage just stopped) were assumed whenever soil moisture tensions reached a value of pF= 2.0. Measurements of volumetric moisture content (θ) were converted to soil water tension via the soil moisture retention curves given in Appendix 25. Discontinuous time series of soil moisture deficits could then be calculated for the Tulasewa and Koromani forest plots

by substracting actual moisture content, as measured with the capacitance probe, from the moisture content at field capacity. A total of 20 days were selected with SMDs ranging from zero to 115 mm for Tulasewa forest (SMD_{max}= 208 mm, Section 4.3.4) and 13 days with SMDs ranging from 0 to 46 mm for Koromani forest (SMD_{max}= 136 mm). The data sets were divided so as to conform to the following conditions:

- Unstable atmospheric conditions (Ri < -0.01)
- No rainfall
- Wind direction such that the fetch was sufficient

For illustrative purposes graphs of r_s against the available energy A, vapour pressure deficit VPD, SMD, wind speed u and temperature T measured at 32.1 m above Koromani forest are shown in Figures 7.17A–E, respectively. Corresponding graphs for Tulasewa forest were similar and are not shown. Figure 7.17A indicates that separate expressions were necessary for the modelling of r_s during daytime (a gradual decreases with increasing A) and during the early morning and late afternoon (sharp increase with decreasing A). Separate data sets were compiled for daytime conditions and early morning – late afternoon conditions. Daytime periods represented data collected between 8:00 h and 17:00 h, with $A > 200$ W m^{-2} at Tulasewa forest and $A > 120$ W m^{-2} at Koromani forest. Multiple linear regression techniques were used to relate r_s (in s m^{-1}) to A (W m^{-2}), VPD, (mbar), SMD (mm), u (m s^{-1}) and T (°C) (*cf.* Shuttleworth, 1988). The following expression was found for r_s in Tulasewa forest for early morning – late afternoon periods:

$$r_s = 677 - 3.46A + 11.07VPD - 44.71SMD$$
$$\text{n= } 35,\ r^2 = 0.64 \qquad (7.26)$$

where most of the variation was explained by the available energy ($r^2 = 0.61$) while the inclusion of VPD and SMD increased the coefficient of determination to 0.64. The inclusion of T and u did not improve the regression significantly ($r^2 = 0.66$) and these were therefore not included. Daytime r_s may be calculated from the equation:

$$r_s = 28.9 - 0.068A - 4.27VPD - 0.11SMD$$
$$\text{n= } 215,\ r^2 = 0.58 \qquad (7.27)$$

where A and VPD explained 52% of the variation in r_s, whereas inclusion of SMD increased the coefficient of determination to 0.58. Inclusion of T and u again did not improve the fit significantly, increasing the r^2 to 0.60.

Similarly, the early morning – late afternoon expression found for Koromani was:

$$r_s = 850 - 5.48A + 60.2VPD - 6.9u - 23.6T$$
$$\text{n= } 35,\ r^2 = 0.53 \qquad (7.28)$$

where A explained 21% of the variation in r_s. Inclusion of VPD, u and T in the regression increased the coefficients of determinations to 0.50, 0.51 and 0.53, respectively. The daytime expression obtained from the Koromani data was:

$$r_s = -87.6 - 0.21A + 5.0VPD - 2.9u + 8.5T$$
$$\text{n= } 183,\ r^2 = 0.59 \qquad (7.29)$$

where 22% of the variation in r_s was explained by A. Inclusion of VPD, u and T increased the coefficients of determinations to 0.49, 0.54 and 0.59, respectively. Unlike

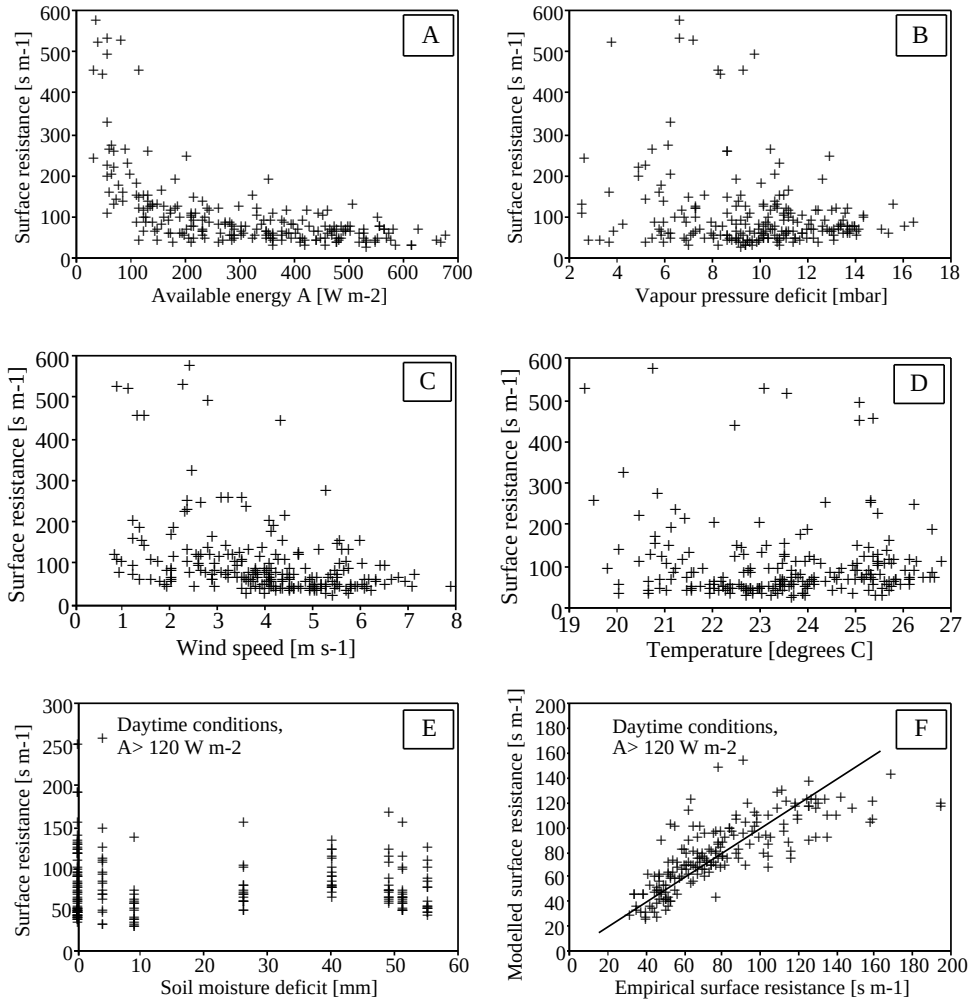

Figure 7.17: *Surface resistance* r_s versus *available energy A (A), vapour pressure deficit (B), wind speed (C), temperature (D) and soil moisture deficit (E) for Koromani forest. Figure F shows empirical values of* r_s*, as derived from the TFEB method, against values obtained with the regression models.*

the situation at Tulasewa inclusion of SMD did not increase the coefficient of determination in Koromani forest. A plot of the r_s values calculated with Equation 7.29 against empirically derived values data (TFEB method plus Equation 7.25) in Koromani forest has been added to Figure 7.17F to illustrate the scatter associated with the use of the above expressions.

Daily values for SMD were required for the calculation of r_s with Equations 7.26 and 7.27 for Tulasewa forest. Since daily soil moisture measurements were not made estimates of SMD for the upper metre of the soil were derived with a model based on a similar model described by Calder *et al.* (1983) . The model required daily rainfall totals (P) and estimates of the Penman open water evaporation (Penman, 1948; Appendix 22.2) as inputs to solve a soil water balance for SMD at a daily time step. When the soil is at or drier than field capacity ($SMD > 0$ mm) drainage was assumed negligible and the change in SMD was described by the following equation:

$$SMD_{i+1} = SMD_i - P + f_i \cdot E_0 \tag{7.30}$$

where i is the day number. When moisture content exceeded field capacity ($SMD <$ 0 mm), Equation 7.30 was modified to simulate drainage according to:

$$SMD_{i+1} = 0.5SMD_i - P + f_i \cdot E_0 \tag{7.31}$$

The factor f_i was introduced to allow for the extraction of moisture by tree roots from depths below the upper metre of the soil. Its value decreased with increasing SMD because the fraction of moisture extracted from the upper metre of soil is likely to decrease with increasing deficits in this layer. As such the following classes were used for the estimate of f_i:

- If SMD_i <0 mm: f_i= 1.0
- If 0< SMD_i <50 mm: f_i= 0.65
- If 50< SMD_i <80 mm: f_i= 0.50
- If 80< $SMD_i < SMD_{max}$ mm: f_i= 0.35
- If $SMD_i > SMD_{max}$ mm: f_i= 0.0

The modelled SMDs matched those derived from soil moisture measurements for the period July – November 1990 rather well (Figure 7.18), with the difference between the two means of 9%. The fit was less good for the period May – June 1990 when the model overestimated mean SMD by 94%. However, the errors did not result in large changes in the calculated r_s as r_s depended mainly on A and VPD. The use of other criteria for f_i did not improve the fit very much.

Half-hourly values of r_s were calculated from Equations 7.26–7.29 and inserted into the Penman-Monteith equation to obtain continuous time series of λE values for Tulasewa (n= 347 days) and Koromani (n= 140 days) forests. The surface resistance was set to zero during periods with rainfall following the stop–go principle (Calder *et al.*, 1986). Examples of the diurnal variation in λE (Penman-Monteith equation as well as TFEB method), H ($A - \lambda$E from Penman-Monteith equation) and A for different weather conditions are shown in Figures 7.19A–C and 7.20A–C for Tulasewa and Koromani forests, respectively. The diurnal patterns of the energy and storage terms on these days have been presented earlier (Figures 7.9 and 7.10). The average daytime

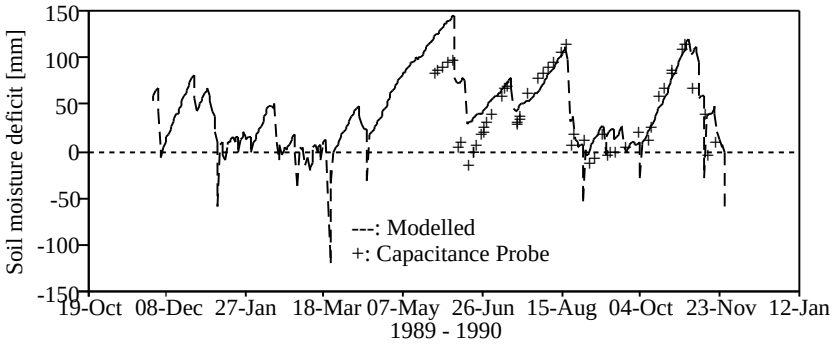

Figure 7.18: *Measured and modelled soil moisture deficits in Tulasewa forest.*

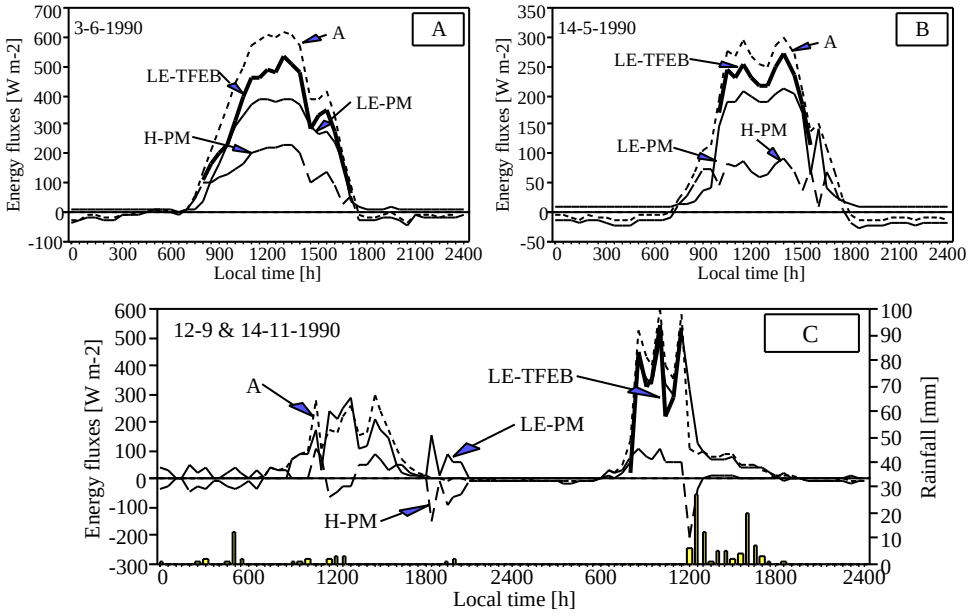

Figure 7.19: *Diurnal patterns of the latent heat flux (LE-PM, LE-TFEB only shown for dry periods with $Ri < -0.01$), sensible heat flux (H-PM) and available energy (A) on selected (A) clear, (B) overcast, and (C) rainy days for Tulasewa forest.*

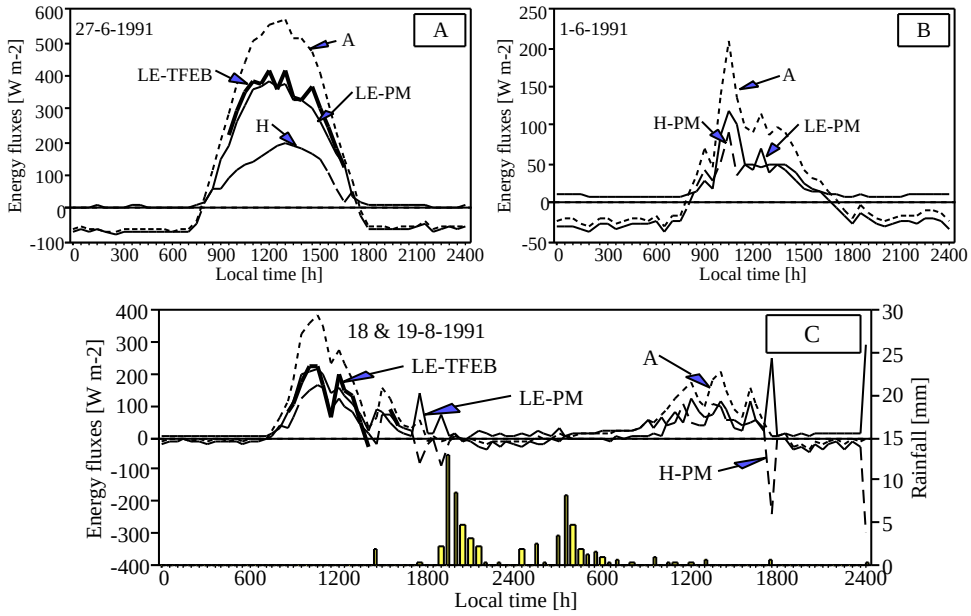

Figure 7.20: *Diurnal patterns of the latent heat flux (LE-PM, LE-TFEB only shown for dry periods with Ri < -0.01), sensible heat flux (H-PM) and available energy (A) on selected (A) clear, (B) overcast, and (C) rainy days for Koromani forest.*

(8:00–17:00 h) wind directions on the selected sunny and overcast days deviated less than 20° from the SE, whereas those on the selected rainy days averaged N138°E and N157°E for Tulasewa forest, and N160°E and N171°E for Koromani forest. Half-hourly estimates of the latent heat fluxes, as calculated with the Penman-Monteith equation, were some 20% lower than those obtained with the TFEB method for both the selected sunny and overcast days at Tulasewa forest, indicating that r_s, as determined from the expressions given earlier, was overestimated for these days. However, much better agreement between the results of the two methods were observed for most other days in the data set (not shown here), as well as for the rainy day. Latent heat fluxes derived with the two different methods also compared well at Koromani forest with differences of less than 10%.

7.7 Summary of Forest Evapotranspiration

Hourly rates of λE in the Tulasewa and Koromani forests, as determined with the Penman-Monteith equation (ET_{pm}) for both dry and rainy (P> 0.8 mm h^{-1}) periods, are given in Table 7.6 for Tulasewa and Koromani forests. The highest rates of ET_{pm} occurred around noon (11:30–12:30 h) and averaged 0.68(±0.25) mm h^{-1} (n= 987) and 0.47(±0.22) mm h^{-1} (n= 402) at Tulasewa and Koromani forests, respectively. Nighttime rates of ET_{pm} under dry conditions were low due to the high r_s and averaged 0.01 mm h^{-1} in both forests. Surprisingly, average hourly rates of ET_{pm} during

Table 7.6: *Averages of ET_{pm}, A and R (rainfall rate), and values of $\bar{E}/\bar{R}$ during periods with rainfall, at Tulasewa and Koromani forests. The number of 30-minute periods is represented by n, standard deviations between parenthesis.*

Location, period & data set	ETpm [mm h-1]	A [W m-2]	R [mm h-1]	E/R	n
Tulasewa forest, Nov '89 - Nov '90, Dry conditions					
Wet season, (8:00-17:00 h)	0.57 (0.28)	474 (226)			2495
Dry season (8:00-17:00 h)	0.44 (0.25)	381 (210)			3576
Wet & dry season (8:00-17:00 h)	0.50 (0.27)	420 (222)			6071
Tulasewa forest, Nov '89 - Nov '90, During rainfall					
Wet & dry season	0.18 (0.25)		5.0 (7.2)	0.04	768
Wet & dry season (8:00-17:00 h)	0.28 (0.28)	119 (124)	6.0 (8.6)	0.05	387
Dry season (8:00-17:00 h)	0.30 (0.30)	120 (131)	3.6 (5.0)	0.08	135
Koromani forest, Apr '91 - Sep '91, Dry conditions					
Dry season (8:00-17:00 h)	0.30 (0.20)	321 (184)			2550
Koromani forest, Apr '91 - Sep '91, During rainfall					
Dry season	0.08 (0.12)		4.2 (6.2)	0.02	143
Dry season (8:00-17:00 h)	0.13 (0.15)	96 (71)	4.6 (6.6)	0.03	68

rainfall were lower than those for dry conditions in spite of zero surface resistance (Calder, 1979). This must be due to the low amounts of (measured) available energy during those conditions (Table 7.6) and the high relative humidity. Corresponding average rainfall rates were calculated to enable the calculation of $\bar{E}/\bar{R}$ for comparison with the $\bar{E}/\bar{R}$ values obtained with the Gash analytical model of rainfall interception (Section 6.4.1). A discussion of the differences in evaporation from a wet canopy obtained with the two methods has been given earlier in Section 6.4.1.

The mean daily ET_{pm} at Tulasewa forest amounted to 4.85($\pm$1.56) mm day^{-1} over a 347-day period between November 30, 1989, and November 27, 1990. The Penman open water evaporation for the corresponding period was 4.61($\pm$1.55) mm day^{-1}, resulting in an ET_{pm}/E_0 ratio of 1.05. The total annual ET_{pm} (November 1989–1990) amounted to 1770 mm, with corresponding totals of E_0 and P of 1672 mm and 1964 mm, respectively. The annual variations in ET_{pm} and E_0 for Tulasewa are shown in Figure 7.21.

ET_{pm} was high during the wet season (November – April), averaging 5.41($\pm$1.52) mm day^{-1} (n= 170). The dry season ET_{pm} (May–November) was lower with an average of 4.32($\pm$1.40) mm day^{-1} (n= 177). This was mainly due to low radiation inputs (table 7.6), rather than to moisture shortages as the dry season of 1990 was relatively wet (table 6.2). Corresponding E_0 values were 5.24($\pm$1.51) and 3.96($\pm$1.34) mm day^{-1}, respectively. The ratio of ET_{pm} to E_0 was usually higher than 1.0, but dropped to 0.7–0.8 during dry periods of several weeks, to be followed by a sharp increase after soil moisture levels were replenished by rainfall (Figure 7.21). A summary of the rates of ET_{pm}, although taken over slightly different periods, will be provided in Table 9.2 in Chapter 9.

The dry season average ET_{pm} at Koromani forest amounted to 2.96($\pm$1.12) mm day^{-1}

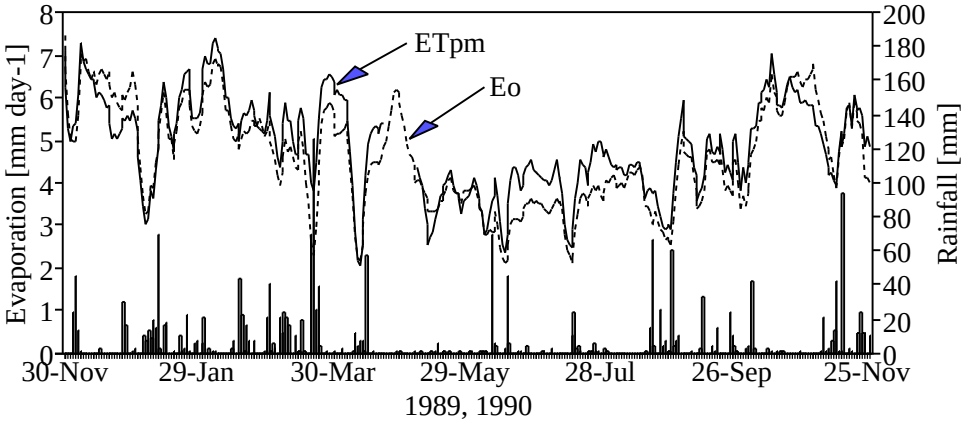

Figure 7.21: *Daily rainfall totals and annual patterns of E_0 and ET_{pm} (5-day moving averages) at Tulasewa forest from November 30, 1989, until November 27, 1990.*

(n= 140), and was much lower than that obtained for the corresponding period a year earlier at Tulasewa forest (3.96(±1.13) mm day^{-1}; n= 135), in spite of a higher average E_0 in 1991 (4.31(±0.96) *versus* 3.63(±1.00) mm day^{-1}). The variations in ET_{pm} and E_0 during the dry season of 1991 at Koromani forest are shown in Figure 7.22.

Total dry season ET_{pm} at Koromani forest amounted to 424 mm (1991) *versus* 573 mm for the same period a year earlier at Tulasewa forest, with corresponding rainfall totals of 321 mm and 467 mm, and E_0 totals of 616 mm and 519 mm (see also Table 9.2, but note the differences in period lenghts). The higher rainfall during the 1990 dry season at Tulasewa cannot be the main reason for its higher evapotranspiration as no water stress was observed in 1991 at Koromani forest (Section 6.5). Rather, the difference in ET_{pm} between the two forests relate to differences in age, and therefore growth rates (Schulze and George, 1987). Furthermore, as stated repeatedly, the canopy of Koromani forest was severely damaged during the passage of cyclone Sina in November 1990, and the foliage biomass had not yet returned to pre-cyclone levels.

The errors in ET totals (computed with the Penman-Monteith equation) as a result of errors in surface roughness parameters were small, with errors in average ET_{pm} values resulting from errors of 15% in d and z_0 and 6% in r_s being lower than 2% and 4% in Tulasewa and Koromani forests, respectively. Errors in R_n or A were thought to be lower than 5%. As such the total error in ET_{pm} values for both forests is probably lower than 10%. The errors associated with daily and half-hourly values may be higher due to uncertainties in the estimation of soil moisture deficit, and therefore r_s.

The ET values derived in this chapter for the two study forests will be compared with estimates of ET in grassland (Chapter 5) in Chapter 9.

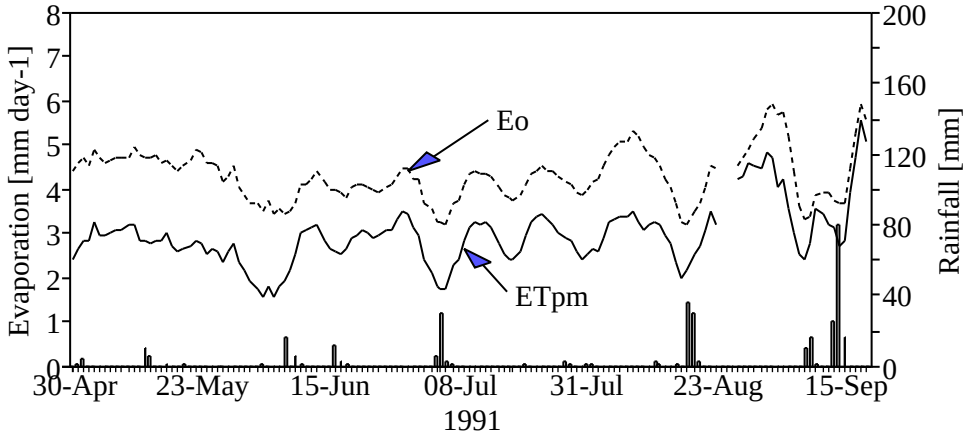

Figure 7.22: *Daily rainfall totals and E_0 and ET_{pm} patterns (5-day moving average) at Koromani forest from April 30 until September 19, 1991.*

Chapter 8

Water Use of the Oleolega Forest

8.1 Introduction

In the previous chapters estimates for the average daily water use of grassland and pine forest have been obtained from a combination of soil moisture depletion, rainfall interception and micro-meteorological measurements. These estimates were obtained for small forest plots in relatively flat terrain, and may not accurately reflect ET rates from steeply dissected terrain covered with patches of pine forest, native forest and grass. The latter situation is far more common in Fiji and an integrated estimate of the overall evaporation rate for this kind of terrain can only be obtained through the quantification of a catchment water balance. Furthermore, ecosystem nutrient exports are generally strongly correlated with streamflow outputs (Likens *et al.*, 1977) whereas the best estimates of nutrient inputs to the system via weathering may be obtained by the catchment nutrient budget technique (Clayton, 1979; Bruijnzeel, 1983a). In this context the following objectives were formulated for the hydrological study in the forested Olelolega catchment:

- To provide baseline information on the water use of mature pine forest, against which the impact of harvesting and subsequent burning on water yield can be assessed
- To allow the calculation of nutrient exports from forested catchment, both for comparison with losses estimated for the respective research plots, and for the assessment of the impacts of harvesting and burning on the water quality *c.q.* nutrient losses
- To evaluate the average annual contribution of rock weathering to the overall pine forest nutrient budget

In this chapter the water budget will be presented for the 63 ha Oleolega catchment (Figure 3.4) which had been planted to pine in 1975, whereas hydrochemical aspects of the catchment in the forested state will be presented in Chapters 13 and 14. Details on the impact of harvesting and subsequent burning of the slash on water yield and quality will be discussed in Chapter 15. A preliminary water budget for the catchment

in the forested state based on the data collected in 1990 was published by Schellekens (1992). However, this budget was slightly in error as a preliminary streamflow rating curve was used, which tended to overestimate peakflows. The corrected water budget is presented in Section 8.3.

8.2 Methods and Instrumentation

Hourly rainfall data were collected from January 4, 1990 onwards with a SIAP UM-8100 pluviograph (orifice at 1.5 m) located near the outlet of the catchment (116 m a.s.l). To obtain an areal estimate of rainfall over the drainage basin two custom-made gauges (OP1, next to the pluviograph; OP5, at the top of the catchment at 245 m a.s.l., orifices at 0.4 m) and a standard rain gauge (OP4, located near sample point 22 at 170 m a.s.l., orifice at 1.0 m) were positioned along the catchment boundary (see Figure 15.3 for locations) between January and March 1990. The mean areal precipitation was estimated using the Thiessen polygons method (Ward and Robinson, 1990) dividing the drainage basin into three parts with 35% of the total area assigned to the pluviograph and gauge OP1, 53% to gauge OP4 and 11% to gauge OP5 (Schellekens, 1992). Topographical aspects were not taken into consideration, in view of the small size of the catchment. The gauges were emptied at least once a week and measurements continued until April 4, 1992. A separate rain gauge (OP2, orifice at 60 cm), similar to those described in Section 6.2, was used to collect rain water for chemical analysis. This gauge was located near the outlet until December, 1990, after which it was moved to the top of the catchment to avoid contamination of samples by logging activities (*e.g.* dust). A total of 23 rain water samples were collected until October 1991.

The water level (H) of the Oleolega creek was measured continuously from January 4, 1990, until April 4, 1992, with an automatic recorder (Leupold & Stevens F4) placed 2.5 m upstream from a culvert. A fixed staff gauge was used as a reference. The approach channel to the culvert was straight. The culvert consisted of four 1.4 m sections of cylindrical concrete (0.91 m diameter) with a slope of 0° at the upstream end, and 2.5° at the downstream end. It had been built on solid rock and leakage underneath the structure could safely be neglected. Both the upstream and downstream walls of the culvert were covered with cement to avoid leakage through the structure. A low V-shaped concrete hump at the joint between the first and the second section of the culvert enabled accurate water level measurements to be made at low discharges. Flood marks indicated that the culvert had been flooded in the past, but this did not occur during the present study.

The waterlevel recorder was serviced once a week. However, when logging started in the area after the forest had been wrecked by cyclone Sina the frequency was increased to twice a week until October 1991, thereby improving the time resolution of the measurements. All charts were digitized at FES–VUA. The water level measurements (H, read to the nearest mm) were converted to discharge (Q, in l s^{-1}) via a stage – discharge relation ship developed for the gauging structure. Regression equations were fitted through 100 simultaneous measurements of Q and H over a range of discharges (Q= 0.6–726 l s^{-1}). Discharge was measured volumetrically at low discharges ($Q < 8.3$ l s^{-1}), with the salt dilution method (Gregory and Walling, 1973) at intermediate discharges (Q= 4.1–34 l s^{-1}) and with the velocity area technique (Ott current meter; Gregory and Walling, 1973) at high discharges (Q= 6.8–726 l s^{-1}). The

following stage–discharge regression equations were calculated (Van Well, 1993b):

$$Q = 0.07274 \cdot \mathrm{H}^{2.2943}$$
$$\mathrm{n}= 99,\ r^2 = 0.99,\ \mathrm{H} \leq 16 \text{ cm} \tag{8.1}$$

$$Q = 0.0296 \cdot \mathrm{H}^{2.6810-0.0039\cdot\mathrm{H}}$$
$$\mathrm{n}= 100,\ r^2 = 1.00,\ \mathrm{H} > 16 \text{ cm} \tag{8.2}$$

During the study water level reached values outside the range of the rating curve (2–70 cm) on three occasions, for a total duration of 8.5 hours. As the discharges for these events were calculated by extrapolation of Equation 8.2 a small error may have been introduced.

Due to maintenance work on the culvert water levels were not measured correctly between January 22 and March 8, 1990. Discharges for this period were simulated using a runoff simulation model developed by Schellekens (1992) for the Oleolega catchment in the forested state. The simulated streamflow total for the whole of 1990, excluding two excessively wet cyclone periods, was within 6% of the measured total (Schellekens, 1992; Van Well, 1993b). Therefore the error in the estimate of total water use by the forest in 1990 introduced by using model predictions for the two weeks during which data were missing can be considered small.

8.3 Catchment Water Balance

To obtain an estimate for the annual ET from the Oleolega catchment the various components of the water balance need to be quantified. The catchment water balance equation reads:

$$P_a = Q + ET + \Delta G + \Delta S + L \tag{8.3}$$

where P_a is the mean areal precipitation, L represents leakage into or out of the catchment, and ΔS and ΔG represent changes in the soil moisture and groundwater storages, respectively (Ward and Robinson, 1989). All amounts are expressed in mm water depth. The accumulated error in ET obtained from such water balance calculations may easily be as large as 20% (Lee, 1970) due to errors in ΔG and ΔS. However, these may be minimized by a careful selection of the period for which the balance is calculated, and the estimates presented below are thought to have an error of less than 10%. Similarly, over- or underestimates of ET because of ungauged amounts of water leaving or entering the catchment via subterraneous pathways can be minimized by selecting a catchment that is watertight. On the basis of the massive character of the bedrock and the very low hydraulic conductivity of the subsoil (Chapter 4.3.3) L was assumed negligible in the present case.

To obtain estimates of ΔG, master baseflow recession curves were calculated for the dry and wet seasons by fitting Equation 8.4 to observed discharges during selected 17–18 day periods of uninterrupted baseflow.

$$Q_t = Q_1 \cdot K_1^t + (Q_2 - Q_1) \cdot K_2^t \tag{8.4}$$

This equation describes the baseflow recession using two so-called linear reservoirs superimposed on each other (Hall, 1968), where Q_t is the discharge (mm h^{-1} at time t in days), Q_1, Q_2, K_1 and K_2 are the initial discharges and recession constants of reservoirs 1 and 2 respectively. Coefficients for the various conditions obtained

Table 8.1: *Regression constants and coefficients of determination (CD) for the prediction of wet and dry season recession curves for the Oleolega catchment in the forested state.*

Recession Curve	Q1	Q2	K1	K2	CD
Wet Season 1990	0.044	0.114	0.967	0.543	1.00
Dry Season 1990	0.025	0.125	0.980	0.238	0.96

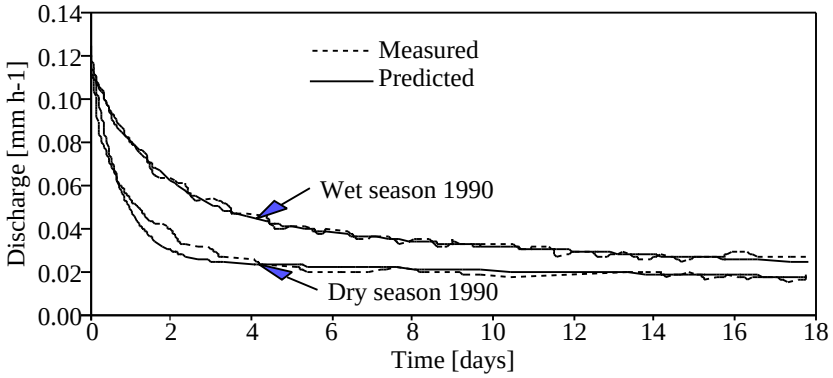

Figure 8.1: *Observed and predicted wet and dry season depletion curves for the forested Oleolega catchment.*

by Schellekens (1992) and Assenberg (1993) were recalculated using the improved stage–discharge relationship derived by Van Well (1993b), using non-linear regression techniques (Marquardt, 1963). The regression constants for both seasons are given in Table 8.1, whereas the observed and predicted recession curves are shown in Figure 8.1.

According to the theory of linear reservoirs ΔG can be calculated from the difference of the discharge at the beginning and at the end of the period under consideration using the following equation:

$$\Delta G = \frac{\partial Q}{\partial t} = \frac{Q_t - Q_0}{\ln K_1} + \frac{Q_t - Q_0}{\ln K_2} \tag{8.5}$$

Equation 8.3 was solved for the period January 4 – November 13, 1990. There were two reasons for chosing this period. Firstly, the discharge at the beginning of this period was 0.007 mm h^{-1}, whereas that at the end of the period was 0.009 mm h^{-1}, leading to the negligibly small value for ΔG of -0.1 mm. Secondly, the catchment was struck by cyclone Sina by the end of November 1990, and this of course altered the situation dramatically. An indication of the importance of ΔS for the selected period was obtained from a comparison of the rainfall totals in the four weeks preceding the beginning and the end of the period. As these compared well (11.5 mm in 1989 *versus* 22.2 mm in 1990 at Nabou station) ΔS could be neglected safely.

The total mean areal precipitation for the selected 314-day period amounted to 1547 mm, whereas total runoff amounted to 246 mm. This implied an ET of 1301

Table 8.2: *Quantification of the components of the water balance for the Oleolega catchment in the forested state between January 4 and November 13, 1990.*

Period	P [mm]	Q [mm]	ET [mm]	Ei [mm]	Eil [mm]	Et [mm]	DeltaS [mm]	DeltaG [mm]	ET [mm day-1]	Eo [mm day-1]	ET/Eo
Whole period											
Jan 4 - Nov 13, 1990	1547	246	1301	290	134	877	(0)	(-0.1)	4.14	4.40	0.94
Wet season											
Jan 4 - May 31, 1990	904	163	741	165	68	508	(0)	(-0.2)	5.04	4.74	1.06
Dry season											
May 24 - Oct 23, 1990	569	98	471	111	59	301	(0)	(0)	3.10	3.86	0.80

mm or 4.1 mm day^{-1}. The average daily ET_{pm} for the corresponding period at Tulasewa forest was only slightly higher at 4.7($\pm$1.5) mm day^{-1} (n= 300) or 1484 mm (Section 7.7). The ET value obtained for the Oleolega catchment with the catchment water balance method therefore seems realistic in view of the lower stocking and growth rate of the mature forest (*cf.* Sections 3.2 and 3.5). In addition, the assumption of zero leakage was not overturned. The Penman open water evaporation as calculated for the nearby Tulasewa site for the selected period was 4.4($\pm$1.5) mm day^{-1}, resulting in a pre-cyclone ET/E_0 ratio of 0.94 for mature pine forest at Oleolega. Blackie (1979) reported a lower value (0.77) for mature *Pinus patula* plantations growing in deep clayey soils at an elevation of 2400 m a.s.l. in Kenya. The runoff coefficient of the Oleolega catchment, defined as the proportion of rainfall that leaves the catchment as streamflow, was low at 0.16.

The ET may be further subdivided into an interception loss component and a transpiration component. An estimate of the former was obtained from the canopy and litter layer interception models discussed in Section 6.4.1 using the daily mean areal precipitation at Oleolega catchment forest as input. The (adjusted) model parameters for Koromani forest (Table 6.6) were used in the calculations since its structure resembled that of the forest in the Oleolega catchment. However, the presence of broad-leaved native vegetation (with different interception characteristics) in the riparian zone could not be accounted for. This may have resulted in small errors in the simulated interception losses. The model predicted an interception loss of 424 mm for the selected period, of which 290 mm was lost from the canopy and 134 mm from the litter layer. This would imply that 877 mm was lost through transpiration by the pines and native vegetation, and that the amount of water reaching the soil surface was 1123 mm. The values obtained for the various components of the water balance are summarized in Table 8.2

Estimates for wet and dry season water use by the forest were also obtained from selected periods during 1990. The accuracy of these estimates must be considered to be somewhat lower than those for the entire period as errors associated with ΔS and ΔG will have a larger impact on the results. An estimate for wet season ET was obtained for the 147-day period between January 4 and May 31, 1990. Groundwater storage, as calculated from Equation 8.5, was again small at -0.2 mm, whereas ΔS was neglected as rainfall totals for the months preceeding the start and the end of the period differed by only 35 mm (67 mm *versus* 32 mm).The error associated with neglecting

ΔS was estimated at less than 5%, and fell therefore within the errors of rainfall and streamflow measurements. The rainfall input during this period amounted to 904 mm, whereas the corresponding streamflow output was 163 mm. As such 741 mm were lost through evapotranspiration, or 5.0 mm day^{-1}. The corresponding daily average for Tulasewa forest (ET_{pm}) amounted to 5.0($\pm$1.6) mm day^{-1} as well, suggesting that the ET rates for young and mature forest during the wet season were similar, and well above the Penman open water evaporation which amounted to 4.7($\pm$1.4) mm day^{-1} (*i.e.* ET/E_0= 1.06). As the soil was wet for most of this period, the observed ET may be assumed to have equalled the potential ET. A summary of the components of the water balance for this period, including interception losses, is given in Table 8.2.

In a similar way, a dry season estimate of ET was obtained for a 152-day period between May 24 and October 23, 1990, when discharges were again similar implying that ΔG could be neglected. ΔS was neglected as well because the difference in rainfall within the 30-day periods before the start (45 mm) and end (72 mm) of the selected period was small. With a rainfall total of 569 mm and a total discharge of 98 mm, the estimated dry season ET amounted to 471 mm, or 3.1 mm day^{-1}. This was much lower than the corresponding ET_{pm} for Tulasewa forest (4.3$\pm$1.4 mm day^{-1}), possibly due to the higher rainfall inputs in the latter area, and differences in soils (*e.g.* amounts of plant available water, Section 4.3.4), forest age and stocking. The daily average E_0, as measured at Tulasewa forest, amounted to 3.9($\pm$1.3) mm day^{-1} for the corresponding period, suggesting a dry season ET/E_0 ratio of 0.80 for the mature forest. This suggested that ET at Oleolega indeed dropped below the potential rate during the dry season, most likely as a result of the higher soil moisture deficits during periods with little rainfall (July, October).

8.4 Contribution of Baseflow and Quickflow to Streamflow

Total streamflow during a storm can be separated into a quickflow and a delayed, or baseflow component (Ward, 1984). The quickflow consists of water reaching the stream channel within a short period following rainfall, and is associated with a peak in the discharge. It may consist of contributions from various types of overland flow, lateral subsurface stormflow and channel precipitation (Dunne, 1978). Baseflow is sustained by water travelling more slowly through the system, and is for a large part derived from the depletion of soil moisture and groundwater storage within the catchment (Ward, 1984).

Schellekens (1992) tested various hydrological (Hewlett and Hibbert, 1967; Pearce *et al.*, 1976; Rogers, 1980) and hydrochemical (Nakamura, 1971) techniques, to separate the quickflow and baseflow components at Oleolega. He decided on a time-based separation method (Hewlett and Hibbert, 1967), with a straight line having a slope of 0.03 mm h^{-1} day^{-1}.

A computer programme was used (Schellekens, 1991) to analyze the streamflow for the period January 4 to November 13, 1990. The results indicated that 88 mm or 35% of the total streamflow occurred as quickflow, whereas 161 mm was assigned to baseflow. Some 85% of the total quickflow was observed during the wet season (January–April and November, 1990) whereas 58% of the quickflow occurred within five days during and after the passage of cyclone Rae in March, 1990. Baseflow during the dry season (May–October) constituted 40% of the total baseflow during the entire

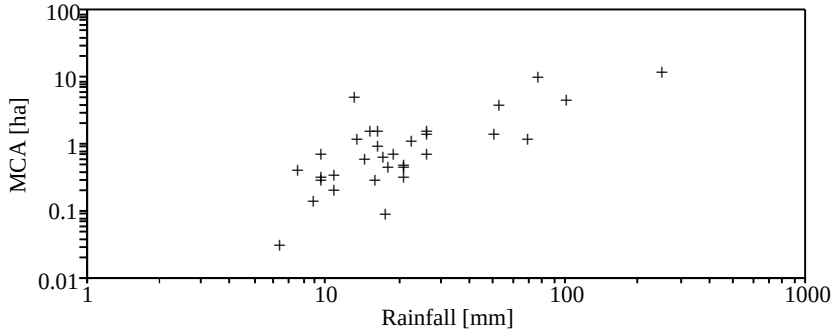

Figure 8.2: *The size of minimum contributing areas (MCA) against mean areal rainfall in the Oleolega catchment for the period January 4 – November 13, 1990.*

period.

The high quickflow percentage, particularly during cyclone events, renders the Oleolega catchment highly responsive to rainfall. Other small forested catchments in the wetter parts of the Austral–Pacific region have been reported to be even more responsive, either as a result of extremely permeable soils (as at Maimai, New Zealand; Pearce *et al.*, 1986; Sklash *et al.*, 1986), or a combination of high rainfall intensities and an impeding layer at shallow depth (as at Babinda, Queensland; Bonell and Gilmour, 1978; Bonell *et al.*, 1981).

The quickflow at Oleolega was analyzed in terms of the minimum contributing area (MCA) concept (Dickinson and Whiteley, 1970; Bruijnzeel, 1983a) by Schellekens (1992). In a general formula the MCA can be defined as:

$$MCA = \frac{Q_q}{P} \cdot A_c \tag{8.6}$$

where Q_q, P and A_c represent the quickflow volume (mm), the amount of rainfall (mm) and the catchment area (ha), respectively.

A graph of the MCAs obtained for the pre-cyclone priod in 1990 against rainfall ($P > 5$ mm) is shown in Figure 8.2. The results indicated that quickflow depended on antecedent wetness and was generally supplied by a relatively small fraction of the catchment area (63 ha) for storms smaller than 50 mm ($MCA < 2$ ha for 82% of the storms) but that the MCA could reach values up to 13 ha during larger storms (*e.g.* during cyclone Rae). The quickflow presumably consisted mainly of subsurface storm flow and valley bottom saturated overland flow with further minor contributions of channel precipitation and hillside hollow saturation overland flow (Schellekens, 1992).

Chapter 9

Summary of Hydrological Effects of Afforestation in SW Viti Levu

Estimates of the water use of *Pennisetum polystachyon* grassland and pine forest of varying age, as well as information on the climate at the respective study sites and various micro-meteorological properties of both vegetation types, have been presented separately in the previous chapters. The impact of the conversion of grassland to pine plantation forest on these various aspects will be summarized in this chapter.

9.1 Impact of Afforestation on Micro-meteorological Parameters

A summary of climatic and micro-meteorological parameters measured above grassland and two pine forests is given in Table 9.1. An attempt at evaluating the impact of afforestation on the microclimate above grassland and pine forest was made by comparing net radiation, average minimum and maximum temperatures, and average minimum and maximum relative humidities as measured above Nabou grassland, with

Table 9.1: *Dry season climatic and micro-meteorological (daytime means) parameters for grassland and pine forest. Standard deviations between parentheses.*

Location	Year	Tmin [C]	Tmax [C]	RHmin [%]	RHmax [%]	Albedo	Rn+	ra [s m-1]	rs [s m-1]
Nabou Grassland	1991	17.9 (3.0)	28.2 (1.9)	59 (9)	98 (6)	0.18 (0.01)*	8.0 (3.5)	30.8 (24.0)	246 (98)
Tulasewa Forest	1990	18.8 (2.0)	26.5 (2.1)	66 (11)	96 (4)	0.10 (0.01)	11.4 (3.6)	14.1 (8.2)	43 (21)
Koromani Forest	1991	20.4 (1.5)	26.1 (1.9)	61 (11)	89 (8)	0.13 (0.01)	10.5 (3.5)	13.5 (7.6)	113 (126)

+: Daytime values (800-1800 h) in MJ m-2 day-1; *: Wet season 1991

those measured above the mature forest at Koromani in the dry season of 1991.

The albedo decreased significantly (α= 0.01) after afforestation from 0.18–0.19 for grassland (wet season) to 0.10–0.13 for pine forest . The decrease in albedo and differences in the net long-wave radiation components caused an increase in the net radiation above the forests compared to grassland, and therefore also in the available energy for evapotranspiration: daytime net radiation totals above Koromani forest were about 24% higher than above Nabou grassland. The comparison between the grassland and Tulasewa forest was more difficult to make as R_n at the latter site was measured a year earlier. However, the even lower albedo of Tulasewa forest (0.10) suggested that the large difference in R_n between the two sites could well be caused by differences in the vegetation type, rather than in the respective seasons. The soil heat flux also showed a larger range below grass (-14 to 19 W m^{-2}) than below mature pine forest (-6 to 7 W m^{-2}), although some of the difference may be attributed to different climatic conditions between the measurement periods.

The minimum temperature and relative humidity above Nabou grassland were significantly lower (α= 0.01) than those measured above Tulasewa and Koromani forests, whereas the maximum temperature and relative humidity were significantly higher (α= 0.01). Afforestation therefore resulted in an attenuation of the diurnal patterns of temperature and humidity during the dry season, in line with the decrease in variation in soil heat flux.

These results are similar to those of Bastable *et al.* (1993), who also observed a much greater diurnal variation in temperature, humidity, and soil heat flux, as well as a reduction in net radiation over a pasture clearing (albedo = 0.16), compared to nearby undisturbed tropical rainforest (albedo = 0.13) in Brazil. The differences between forest and clearing were most pronounced during dry periods. Similarly, contrasts have been reported by Schulz (1960) for rainforest canopies and grassy clearings in Surinam, whereas various other examples of changes in microclimate after forest clearing can be found in Lal (1987).

The aerodynamic properties of the grassland were also different from those of pine forest, which presents a much rougher surface. This must have resulted in a gradual decrease in r_a during the first few years after the planting of the pine forest. However, the decrease seemed to level off after canopy closure as differences in r_a between the young and the mature stand were not significant (*cf.* Section 7.6.3). As will be shown below, the combined effect of increases in LAI and reductions in r_a associated with afforestation resulted in a large increase in amounts of rainfall interception by the respective vegetation types (Table 9.2; *cf.* Calder, 1979; Calder, 1982).

The *Pennisetum polystachyon* grassland vegetation was strongly seasonal and started to die off at the start of the dry season. Stomatal resistances were high during the dry season and this, in combination with a gradual decrease in LAI, resulted in a corresponding increase in daytime r_s from about 80 s m^{-1} in May to 300–400 s m^{-1} at the end of the dry season. Differences in r_s of grassland and pine forest were small at the beginning of the dry season (Calder, 1979), but increased as the dry season progressed because the r_s of the pines, which did not show a seasonal trend, remained fairly constant (*cf.* Sections 5.4.4 and 7.6.3).

Table 9.2: *Dry season (May 11 – September 19, n= 132) and annual estimates of ET, E_0, modelled interception losses, and rainfall amounts (P) for Nabou grassland and Tulasewa, Korokula, Koromani and Oleolega forests .*

Location	Period/Year	ET [mm]	ET [mm day-1]	Eo [mm]	ET/Eo	I-loss Canopy [mm]	I-loss Litter [mm]	I-loss Total [% of P]	Rainfall Total [mm]
Dry Season Estimates									
Nabou Grassland	1991	128	0.97 (0.34)	485	0.26	14	25	12	319
Tulasewa Forest	1990	521	3.95 (1.14)	468	1.11	92	51	31	465
Koromani Forest	1991	382	2.96 (1.14)	551	0.69	49	45	30	317
Oleolega Forest*	1990	438	3.3 (-)	506	0.87	100	50	29	525
Annual Estimates									
Tulasewa Forest	Nov'89-Nov'90	1772	4.85 (1.56)	1681	1.05	357	159	27	1932
Korokula Forest	1990					365	154	29	1779
Koromani Forest	1990					335	155	26	1908
Oleolega Forest+	1990	1512	4.1 (-)	1605	0.94	338	156	27	1798

*: ET and Eo based on data collected in the period May 24 - October 23, 1990
+: Annual totals of ET, Eo, I-loss, rainfall and runoff obtained by extrapolation from 314 days of data

9.2 Impact of Afforestation Dry Season on Water Use

Grassland ET rates in the dry season were determined from a combination of the Penman-Monteith equation and soil moisture depletion measurements (Sections 5.3 and 5.4.4). Estimates for the dry season water use of Tulasewa and Koromani forests were obtained from soil moisture depletion measurements (Section 6.5), and particularly from micro-meteorological measurements (Section 7.7). A comparison of the results obtained with the two approaches indicated that the former method underestimated ET at Tulasewa and Koromani forests by 24% and 38%, respectively, due to water extraction by tree roots at depths beyond those reached by the soil moisture probe access tubes. Because the access tubes in the grassland plot extended below the rooting depth of grass, the ET_{sm} data obtained with the soil moisture depletion method were considered realistic in this case. Finally, the catchment water balance method was used to obtain a dry season estimate of water use by mature pine forest at Oleolega.

Dry season and annual estimates of ET, E_0, rainfall and interception losses for Nabou grassland (no annual values), and Tulasewa, Korokula (no estimates for ET, E_0), Koromani and Oleolega forests are summarized in Table 9.2. It should be noted that that the estimates presented here were collected over part of the respective dry seasons (only 132 days), and that totals pertaining to a whole dry season (184 days) will therefore be considerably higher. The post-cyclone dry season water use of Koromani forest was 254 mm higher than that of Nabou grassland in 1991. This was largely due to differences in transpiration (calculated as the difference between ET and interception loss) between the two vegetation types (79 mm for grass *versus* 288 mm for mature pine forest) and to a lesser extent to differences in interception loss (39 *versus* 94 mm, respectively). The dry season ET for grassland would probably have been higher in 1990, due to the higher 1990 rainfall total which would have resulted in

a larger interception loss. It should be mentioned here (*cf.* Section 5.1) that the *Pennisetum polystachyon* grasslands in SW Viti Levu were observed to die anyway during the dry season, regardless of soil water conditions. Therefore no major increases in transpiration as a result of increased rainfall were to be expected for 1990. Further support for the latter contention comes from the fact that E_0 values differed by less than 5% for the two dry seasons. The total interception loss for the grassland during the dry season of 1990 was approximated at 12% of total rainfall (Section 5.5) or 60 mm. Together with the estimated transpiration rate of 80 mm (1991 value) a total dry season ET of 140 mm was calculated. Using this value, corresponding ET losses at Tulasewa and Oleolega were 380 and 300 mm higher than that of the Nabou grassland, respectively.

The annual ET in the fast-growing and well-stocked Tulasewa forest was high, amounting to 92% of the annual rainfall, and somewhat lower in the cyclone damaged mature Oleolega forest where it amounted to 82% of the annual rainfall (Table 9.2). The interception losses, again expressed as fractions of total rainfall, did not show much variation between forest sites and were in the order of 500 mm year^{-1} for a year of average rainfall. Annual transpiration totals ranged from about 1050 mm at Oleolega to 1256 mm at Tulasewa, which is within the range for natural forest in humid tropical lowlands (885–1285 mm year^{-1}) given by Bruijnzeel (1990).

Summarizing, conversion of *Pennisetum polystachyon* grassland to *Pinus caribaea* forest resulted in increases in dry season transpiration rates and in amounts of water lost by rainfall interception (Table 9.2). Annual differences in ET between grassland and pine forest will be larger than the quoted 250–380 mm, as measurements pertained to (part of) the dry season only. The water use of *Pennisetum polystachyon* grass during the wet season remains unknown as yet, but is almost certainly lower than that of the pine forest due to its lower rainfall interception (estimated at 12% *versus* 26–29% of rainfall in mature pine; *cf.* Sections 5.5 and 6.4.1), and the lower net radiation total observed above the grass.

The annual streamflow total of the forested Oleolega catchment was 288 mm in 1990 (Section 8.3), and since the difference in the dry season ET between the vegetation types was 250–380 mm, the annual streamflow total from a similar catchment under grass was likely to exceed 540 mm. This suggests that a reduction in annual water yield of at least 50% may be expected several years after grassland catchments have been converted to pine plantation forest (*cf.* Kammer and Raj, 1979). However, further work on wet season stomatal behaviour and LAI, preferably in combination with a micro-meteorological study involving the determination of ET_{pm} from a combination of the temperature fluctuation energy balance method (to obtain expressions for r_s; see Section 7.6.3) and the Penman-Monteith model, of *Pennisetum polystachyon* grassland is necessary before grassland ET in the wet season can be quantified properly.

9.3 Effect of Cyclone Sina on Forest Water Use

Temporary reductions in transpiration as well as in interception losses may be expected after the passage of a cyclone due to the decrease in foliar biomass (LAI) (*cf.* Frangi and Lugo, 1991; Lodge *et al.*, 1991).

Comparison of pre- and post-cyclone dry season ET_{sm} (Table 6.8) indicated that water extraction from the top 0.6–1.0 m of the soil decreased by 31%, 38% and 8% in Tulasewa, Korokula and Koromani forests, respectively, 6–9 months after the forests

had been damaged severely by cyclone Sina in November, 1990. In the Tulasewa forest plot where tree density was reduced by some 40% this resulted in much higher soil moisture levels throughout the dry season of 1991 compared to 1990 (Figure 6.5 in Section 6.5).

Cyclone damage was less in Korokula and Koromani forests, however, and no such differences in minimum soil moisture levels between the pre- and post-cyclone dry seasons were observed there. The relatively large reduction in ET observed for the Korokula forest plot in 1991 could partly be attributed to differences in rainfall amounts between the respective periods. However, the fact that moisture stress was observed during the rather wet dry season of 1990 (as indicated by increased litter fall; Section 12.3.1), but not during that of 1991, which was much drier, suggested that a reduction in ET as a result of cyclone damage had occurred at this site as well.

Comparison of the pre-cyclone dry season ET of Oleolega forest with the post-cyclone ET in Koromani forest (which was similar in structure) suggested a 10% reduction in ET as a result of damage afflicted by cyclone Sina. The actual reduction may have been somewhat higher as E_0 in 1990 was lower than that for the corresponding period in 1991 (table 9.2).

Interception losses from the canopy decreased at all sites (Section 6.4), as indicated by the larger amounts of relative throughfall collected during the post-cyclone period. The largest decrease was observed at Korokula forest, where the observed amount of throughfall increased from 77% of total rainfall during the pre-cyclone period to 87% during the post-cyclone period. At Tulasewa forest relative throughfall increased from 79% to 85% of total rainfall. No pre-cyclone measurements had been made during the 1990 wet season in the Koromani forest plot, and the observed 82% of total dry season rainfall in 1990 *versus* 83% of post-cyclone rainfall may not accurately reflect the effect of cyclone Sina. However, the decrease in interception loss from the canopy was partly compensated by higher interception in the litter layer, which increased from 9.9% to 11.6% of total rainfall in Korokula forest, and from 9.5% to 10.5% in Tulasewa forest. We are not aware of any other studies in the literature reporting the effects of forest disturbance by tropical cyclones on rainfall interception or forest evapotranspiration.